Project No. ___ **COPY No..**

NCHRP Project 9-22B: Comparing HMA Dynamic Modulus Measured by Axial Compression and IDT Methods

PROJECT FINAL REPORT

Prepared for

NCHRP
Transportation Research Board
of
The National Academies

LIMITED USE DOCUMENT

This Quarterly Progress Report is furnished only for review by members of the NCHRP project panel and is regarded as fully privileged. Dissemination of information included herein must be approved by the NCHRP.

Leslie Myers McCarthy, Ph.D., P.E.
Villanova University
Villanova, PA

Thomas Bennert, Ph.D.
Rutgers University
Piscataway, NJ

May 2012

ACKNOWLEDGMENT OF SPONSORSHIP

This work was sponsored by one or more of the following as noted:

☒ American Association of State Highway and Transportation Officials, in cooperation with the Federal Highway Administration, and was conducted in the **National Cooperative Highway Research Program,**

☐ Federal Transit Administration and was conducted in the **Transit Cooperative Research Program**,

☐ American Association of State Highway and Transportation Officials, in cooperation with the Federal Motor Carriers Safety Administration, and was conducted in the **Commercial Truck and Bus Safety Synthesis Program,**

☐ Federal Aviation Administration and was conducted in the **Airports Cooperative Research Program,**

which is administered by the Transportation Research Board of the National Academies.

NCHRP Project 9-22B: Comparing HMA Dynamic Modulus Measured by Axial Compression and IDT Methods

FINAL REPORT

Prepared for

NCHRP
Transportation Research Board
of
The National Academies

LIMITED USE DOCUMENT

This Quarterly Progress Report is furnished only for review by members of the NCHRP project panel and is regarded as fully privileged. Dissemination of information included herein must be approved by the NCHRP.

Leslie Myers McCarthy, Ph.D., P.E.
Villanova University
Villanova, PA

Thomas Bennert, Ph.D.
Rutgers University
Piscataway, NJ

May 2012

CONTENTS

LIST OF FIGURES AND TABLES

List of Figures

List of Tables

ACKNOWLEDGMENTS

The research reported herein was performed under NCHRP Project 9–22B by the Department of Civil and Environmental Engineering at Villanova University and the Rutgers University Advanced Pavement Laboratory. Villanova University was the contractor for this study, with Rutgers University serving as subcontractor. The Federal Highway Administration provided laboratory data from testing conducted in the Mobile Asphalt Mixture Testing Laboratory. The Rhode Island Department of Transportation, Maine Department of Transportation, and Delaware Department of Transportation actively participated in this project by generously supplying project data, materials, and coordination with contractors and the NCHRP 9-22B project team.

Dr. Leslie Myers McCarthy, Ph.D., P.E., Assistant Professor of Civil and Environmental Engineering at Villanova University, was the Principal Investigator. The other authors of this report are Dr. Thomas Bennert, Assistant Research Professor at Rutgers University and co-Principal Investigator; Ms. Maria C. Guercio and Mr. Van DeJarnette, Research Assistants and M.S. Candidates at Villanova University; and Mr. Darius Pezeshki, Laboratory Technician at Rutgers University Asphalt Pavement Laboratory. The work was done under the general supervision of Professor McCarthy at Villanova University and Dr. Bennert at Rutgers University.

ABSTRACT

This report documents the results of a scoping study on the impacts of asphalt mixture specimen type and test methods on flexible pavement performance. Laboratory tests in combination with computer simulations were conducted to investigate asphalt mixture behavior at a range of temperatures and load frequencies when tested by two different methods for measuring dynamic modulus. Asphalt mixtures included in the study included both those commonly used and those modified with emerging technologies. Three different laboratory specimen preparation types were given consideration in the study. The dynamic modulus data was then investigated using three pavement performance tools. Pavement distresses that were observed and evaluated included rutting in the surface and binder layers, and fatigue cracking. The pavement predictive model results correlated well with one another. The findings of the study suggest that agencies can choose their test procedure and specimen preparation method and expect similar performance from pavement life predictions. Agencies should base their decision of which method to use upon the type of pavement distress most likely to occur at the design location.

EXECUTIVE SUMMARY

The Mechanistic-Empirical Pavement Design Guide (MEPDG) and the NCHRP Project 9-22 Quality-Related Specification(QRSS) analytical software require the user to input the dynamic modulus (|E*|) of the hot mix asphalt (HMA) mixture in order to utilize the rutting and fatigue cracking distress prediction equations of the hot mix asphalt pavement section. However, there are various methods and sample types available for the determination of |E*| of the HMA. Therefore, the primary objective of this research project was to evaluate the effects of testing different sample types/configurations on the distress predictions resulting from the MEPDG, QRSS, and SPT Program tools.

In Phase I of the research, asphalt mixtures were sampled during construction and brought back to the laboratory for testing. Along with the collect loose asphalt mixture, field cores were also procured, as well as the asphalt plant quality control production information. The loose mix was utilized to compact test specimens for dynamic modulus testing, in accordance with AASHTO TP79. Meanwhile, the collected field cores were also measured for their respective dynamic modulus properties utilizing a newly developed testing and analysis procedure that allows the dynamic modulus to be measured with the test specimen in the indirect tensile mode (IDT) configuration. In Phase II, the measured dynamic modulus was inputted into various pavement performance software programs to predict pavement distress levels and resultant performance-based pay adjustment factors. The analysis programs included the Mechanistic Empirical Pavement Design Guide (MEPDG), Arizona State's SPT program (a product of NCHRP Project 9-22A, and also the Quality Related Specification Software, QRSS (a product of NCHRP Project 9-22).

In general, differences in measured dynamic modulus were found between the different specimen types (laboratory compacted vs. field cores). However, the trend in the differences was not consistent. Dynamic modulus measurements of the field cores were found to be higher and lower than the laboratory reheated and compacted test specimens. The dynamic modulus properties of the mixture were also found to sometimes vary greatly from a Lot to Lot basis. Collected information shows that this difference may be due to the contrast in volumetric properties from one Lot to the next. Overall, it was determined that the IDT test mode to determine dynamic modulus of asphalt mixtures could be utilized to generate inputs for the various pavement performance software programs that required dynamic modulus as an input parameter.

When utilizing the pavement performance programs with the generated dynamic modulus values, the resultant data suggests that it is not necessary to require plant-compacted or field-compacted asphalt specimens. Test results based on the laboratory reheated and compacted specimens resulted in pavement performance predictions equivalent to the plant-compacted and field-compacted specimens. A comparison of the different software programs also suggests that the Mechanistic Empirical Pavement Design Guide (MEPDG or DARWIN-ME) can be used effectively with Level 2 inputs in lieu of requiring Level 1 inputs to predict the life expectancy of the pavement. It was also found that the MEPDG can be an effective substitute for the QRSS software. Some improvement can be made to the QRSS and SPT programs to make them more user-friendly and stable during pavement analysis runs.

CHAPTER 1

BACKGROUND

1.1 Problem Statement and Research Objective

1.1.1 Problem Statement

The primary input parameter utilized in the American Association of State Highway and Transportation Officials (AASHTO) Mechanistic-Empirical Pavement Design Guide (MEPDG) and National Cooperative Highway Research Program (NCHRP) Project 9-22 performance-related specification (PRS) software packages is the dynamic modulus (|E*|). In the MEPDG, stresses and strains within the asphalt pavement structure are computed using layered elastic theory. The dynamic modulus is required to conduct these calculations. The dynamic modulus represents the linear-elastic stiffness property of hot mix asphalt (HMA) when subjected to a continuous sinusoidal, stress-controlled load in compression. Both the applied stress and the resulting strain are recorded with time as shown in Figure 1.

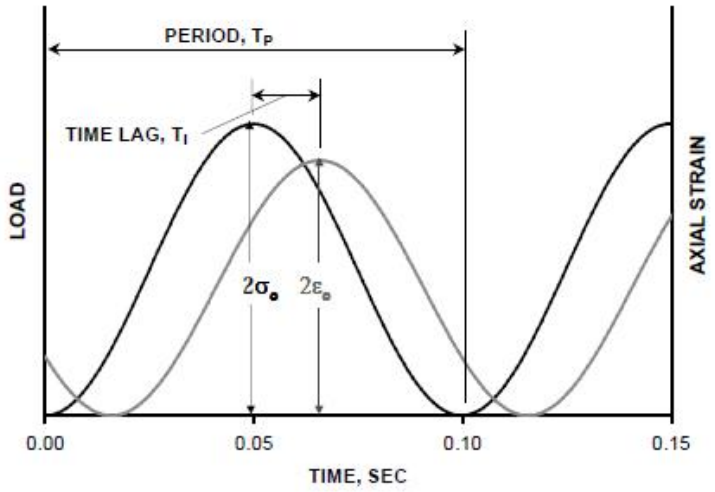

Figure 1. Schematic of Stresses and Strains in the Dynamic Modulus Test [data from Bonaquist, 2009].

During testing, the asphalt specimen is typically subjected to varying temperatures and loading frequencies in order to generate a master stiffness curve, which represents the stiffness of the asphalt mixture at any given time and temperature. Currently, the dynamic modulus (|E*|) is tested in accordance with AASHTO T 342, *Standard Method of Test for Determining Dynamic Modulus of Hot-Mix Asphalt (HMA)*, or AASHTO TP79, *Determining the Dynamic Modulus and Flow Number for Hot Mix Asphalt (HMA) Using the Asphalt Mixture Performance Tester (AMPT).* However, these AASHTO test procedures require a specimen height of six (6) inches (150 mm) and diameter of four (4) inches (100 mm). The restriction on specimen dimensions often leads to difficulties in testing field-compacted cores, which are commonly placed in lifts less than three (3) inches (75 mm) thick. In practice, this restriction has resulted in limiting laboratory analyses to either test specimens compacted at the asphalt plant's Quality Control (QC) laboratory or to sampled loose mix brought back to the laboratory, reheated, and then compacted to provide dynamic modulus test specimens. Both conditions may not fully represent the in-situ stiffness of the field-compacted material that is presumed to best represent the ultimate performance of the asphalt pavement.

The use of the Indirect Tension (IDT) mode for dynamic modulus testing was developed by Kim et al. (2004) to possibly resolve some of the specimen dimension issues. The findings presented by Kim et al. (2004) provided an analytical solution that can be used as a standard test procedure to determine the dynamic modulus and phase angle of asphalt mixtures using the IDT testing configuration. The test procedure has also been presented at the Federal Highway Administration (FHWA) Asphalt Mixture Expert Task Group (ETG) a number of times with the most recent resulting in the establishment of a task group to conduct a ruggedness study on the test procedure (Kim et al., 2009).

Rutgers University conducted preliminary tests using both the AASHTO TP79 and the IDT |E*| procedure (Kim et al., 2004) on asphalt mixtures placed at the Federal Aviation Administration's (FAA) National Airport Pavement Testing Facility (NAPTF) in Atlantic City, New Jersey. The preliminary laboratory investigation consisted of testing both extracted field cores (referred to as Plant-Mixed/Field-Compacted) and loose mix (referred to as Plant-Mixed/Laboratory-Compacted) sampled during production. The field cores were extracted from a 6-inch thick pavement section that contained two 3-inch lifts of identical mixture, in order to test in accordance with AASHTO TP79. As shown in Figure 2, the use of the IDT |E*| procedure provides a viable comparison to the dynamic modulus determined using AASHTO TP79. Although Figure 2 is only from one dataset, the data complemented the continued work presented by Kim et al., (2009), that indicates the IDT |E*| test may be used in lieu of either AASHTO T 342 or AASHTO TP79 for determining the dynamic modulus properties of asphalt mixtures.

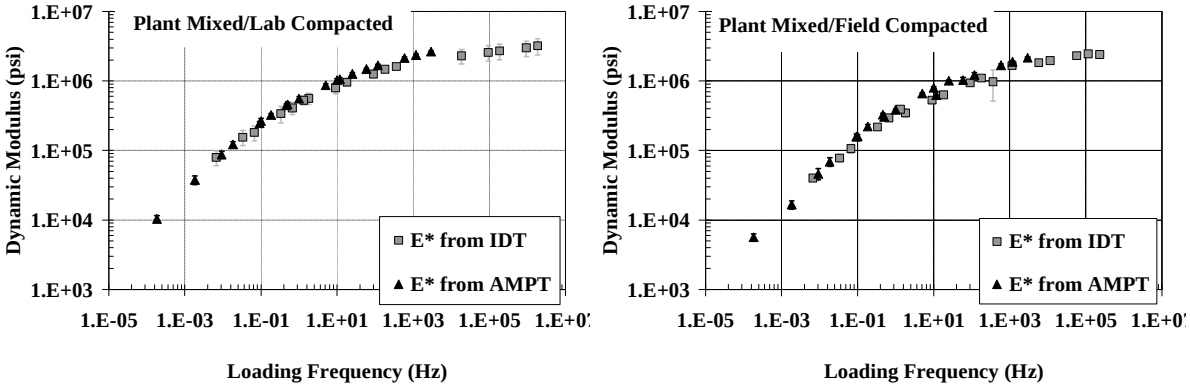

(a)
Plant-Mixed/Laboratory-Compacted

(b)
Plant-Mixed/Field-Compacted

Figure 2. Dynamic Modulus Master Curves Generated from the Asphalt Mixture Performance Tester (AASHTO T 342) and IDT Test Device [Kim et al., (2004)].

As more state transportation agencies (DOTs) move toward implementation of the AASHTO MEPDG software, more information is required regarding how the specimen type may affect predicted pavement performance. Key questions that arise include:

- Should a DOT pursue development of HMA Material Input Catalogs using laboratory-mixed or plant-mixed materials?
- What can DOTs expect if they use field-compacted versus laboratory-compacted specimens?

An example from the MEPDG shows HMA rutting and top-down fatigue cracking predictions for laboratory-compacted and field-compacted samples in Figure 3. The MEPDG distress predictions were determined using the dynamic modulus test results for the Asphalt Mixture Performance Tester (AMPT) results that were shown previously in Figure 2. Based on the pavement structure, climate, and traffic level used in the example, initial results indicated that specimen type will result in different levels of pavement distresses as generated by the predictive models in the MEPDG software. Thus, it may be possible that similar differences in predicted distress could be found in the NCHRP Report 704 PRS software tool, Quality-Related Specification Software (QRSS), and the beta-version SPT Program from NCHRP Project 9-22A (2011).This assumption is based on the fact that the rutting and fatigue cracking predictive models in the QRSS software and SPT Program are based on the same analysis procedures used in the MEPDG software.

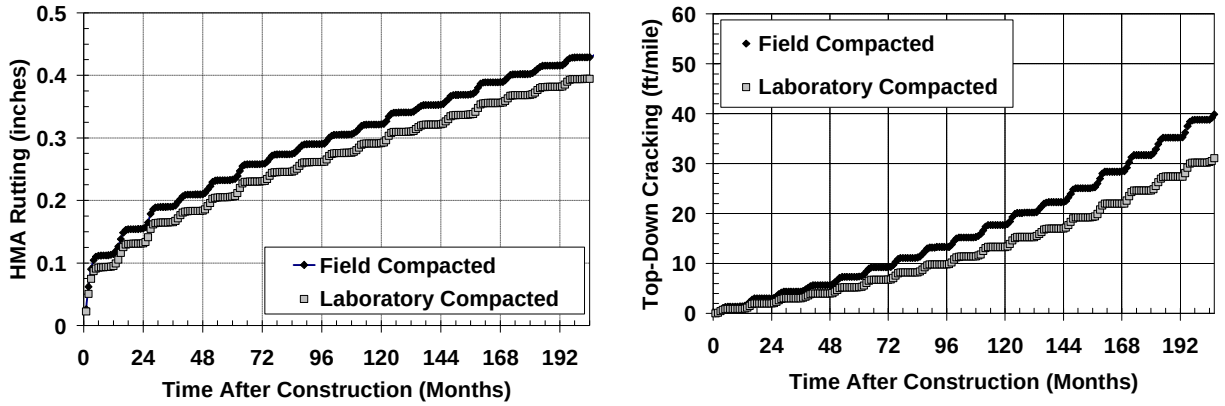

(a) **(b)**

Plant-Mixed/Laboratory-Compacted Plant-Mixed/Field-Compacted

Figure 3.Influence of Plant-Mixed Compaction Method on Predicted Distresses from the AASHTO MEPDG Software [data from Bennert et al., 2008].

The results shown in Figure 3 raise some interesting questions:

- If a DOT would like to utilize the MEPDG or NCHRP 9-22 PRS software tools in their pavement design or QC analysis, how much does specimen type influence the HMA rutting and fatigue cracking predictions; and
- Are these differences acceptable when compared with DOT criteria?

As can be seen in Figure 3, for the pavement structure, climate, and traffic conditions selected, a prediction of 0.3 inches in total HMA rutting and 10 ft/mile in top-down cracking were found, simply by changing the specimen type used during testing (i.e., plant-mixed/field-compacted and plant-mixed/laboratory-compacted with loose mix sampled during production).

1.1.2 Research Objectives

The Mechanistic-Empirical Pavement Design Guide (MEPDG) and the NCHRP Project 9-22 Quality-Related Specification(QRSS) analytical software require the user to input the dynamic

modulus (|E*|) of the hot mix asphalt (HMA) mixture in order to utilize the rutting and fatigue cracking distress prediction equations of the hot mix asphalt pavement section. However, there are various methods and sample types available for the determination of |E*| of the HMA. The primary objective of this research project was to evaluate the effects of testing different sample types/configurations on the distress predictions resulting from the MEPDG, QRSS, and SPT Program tools.

1.2 Scope of Study

The research was conducted in a four-phase approach, starting with asphalt binder and mixture procurement and collection of quality control data during plant production. State transportation agencies in the northeastern United States were contacted to participate in the study by providing QC information that includes volumetric and gradation properties of the asphalt mixture, asphalt binder sampled during production, loose mix sampled during production and prior to leaving the asphalt plant, gyratory specimens produced during production at the asphalt plant's Quality Control laboratory, preferably at air void levels representing the density of the field cores, and field cores (six inches in diameter) extracted after production and preferably within 1 week after placement.

Laboratory evaluation of the different asphalt mixture specimen types was conducted by testing volumetric properties, asphalt binder properties, and dynamic modulus values. Each of the asphalt binders collected during the study was tested for performance grade in accordance with AASHTO R29, *Grading or Verifying the Performance Grade (PG) of an Asphalt Binder*, as well as determining the shear modulus (G*) and phase angle (δ) at various temperatures and loading frequencies (commonly referred to as master curve testing). By testing the asphalt

binders with these two tests, input parameters for the asphalt binder were produced for use in the MEPDG Level 1, Level 2, and Level 3 analyses. The dynamic modulus of the asphalt mixtures was tested for the following specimen types:

- Plant-Produced/Field-Compacted (PP/FC) – six inch diameter field cores tested using the IDT |E*| test procedure proposed by Kim et al., (2004);
- Plant-Produced/QC Lab Compacted (PP/QLC) – gyratory specimens produced during production at the asphalt plant's contractor Quality Control lab;
- Plant-Produced/Laboratory-Compacted (PP/LC) – gyratory specimens were compacted at the research laboratory using loose mix collected during production. The loose mix was reheated to compaction temperature, for no longer than 4 hours, and compacted into gyratory specimens of similar air voids as to the collected field cores.

Although both the PP/QLC and PP/LC configurations appear to be identical, the reheating of the loose asphalt mixture may increase the age hardening of the asphalt binder and could thereby result in higher dynamic modulus values. If this condition exists, DOTs interested in using the MEPDG and NCHRP Project 9-22 PRS programs may need to determine the magnitude of the increased stiffness and how it affects the pavement performance predicted.

Coordination with FHWA was done to obtain pavement structural and materials information and data from state projects with similar characteristics to those included in this study. This data was used in MEPDG simulations as additional inputs for pavement performance predictions.

Once the laboratory evaluation was complete, the data was used to conduct pavement performance analyses in the MEPDG and NCHRP Project 9-22 PRS programs (the QRSS and NCHRP Project 9-22A SPT Program).For each of the three pavement structures, the MEPDG and NCHRP Project 9-22 PRS analyses were conducted using laboratory and volumetric data for

the three different specimen types. Both the rutting in the surface and binder lifts and fatigue cracking distresses were evaluated for each of the specimen configurations. Along with the MEPDG Level 1 analysis using measured dynamic modulus and binder properties, the Level 2 and Level 3 material inputs were also analyzed. Not only were the performance predictions compared based on the specimen type, but also comparisons were made among the analysis tools. The results of the QRSS analysis were compared to the MEPDG Level 2 distress predictions since both are based on volumetric properties and binder inputs for HMA. The results of the NCHRP Project 9-22A SPT Program analysis were compared to the MEPDG Level 1 distress predictions since both are based on dynamic modulus inputs for HMA. Finally, a limited sensitivity analysis was conducted using the MEPDG software to test the impacts of different traffic levels and structural profiles on distress predictions.

CHAPTER 2

RESEARCH APPROACH

An overview of the research approach for this project is included in Figure 4. It should be noted that each of the three analysis programs (QRSS, NCHRP 9-22A SPT Program, and MEPDG) calculate the pavement temperatures differently. All three programs calculate the average values for the as designed mix analysis across all production lots used for input. However the as-built mix analysis portion of the SPT QA and QRSS analyze the materials on a lot by lot basis compared to the MEPDG which utilizes average values for both the as designed and as built mix analysis. |E*| is a function of frequency and temperature. The frequency is a minor issue since speed is used to simulate the frequency at different depths in the pavement layers. This approach is consistent between MEPDG and QRSS mix design only (which does not include a Pay Factor analysis). Rather, it is the temperature is represented differently in that the MEPDG generates five monthly temperatures, while the QRSS and SPT Program use a calculated effective temperature. Due to these reasons, the comparison between programs was done by focusing on the variation in total distress values at the end of each pavement's life.

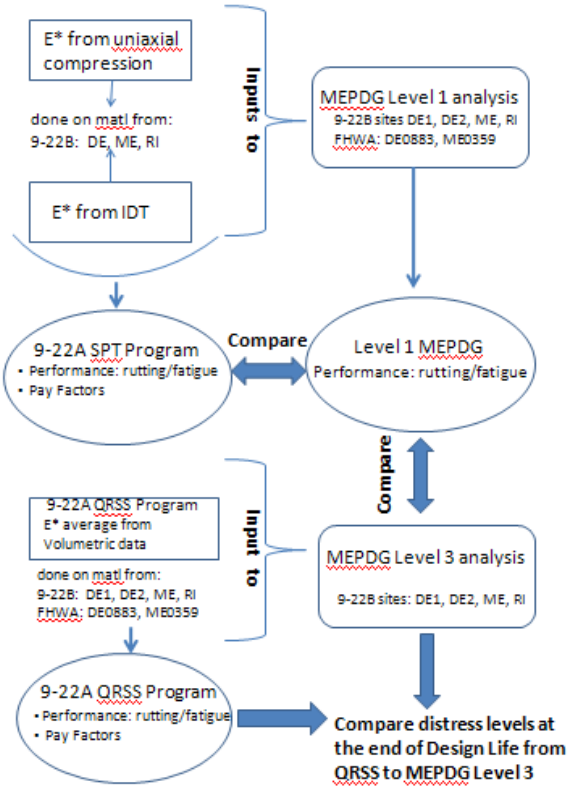

Figure 4. Flowchart of Research Approach to NCHRP 9-22B Project.

2.1 Project Identification and Material Procurement

2.1.1 Identification of Candidate Projects

A questionnaire was developed and distributed to 12 state transportation agencies (DOTs) in the northeastern United States to solicit candidate projects. Fifty percent of the agencies responded and Table 1 presents the results of the questionnaire and identification of the three participating DOTs: Delaware (DelDOT), Maine (Maine DOT), and Rhode Island (RI DOT).

Table 1. Participating Transportation Agencies (DOTs).

State	2011 Paving Season		
	Response	Available project?	Expected month/date for paving?
CT			
DE	X	Y	June
ME	X	Y	September
MD	X	N	N/A
MA			
NH	X	N	N/A
NJ	X	Y	Unknown
NY			
OH			
PA			
RI	X	Y	August
VT			

After the candidate projects were identified, data and material requirements plan was developed and distributed to the three participating DOTs as part of the project kickoff meetings. The purpose of the plan was to provide general direction to the participating states as to the information and materials necessary for the NCHRP Project 9-22B research team to complete the study.

To help in the analysis of pavement performance, information about the general pavement structure, traffic characteristics, and quality assurance techniques for each DOT project was collected. Information that was gathered for each pavement section included:

- Layer (bound and unbound) thicknesses,
- Asphalt mixture type/designation (if present on project),
- Soil/aggregate classification for unbound materials (AASHTO equivalent designation),
- Average annual daily traffic (AADT),
- Percent trucks (heavy and light),

- Equivalent Single Axle Loads (ESALs),
- State Specific Growth Factors, and
- Directional Distribution Factor (if available).

The state-approved asphalt mixture design and the quality control (QC) data generated during production was collected and used in the Performance Related Specifications (PRS) software tools to establish a baseline performance level of the pavement structure using the models developed for the MEPDG software. The quality control data are inputs required by the QRSS and SPT Program evaluation tools to determine the relative pavement performance changes (positive or negative) due to variations in mixture components during production (NCHRP Report 704, 2011). This resulted in the calculation of pay factors (incentive or disincentive) for the project.

Information that was gathered for each mixture design and QC data included:

- Aggregate blend gradation from the following sieves: ¾-inch, 3/8-inch, No. 4, and No. 200,
- Asphalt binder content,
- Asphalt binder grade,
- Maximum specific gravity, and
- Bulk specific gravity of the aggregate blend.

2.1.2 Material Procurement

One of the most important components of the study was the evaluation of the asphalt mixture materials themselves. Therefore, the breakdown of material needs was based on minimum materials provision requirements (Table 2) and optimal materials provisions requirements (Table 3). For material requirements, asphalt binder, field cores, loose mix and gyratory samples compacted at the plant's QC laboratory were requested.

Table 2. Minimum Materials Collection from Candidate Projects.

Material	Quantity	Notes
Asphalt binder	One 1-gallon can	Sampled during actual project production
Loose mix	Two 5-gallon buckets	Sampled during actual project production
Field cores	Three (3) full depth cores	Sampled from project limits
		Rutgers University will trim samples
Plant-compacted gyratory samples	Three 170-mm tall samples Compacted to air void levels of 6.5 to 7.5%	Loose mix sampled during time of project production
		Mix compacted as soon as possible after sampling

Table 3. Optimal Materials Collection from Candidate Projects.

Material	Quantity	Frequency	Notes
Asphalt binder	One 1-gallon can	Beginning, middle, and end of production	Total of 3 1-gallon containers
Loose mix	One 5-gallon bucket	Each lot or per day's production	Assumes minimum of 2 lots or 2 day's production
Field cores	Two (2) full depth cores	Each lot or per day's production	Assumes minimum of 2 lots or 2 day's production
			Rutgers University will trim samples
Plant-compacted gyratory samples	Two170-mm tall samples Compacted to air void levels of 6.5 to 7.5%	Each lot or per day's production	Assumes minimum of 2 lots or 2 day's production
			Loose mix sampled during time of project production
			Mix compacted as soon as possible after sampling

There were four paving mixtures analyzed as part of the research study: one from ME DOT, two from DelDOT, and one from RI DOT. It was determined that an assortment of conventional dense-graded asphalt mixtures and modified mixtures should be included. The inclusion of conventional mixtures was done to ensure that the Witczak predictive equation (WPE) model. The WPE model was the default method for determining |E*| in the PRS software and has been reported to give good estimates of |E*| for unmodified mixtures; it can perform as designed on

half of the candidate projects (Dongre et al, 2005).Information on the case study projects is summarized in Table 4. Maine DOT provided the optimal materials collection and provided material samples from the asphalt base, binder, and surface layers. In all of the other candidate projects, the materials were sampled from the paving structure's surface lift.

Table 4.Candidate Project Mixture Information.

State	Project ID	Mixture Type	Binder Type	Additive Type	Loose Mix Lots	Mix Sampling Location	Plant Compacted Samples	Field Compacted Samples	Liquid Binder Samples
DE	DE US-13 WMA	WMA SMA	PG 70-22	10% RAP	5	Truck at plant	--	16	1
	DE US-13 C/160	Hi-RAP HMA	PG 64-28	35% RAP	2	Truck at plant	--	8	1
	FHWA DE0883	SMA	PG 58–22	30% RAP	N/A	N/A	--	--	X (data sent)
ME	Township D	DGA	PG 64-28	15% RAP	5	Hopper	8	7	1
	FHWA ME0359	HMA	PG 64-28	30% RAP	N/A	N/A	N/A	N/A	X (data sent)
RI	Dunn's Corner	DGA	PG 64-28	None	2	Truck at plant	--	--	1

2.1.3 Details on Candidate Project Pavement Sections

2.1.3.1 Delaware

In Delaware, the two-lane route US-13 was represented as a 2-inchflexible overlay over existing pavement of unknown cross-section. For purposes of the research analysis, one section of roadway was modeled as overlaid with a 12.5mm PG70-22 Warm Mix (WMA) Stone Matrix Asphalt (SMA) with up to 10% Reclaimed Asphalt Pavement (RAP)and another section of US-13 was overlaid with a 9.5mm PG64-28HMA with a RAP portion of up to 35% (designated as HMA Hi-RAP). Because both of the US-13 projects were overlays, there was very little job mix formula (JMF) or pre-existing material data available. An approach was taken to approximate this information by utilizing data from previous QRSS and MEPDG software analyses from the NCHRP Project 9-22A to fill in the gaps in the JMF and QA material information for the sub-

surface lifts and by replacing the pavement profiles with the ones specific to the current candidate projects. The data from a pavement section of Rhode Island DOT's State Route 102, a candidate project used in the NCHRP Project 9-22A, was used for providing JMF material data. It was replaced in the pavement profile data with the project-specific values such as layer thickness from DE US-13where available in order to run the QRSS analysis. This approach was taken for all of the other candidate projects, with the exception of that of Maine DOT which was a fully reconstructed section. Table 5presents a summary of the sources of material data for each of the six projects.

Table 5. QRSS Input Material Data Source Summary.

Project	Overlay?	Material Properties Source			
		Surface Lift	Binder Lift	Base Lift	Subgrade
DelDOTUS-13 WMA SMA	Yes	Del DOT	RI Rt 102	RI Rt 102	RI Rt 102
DelDOTUS-13 HMA Hi-RAP	Yes	Del DOT	RI Rt 102	RI Rt 102	RI Rt 102
FHWA DE0883 HMA	No	FHWA	RI Rt 102	RI Rt 102	RI Rt 102
MEDOT Township D HMA+RAP	No	ME DOT	ME DOT	ME DOT	ME DOT
FHWA ME0359 HMA	Yes	FHWA	RI Rt 102	RI Rt 102	RI Rt 102
RIDOT Dunn's Corner HMA	Yes	RI DOT	RI Rt 102	RI Rt 102	RI Rt 102

This "default" pavement material data was required to utilize the QRSS program. Currently, the QRSS can only be used in new construction/reconstruction pavement projects. The current form of the QRSS is not capable of handling typical rehabilitation projects, generally classified as "mill and fill" type projects. The QRSS requires all the material properties of the binder, base, subbase (if applicable), and subgrade. The full pavement profiles were available for five of the seven candidate projects and only details on the pre-existing US-13 roadway profile were unavailable. As a result, analyses on the DelDOT projects utilized the same pavement cross section as RI Route 102 (shown in Figure 5) from the NCHRP 9-22A project.

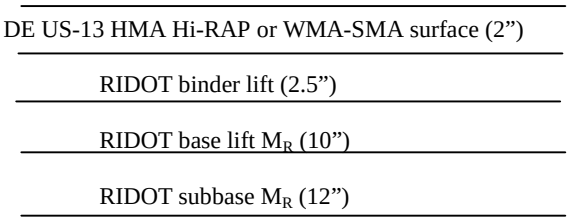

Figure 5. DelDOT US-13 Pavement Cross-Section Analyzed.

2.1.3.2 Maine

The candidate pavement from Maine DOT was a two-lane section of Rumford Road in Township D (Franklin County, Maine). The surface was a fine-graded HMA with up to 15% RAP full depth construction project over existing pavement. The pavement cross-section is presented in Figure 6.

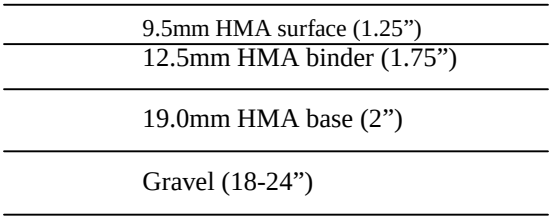

Figure 6. Maine DOT Township D Pavement Cross-Section.

2.1.3.3 Rhode Island

The candidate project from Rhode Island DOT was a two-lane section of Dunn's Corner Road (Westerly, RI) and was a full depth construction project consisting of a 1.5-inch thick 12.5mm HMA surface lift over a 2.5-inch 19.0mm HMA binder lift, placed over a base course of reclaimed asphalt pavement and gravel base. Due to compaction issues with the 12.5mm surface lift, the contractor overlaid the previously described pavement cross section with an additional

1.5-inch thick 9.5mm HMA lift. Unlike the other projects, there was no RAP allowed in the HMA mix design per RIDOT specs for this project.

2.2 Laboratory Evaluation of Collected Materials

2.2.1 Specimen Preparation

As previously described, different specimen types were researched as part of this project. Loose mix, received from the three participating DOTs, was reheated to the estimated field compaction temperature for each particular lot and then compacted into five or six tall gyratory specimens. Dynamic modulus test specimens were prepared in accordance with AASHTO PP60-09, Preparation of Cylindrical Performance Test Specimens Using the Superpave Gyratory Compactor (SGC).These specimens were cored using a standard coring drill and saw-cut by hand to the following dimensions to create four different specimen types:

- Laboratory-Compacted Uniaxial Compression Gyratory Specimens: three tall specimens per lot fabricated to 150mm tall (three specimens total per lot);
- Laboratory-Compacted Indirect Tension (IDT) Gyratory Specimens: two tall specimens per lot cut to 150mm diameter and 50mm height (four specimens total per lot);
- Plant-Compacted (Uniaxial Compression) Gyratory Specimens: These samples were compacted in the contractor quality control laboratory at the asphalt plant. For this project, the only specimens of this type were provided by Maine DOT from the Township D HMA project;
- Field-Compacted IDT Specimens from Field Cores: Field cores delivered by the DOTs produced according to the IDT method [Kim et al, 2004].

Specimens were compacted to match the average air voids from the field core samples taken from each lot of the respective projects. Three specimens from each lot were cored and cut to make three 150mm tall gyratory samples, and two others were cut into four 50mm tall IDT samples, leaving one extra specimen. A summary of the gyratory specimen laboratory data for the DelDOT mixtures is shown in Table 6.

Table 6. DelDOT Gyratory Specimen Laboratory Compaction Data.

Mixture Information	WMA-SMA					HMA Hi-RAP	
Lot #	Lot #1**	Lot #2	Lot #3	Lot #4	Lot #5	Lot #1	Lot #2
Date	6/13/11	6/22/11	7/11/11	7/20/11	8/4/11	6/7/11	7/7/11
Asphalt PG	76-22					64-28 equivalent	
Mix Temp on Truck (°F)	280	270	285	280	295	290	315
Gmm	2.635	2.63	2.624	2.629	2.628	2.516	2.51
Gsb	2.904	2.89	2.897	2.891	2.89	2.703	2.695
AC Content	6.2	6.2	6.3	6.3	6.3	5.5	5.5
Measured AC Content	6.41	6.21	6.53	6.36	6.29	5.68	5.67
Average Target Air Voids	6.1**	6.4	5.6	6.4	6.3	11.2	9.6

** cores lost by DOT; assumed value

After completion of testing a full lot of three tall specimens (and four specimens for IDT), dynamic modulus master curves were created for each lot utilizing an Excel-based worksheet created by Rutgers University.

2.2.2 Summary of Binder Testing

Binder testing was conducted on liquid samples from all four of the candidate projects, including the two from DelDOT (modified PG76-22 and modified PG64-28), one from Maine DOT (modified PG64-28), and one from RIDOT (unmodified PG64-28). Table 7summarizes the binder A and VTS experimental values determined from binder testing. This data was used as direct inputs for the QRSS and SPT Program, as well as Level 1 and 2 inputs to the MEPDG

software. Additionally the G* master curve of the asphalt binder was measured for the Hirsch Model for use by the MEPDG Level 1 analysis.

Table 7.Summary of Key Binder Input Values.

Binder Type	A	VTS
DelDOTPG76-22 (SMA)	9.333	-3.079
DelDOT PG64-28 (HMA)	11.237	-3.764
MEDOT PG64-28	9.664	-3.224
RIDOT PG64-28	9.823	-3.276

2.3 Summary of Dynamic Modulus Master Curve Analysis

2.3.1 Dynamic Modulus Testing Approach

Specimens were tested in the asphalt mixture performance tester (AMPT) using a version of the reduced testing method developed in *Practical Procedure for Developing Dynamic Modulus Master Curves for Pavement Structural Design* [Bonaquist and Christensen (2005)]. Using the NCHRP 1-37A/AASHTO TP62-03 protocol as a baseline, Bonaquist and Christensen (2005) proposed a modification to replace the extreme temperature data sets with predicted data based on the limiting maximum modulus $|^*|_{max}$ from binder stiffness and volumetric data. The theoretical basis for this modification was that asphalt binders reach approximately the same dynamic modulus at very low temperatures, commonly called the “glassy modulus” [Bonaquist and Christensen (2005)].

Table 8. Dynamic Modulus Testing Protocol Comparison.

Test Parameter	AASHTO T 342	NCHRP 9-22B Reduced Test Protocol
Temperature (°C)	-10, 4.4, 21.1, 37.8, 54.4	4, 20, 35
Frequency (Hz)	25, 10, 5, 1, 0.5, 0.1	25, 10, 5, 1,0.5, 0.1 (0.01 at 35°Cin Uniaxial Compression only)

While the standard test method developed for AASHTO T 342 requires testing at five standard temperatures, the reduced method requires only three test temperatures. As a result, a full sweep for two lots of uniaxial samples can typically be completed in two days based on six tall specimens over approximately 12 hours. Likewise, a full sweep of one lot of IDT samples based on four specimens can be completed in two days. This procedure resulted in better precision as the greatest variability in |E*| testing was found to be at the lowest and highest test temperatures recommended in AASHTO T 342 [Bennett and Williams(2009)].

2.3.1.1 Estimation of Variance

Log plots comparing the experimental |E*| results at each of the three test temperatures were created to determine the source of the variation of the average data within the mixes and are included in Appendix A. Since there are only two lots of experimental HMA Hi-RAP samples, the data was plotted with standard deviation ranges. Figure 7 shows that the data points are shifted by more than one standard deviation between the two lots. Data at 4°C and 35°C are included in Appendix A. This agrees with COV% calculations which displayed a high level of precision for the Lot #2 HMA Hi-RAP specimens (COV% of 3.1) while displaying slightly above the acceptable COV% level of 13.1% for Lot #1. All of the 4°C and 20°C sweeps displayed COV% less than 11.5%, which is considered acceptable. This finding indicated that both lots showed high correlation within the lots, but not between each other. One reason for

this could be the disparity between air voids for these two lots. It is also possibly due to the amount of RAP used in the mixture. Higher RAP percentages lead to higher dynamic modulus results and the test data could have been a caused by this fact. The air void level of Lot#1 was 10.8% and is high for typical compaction of Superpave mixes, which may account for the lower stiffness than the Lot #2 which had an air void level of 8.8%.

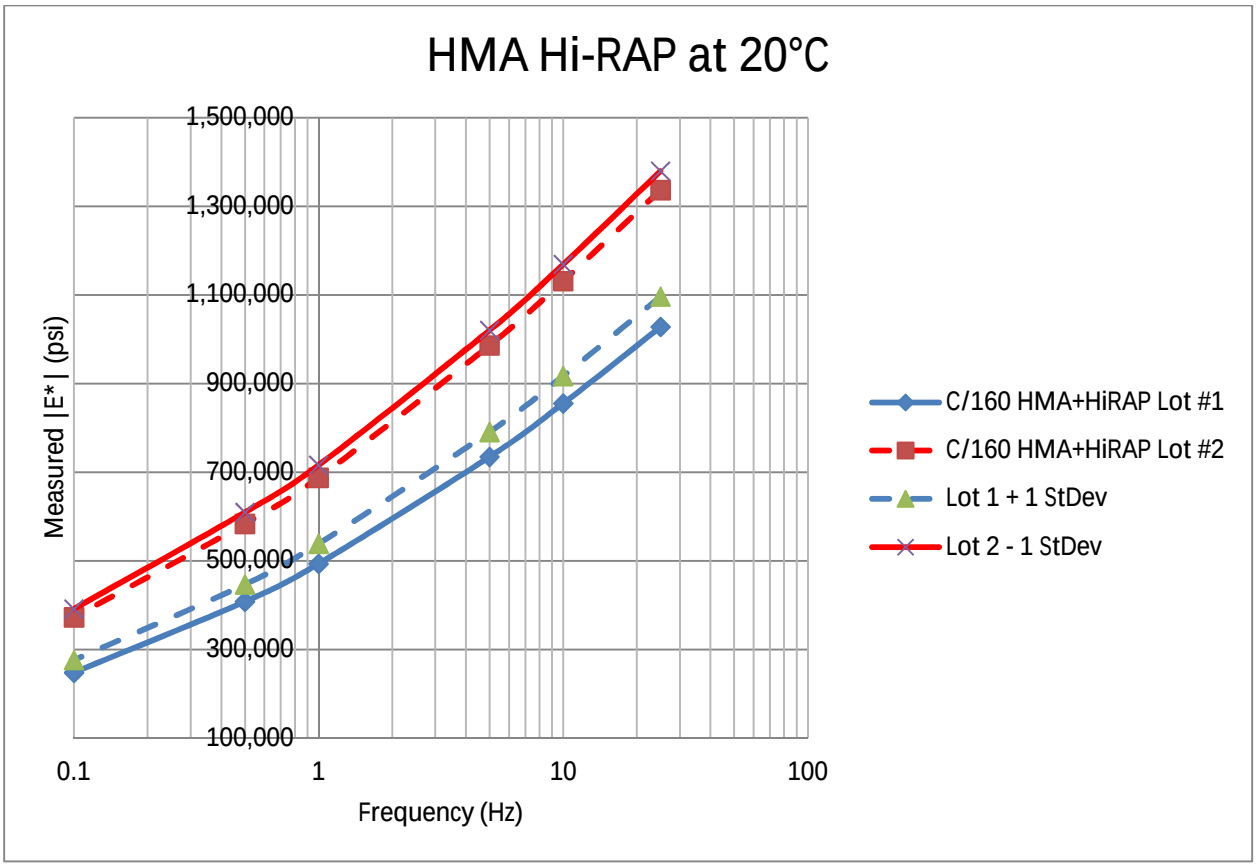

Figure 7. Laboratory-Compacted HMA Hi-RAP |E*| Plotted with Log Frequency.

Log plots of the |E*| results from the WMA-SMA specimens showed relatively low variation between Lots #1 through 4, with the Lot #5 |E*| results measuring significantly lower than the average results from the other four lots, as shown in Figure 8. Data at 4°C and 20°C are included in Appendix A.

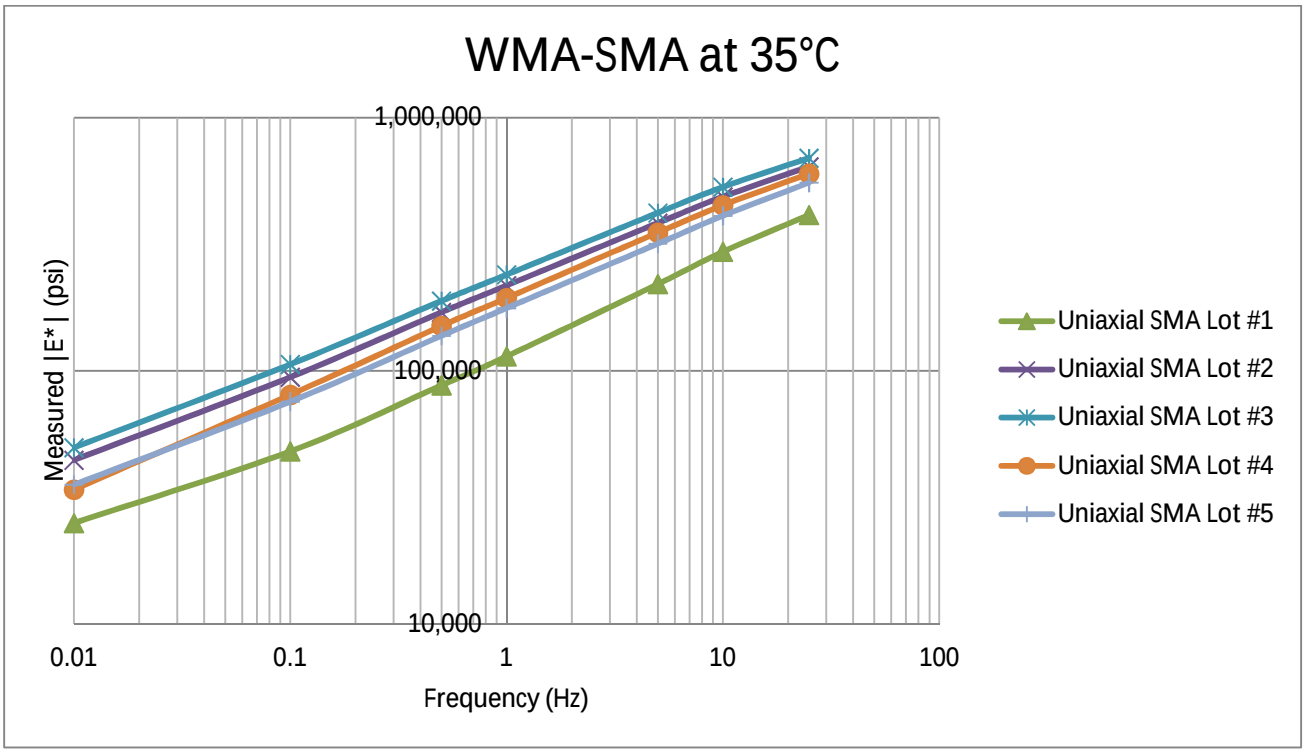

Figure 8. Laboratory-Compacted WMA-SMA Experimental |E*| Results vs. Log Frequency.

One reason for the variation between the WMA-SMA Lot #1 and the other four lots is most likely from the material property differences between them, particularly the percent voids in the mix. Mixture air voids in Lot #1 was only 2.5%, as compared to between 3 to 5% for the other four WMA-SMA lots (Appendix A). Mixture production temperatures of the WMA-SMA were compared to assess the possibility of production temperature variability. The assumption being that lower production temperatures would cause lower levels of oxidative aging in the asphalt binder, thereby resulting in "softer" asphalt mixtures. Lots #2 and #5 had truck mix temperatures of 270°F and 295°F respectively, as compared to 280°F for Lot #1. Figure 8 clearly shows that both Lots #2 and #5 resulted in experimental stiffness values greater than Lot #1.

Bennert and Williams [2009] recommended that the allowable microstrain range should be limited to 75 to 125microstrainssince laboratory data measured at these levels resulted in high precision. A check of the microstrain ranges for all specimens tested as part of this project showed a range from 85 to 115microstrains, which is within the allowable limits for high precision results.

The master curve graphs included in Appendix A show that the uniaxial compression testing typically yielded high correlation between the experimental results and the predictive results. A comparison between the Hirsch Model and Witczak Predictive Equation (WPE), and the experimental |E*| data collected in the AMPT, showed that the predictive models appear to over predict the |E*| of a pavement sample at the highest temperatures and under predict the |E*| values at lower temperatures.

A comparison between the two predictive models in Figure 9 and Table 9 indicates that the Hirsch model appears to be a more accurate predictor of the experimental |E*| results for a given sample. At the 4°C test temperature, error between the Hirsch Model and experimental values was below 25% for all frequencies in six out of seven lots. For all test temperatures, the Hirsch Model typically displayed error under 50% at all frequencies, as compared to up to 70% error between predicted and experimental |E*| using the WPE. However, the Witczak Prediction Equation showed a tendency of being more accurate at the highest test temperature, particularly in the WMA-SMA Lots #2 and 3. This may be explained by the Hirsch Model using a typical limiting modulus of around 30,000 psi. As a result, when the measured modulus is significantly lower than this value, the Hirsch model may become less accurate.

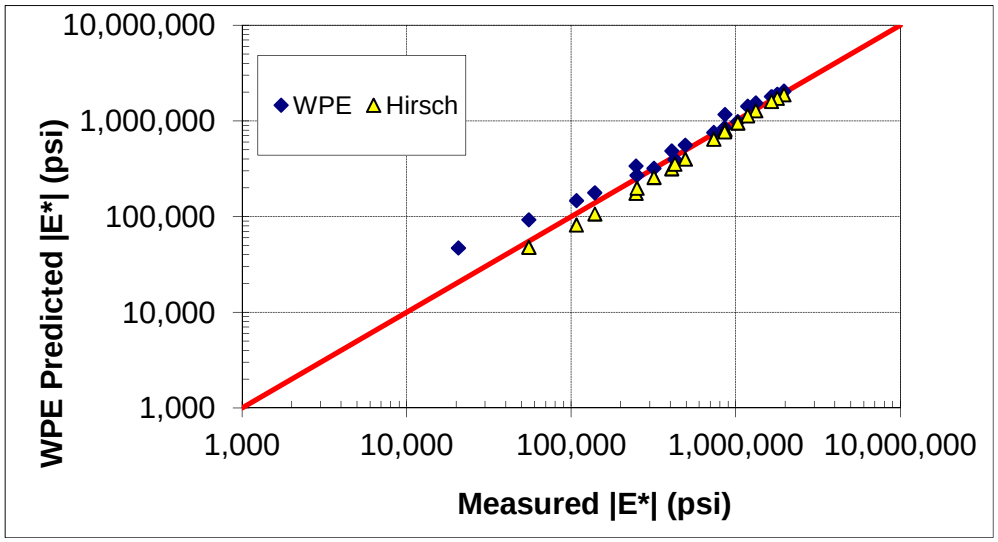

Figure 9. Comparison of WPE and Hirsch Model |E*| Results (Based on HMA Hi-RAP Lot #1, Uniaxial Compression).

Table 9. Summary of WPE |E*| and Hirsch Model |E*| Results (Based on HMA Hi-RAP Lot #1, Uniaxial Compression).

Temp (°F)	Measured |E*| (psi)	WPE Predicted |E*|		Hirsch Model	
		|E*| (psi)	% Error	|E*| (psi)	% Error
39	1,960,571	2,046,961	-4.2204	1,883,719	3.919875
	1,786,284	1,907,393	-6.34942	1,729,257	3.192514
	1,646,420	1,798,740	-8.46815	1,602,216	2.684846
	1,322,841	1,539,921	-14.0969	1,281,204	3.14748
	1,178,963	1,427,370	-17.4031	1,136,981	3.56092
	858,623	1,169,448	-26.5788	810,131	5.647678
68	1,027,834	986,083	4.23404	954,217	7.162336
	855,046	853,258	0.209544	773,390	9.549797
	734,471	758,436	-3.15984	646,711	11.94877
	493,225	560,663	-12.0283	399,935	18.91423
	407,798	486,149	-16.1167	316,758	22.32473
	247,434	339,245	-27.0632	175,587	29.03681
95	426,217	395,969	7.638962	354,461	16.83572
	318,116	319,977	-0.5816	257,182	19.15466
	250,915	270,127	-7.1123	198,973	20.70107
	139,023	177,809	-21.8129	106,882	23.11919
	107,429	147,086	-26.9614	82,013	23.65893
	55,206	93,022	-40.6524	47,863	13.30144
	20,629	47,014	-56.1208		

2.3.2 Summary of Dynamic Modulus Test Results

Dynamic modulus test results and the results of the VTS-shift |E*| master curve analysis for all projects are presented in Appendix A. The information in Appendix A is formatted to be a summary of the average |E*| data values organized by project and lot number. The IDT testing follows the method developed in *Dynamic Modulus Testing of Asphalt Concrete in Indirect Tension Mode* [Kim et al. (2004)], but utilizes the same frequency and temperature test protocol as the uniaxial compression testing for comparison purposes. The IDT samples were not tested at 0.01 Hz. The practical benefit of the IDT test is that it requires core samples that are of a size (1.5 to two inches) that can be easily extracted from a field pavement section. The Indirect Tension Method creates a biaxial state of stress in the core sample by applying the principles of the Poisson's ratio and Hooke's Law for relating biaxial stress and strain. Figure 10 provides a view of the test apparatus used to conduct experiments as part of this research project.

Figure 10. IDT Test Apparatus for Measuring Dynamic Modulus (courtesy of Rutgers University).

Four IDT samples were created for testing from two tall gyratory specimens. Each of the four specimens were tested and included in the master curve construction. The original master curve file created for uniaxial testing with three specimens was adjusted to include the average of all four IDT specimens. The results of the master curve analysis were plotted within each lot according to each sample and test type. From the master curve program, the VTS-shift |E*|curve was plotted for each of the four projects over all lots and for all three sample types. Generally, the |E*| master curves by uniaxial compression (UC) testing as opposed to indirect tension (IDT) testing were very similar for all mixtures. This finding corresponded with previous research conducted by Kim et al. (2004) who concluded the uniaxial compression and IDT testing modes produced equivalent results when testing equivalent samples.

2.3.2.1 WMA-SMA Mixture

Five lots of the WMA-SMA were tested as part of the research study. As previously shown in Table 10, there were no field core samples for the WMA-SMA Lot #1 and therefore only the two laboratory-compacted sample types were tested: in uniaxial compression (UC) and in IDT. Figures 14 through 18present the lot-by-lot master curve results for the WMA-SMA mixture.

The WMA-SMA Lot #2 did not have enough material to produce both laboratory-compacted (LC) uniaxial compression samples (UC/LC) and IDT samples (LC/IDT); therefore, only the UC/LC samples were compared to the field core samples (FC/IDT). In contrast to Lot #1 where equivalent samples were tested using the two different methods, Lots #2 and #5 show the disparity in dynamic modulus results between laboratory-compacted samples and field cores (Figures15 and 18). Typically, additional age hardening is induced in the binder when loose mix materials from the plant are compacted at some later point in the laboratory, due to the reheating

that the binder must undergo to produce gyratory samples. Peterson et al. (2004) reported that this can result in age-hardened LC samples which display values up to twice the stiffness of the field core samples that have not undergone additional age-hardening in the laboratory.

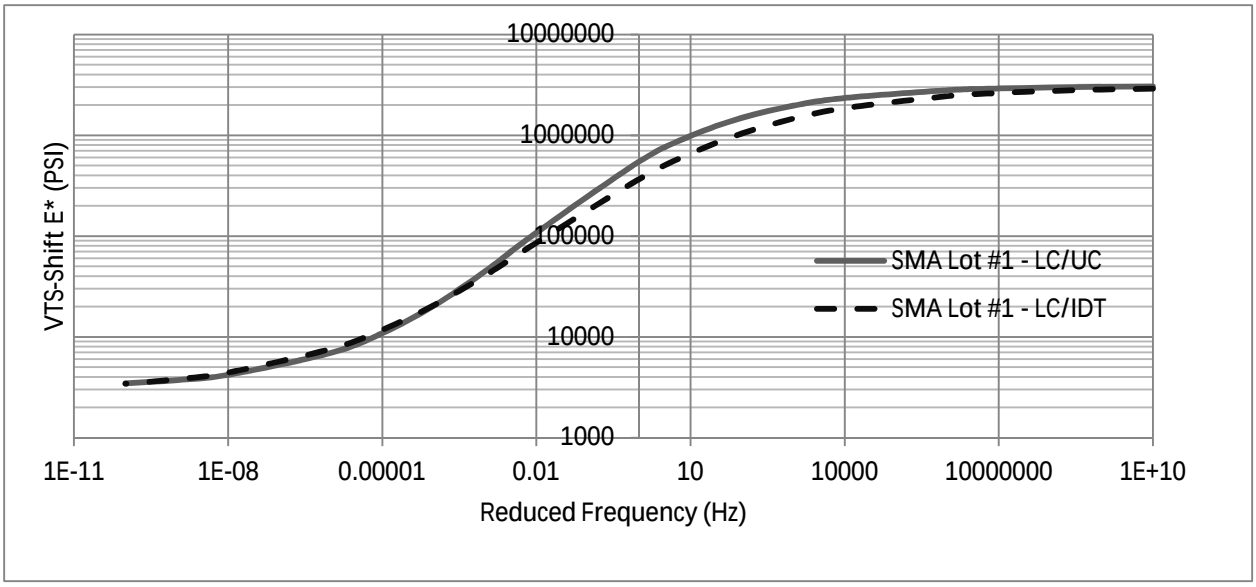

Figure 11. VTS-Shift Dynamic Modulus Master Curve, WMA-SMA Lot #1.

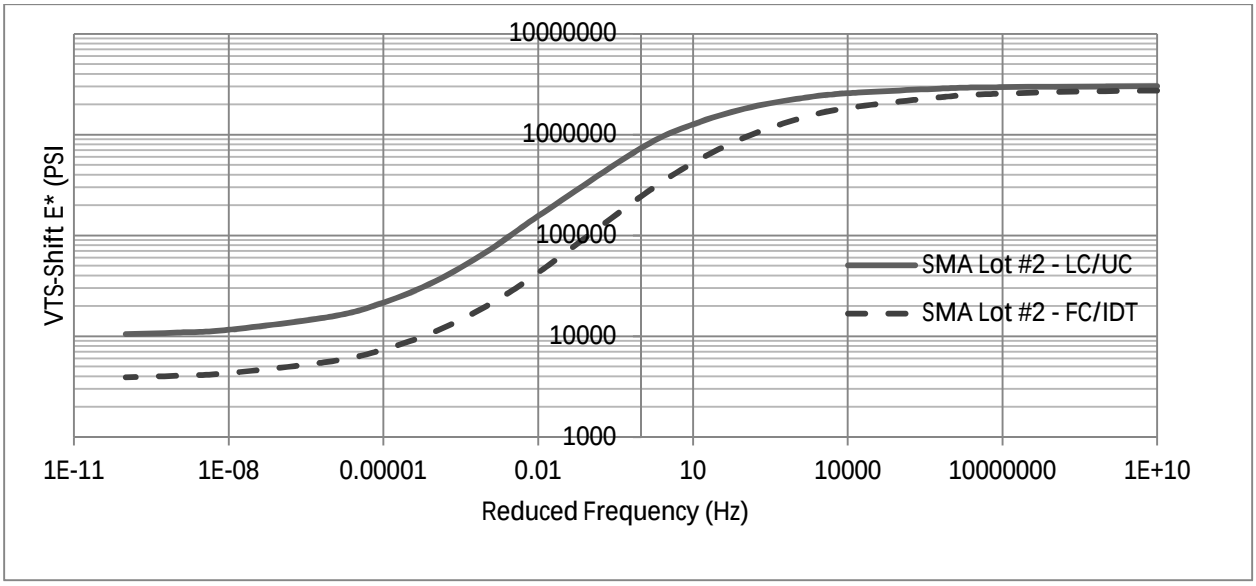

Figure 12. VTS-Shift Dynamic Modulus Master Curve, WMA-SMA Lot #2.

Consistent with the data displayed in Lots #1 and #2, SMA Lots #3 and #4 (Figures 16 and 17) also displayed high correlation between the results of the tests run on LC samples, as well as showing the LC samples to produce higher stiffness results than the field core samples.

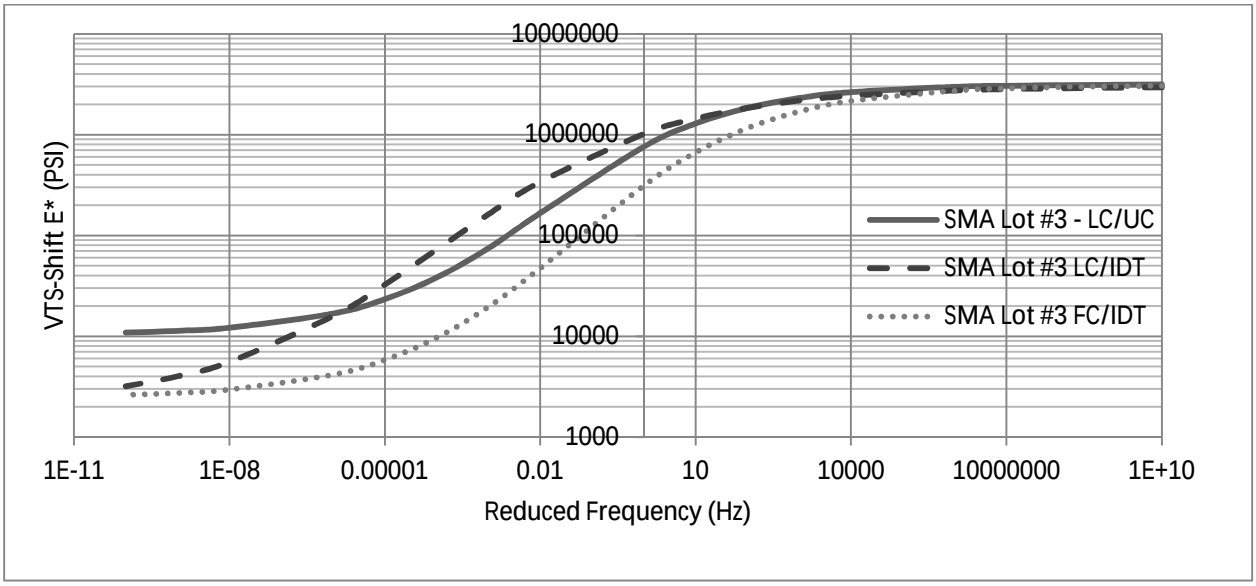

Figure 13. VTS-Shift Dynamic Modulus Master Curve, WMA-SMA Lot #3.

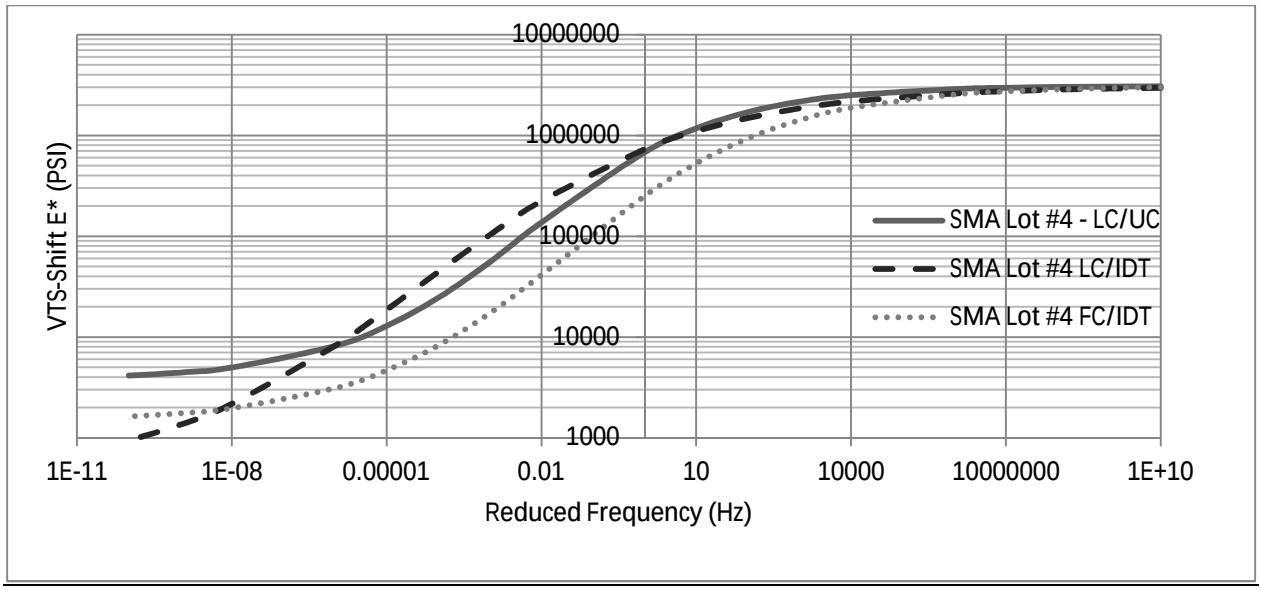

Figure 14. VTS-Shift Dynamic Modulus Master Curve, WMA-SMA Lot #4.

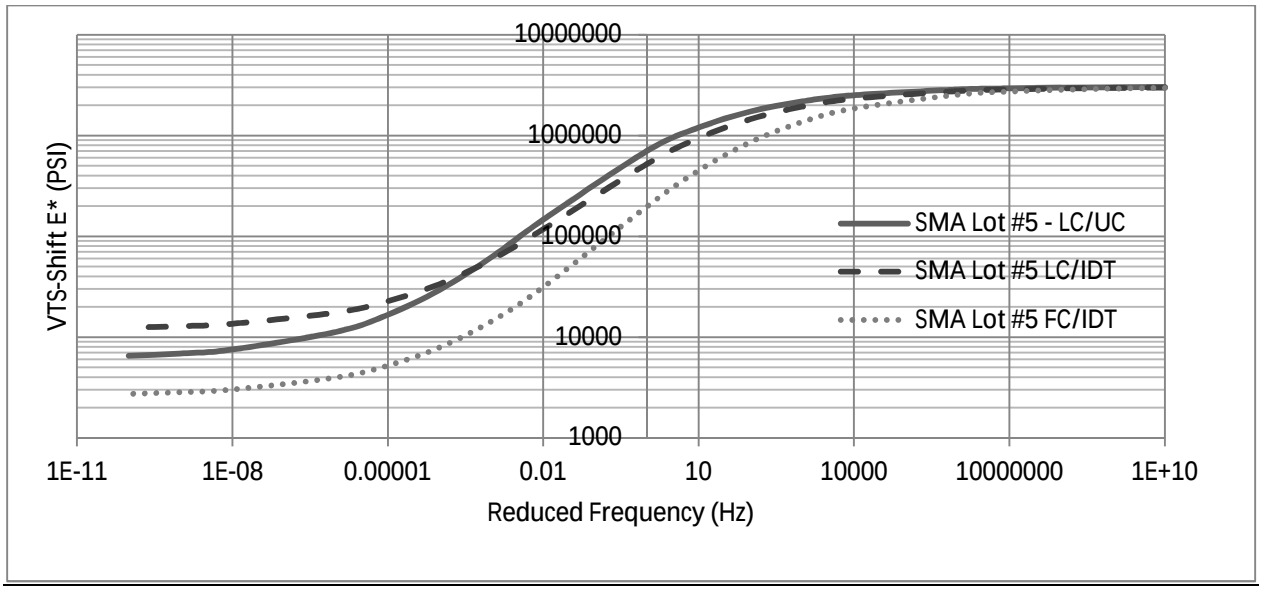

Figure 15. VTS-Shift Dynamic Modulus Master Curve, WMA-SMA Lot #5.

2.3.2.2 HMA High-RAP Mixture

The master curve data for the HMA mixture produced with 35% RAP (referred to as HMA Hi-RAP) mixture is plotted by lot in Figure 16 and Figure 17. Figure 16 illustrates that at the high and middle reduced frequency values, corresponding to the 4°C and 20°C dynamic modulus test series, the data trend is equivalent to as was observed in the WMA-SMA mixture. However, in this case, both the laboratory-compacted and field core IDT samples displayed significantly stiffer dynamic modulus values at the low reduced frequency (very high temperature) level as compared to the uniaxial compression sample.

This finding may be related to issues with reaching the axial strain limit during 35°C temperature testing for HMA Hi-RAP Lot #1, both on the field cores and laboratory-compacted samples. The UC/LC samples from HMA Hi-RAP Lot #1 measured low stiffness on the whole, with an air void range between 10.2% and 11.8% that was significantly higher than the typical 5% to 7% in-situ air void levels acceptable by Superpave. After each time a sample reaches the axial strain limit, the deviator stress was reduced for that particular frequency data point, and the entire high temperature frequency series had to be re-run from the beginning. As a result, the dynamic modulus results at these temperatures are most likely artificially inflated for the IDT samples due to lowering the applied deviator stresses to complete the tests. In contrast to HMA Hi-RAP Lot #1, Lot #2 shows strong correlation between the LC samples throughout the entire reduced frequency spectrum. While the disparity between the field core and LC samples is not as strong in Lot #2, it is still apparent at the lower reduced frequency values as seen in Figure 17.

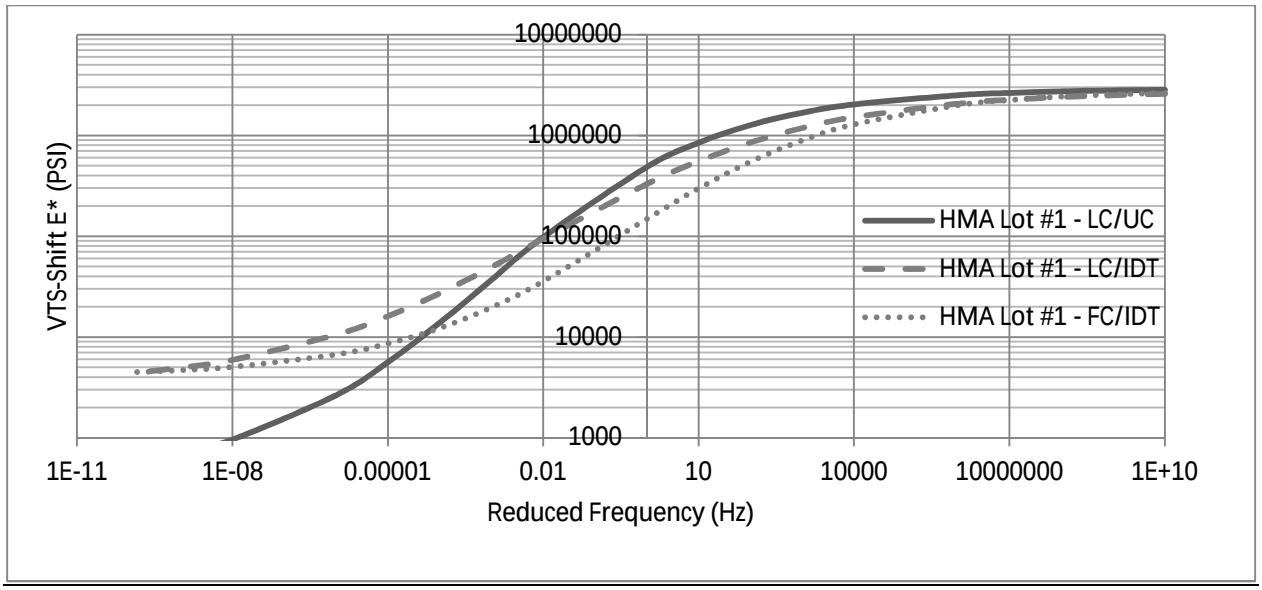

Figure 16. VTS-Shift Dynamic Modulus Master Curve, HMA Hi-RAP Lot #1.

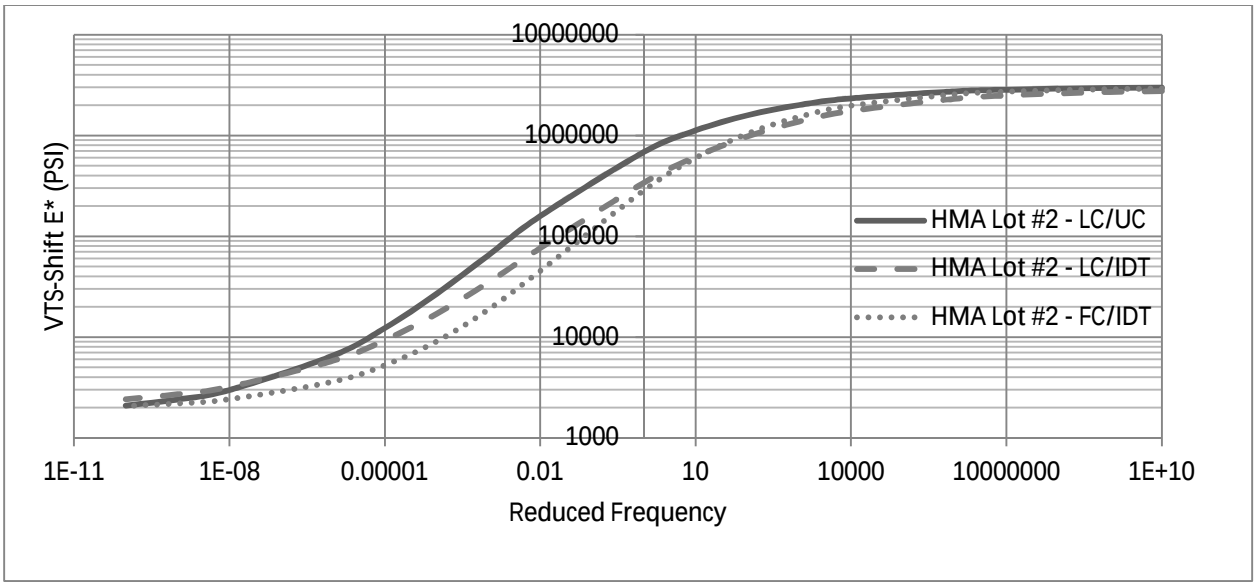

Figure 17. VTS-Shift Dynamic Modulus Master Curve, HMA Hi-RAP Lot #2.

2.3.2.3 Conventional Dense-Graded HMA+RAP Mixture

A total of five lots of plant-produced conventional dense-graded (DGA) HMA+RAP (modified with 10% reclaimed asphalt pavement) loose mix were provided. Table 10 summarizes the types

and number of samples tested, organized by pavement layer and production lot. Plant-compacted (PC) tall specimens were tested exclusively using the Uniaxial Compression (UC) method. Laboratory-compacted (LC) specimens were tested according to both the UC and IDT methods and field cores (FC) were only tested using the IDT method. Master curves were constructed based on a maximum of three specimen's worth of dynamic modulus data sets per lot (for the LC IDT samples) and a minimum of one sample (Lot #2 from the FC IDT).

Table 10. Summary of DGA HMA+RAP Samples Tested.

Lot #	NMAS	AC Layer	Date	PP-PC (UC)	PP-LC (UC)	PP-LC (IDT)	Field Cores (IDT)
1	19mm	Base	7/29/2011	0	3	0	0
2	19mm	Base	8/27/2011	2	3	4	1
3	12.5mm	Binder	9/1/2011	2	3	4	0
4	12.5mm	Binder	9/2/2011	2	3	4	2
5	9.5mm	Surface	9/17/2011	2	3	4	4

The master curve plots are organized and compared according to production lot in Figures 18 through 21. The results are generally similar to those of the HMA Hi-RAP and WMA-SMA mixtures tested, in which laboratory-compacted samples from both the IDT and UC modes of testing displayed dynamic modulus results nearly double the stiffness of the equivalent field core dynamic modulus values measured. Additionally, the IDT dynamic modulus (FC-IDT and LC-IDT) curves typically flattened out at more steep a curve along the low end of the reduced frequency scale. This resulted in IDT dynamic modulus values which were stiffer than the corresponding LC-UC or PC-UC samples.

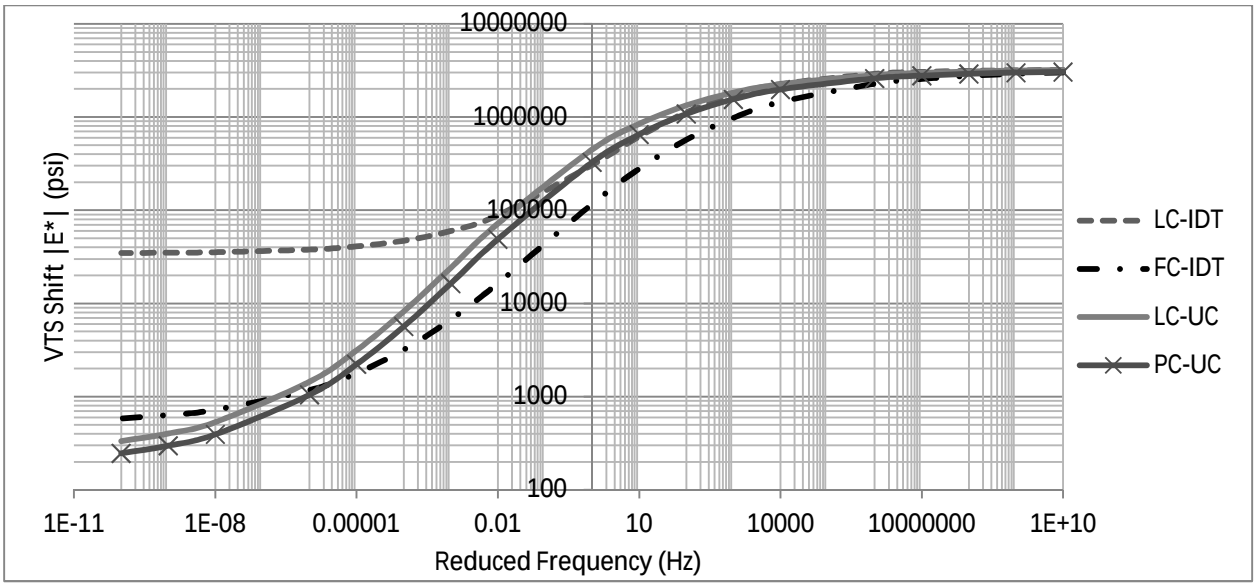

Figure 18. Master Curves for Conventional DGA HMA+RAP Base Lift.

However, while this effect was expected based on the test results from the previous modified mixes, an unexpected result was the large variation between the LC-IDT dynamic modulus results and the other three specimen types tested on this mixture at the low end of the reduced frequency scale. The differences seen in the dynamic modulus values ranged from up to 40,000 psi for the LC-IDT samples to less than 1,000 psi for the other specimen types at the lowest reduced frequency (Figure 18) and almost 100,000 psi for the LC-IDT samples (Figure 20) compared to approximately 100 psi for the other three specimen types.

Upon further review of the raw data files, it was found that the vertical strain applied to the test LC-IDT test specimens were well under the minimum 50 microstrains recommended by Kim et al., (2004). It is hypothesized that the lower applied strain resulted in an erroneous increase in measured dynamic modulus of the LC-IDT test specimens. As a result, IDT testing was halted prior to completion of the RIDOT samples and the remaining mixture from Lot #1of the HMA base lift of the Maine DOT Township D project.

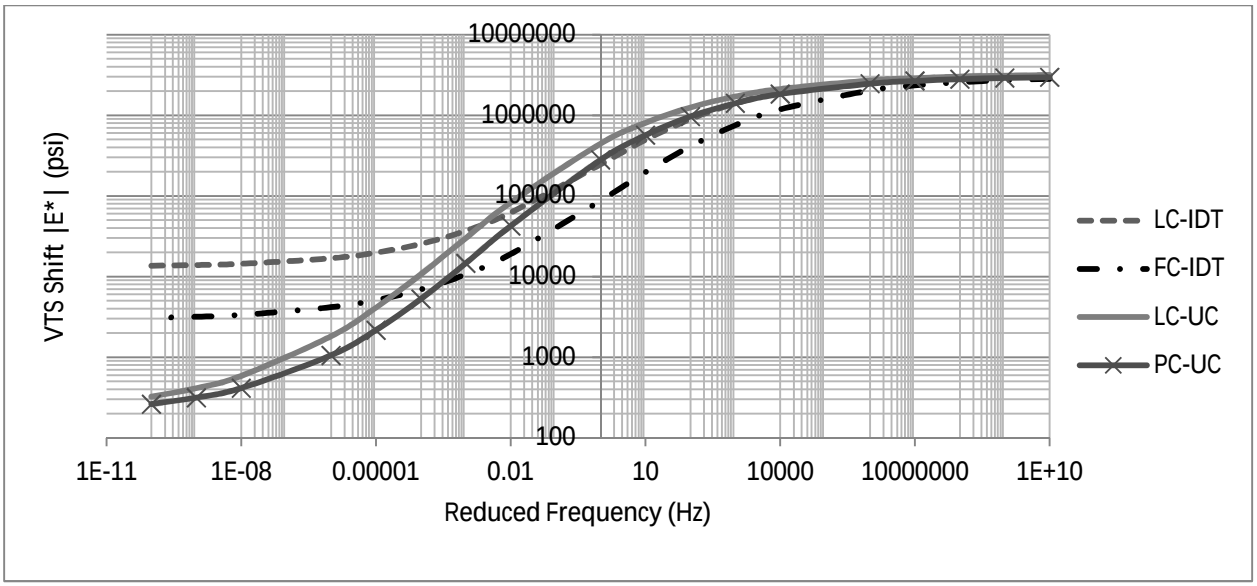

Figure 19. Master Curves for Conventional DGA HMA+RAP Binder Lift, Lot #1.

Another unexpected result was that the PC-UC samples displayed nearly identical dynamic modulus results when compared to the LC-UC samples. Based on the same age-hardening factors that explained the differences between the field core materials and the laboratory-compacted materials, it was anticipated that the PC-UC samples would be softer and exhibit dynamic modulus master curves similar to the field core samples (FC-IDT). While the effects of age-hardening are observed by the LC-UC dynamic modulus values being slightly stiffer than the equivalent PC-UC values, the difference is not to the level that was expected, based on the results seen in the other candidate project mixtures.

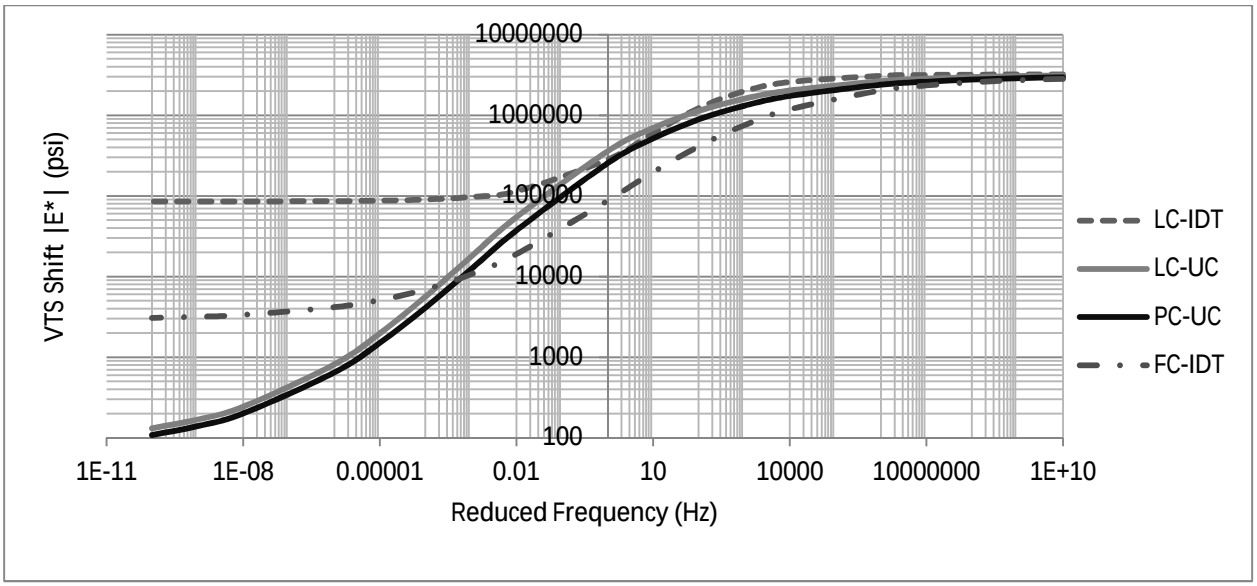

Figure 20. Master Curves for Conventional DGA HMA+RAP Binder Lift, Lot #2.

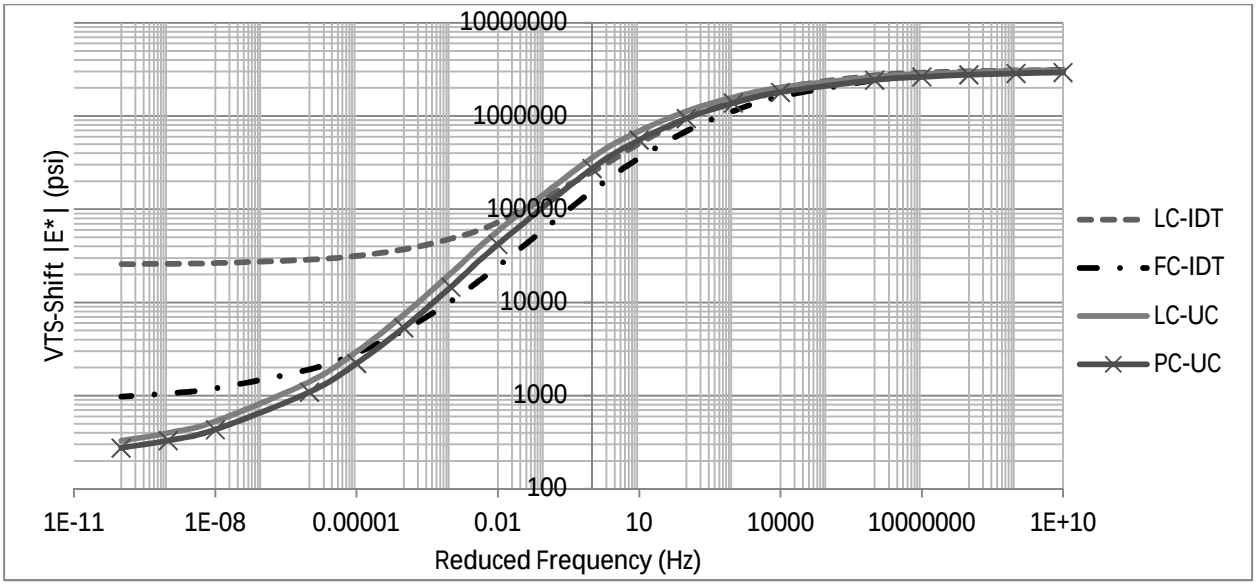

Figure 21. Master Curves for Conventional DGA HMA+RAP Surface Lift.

2.3.2.4 Conventional Dense-Graded HMA Mixture

Two lots of conventional dense-graded unmodified HMA loose mix were tested using the Uniaxial Compression (UC) method. The results of the master curve analysis of these two lots are shown in Figure 22. The average air voids and effective binder content for the two lots are

shown in Table 11. The air void content at 7.8% (outside the typically accepted Superpave range) for Lot #1 (10/5/11) likely contributed to the softness of the materials compared to the Lot #2 (10/6/11) specimens with an average air void content of 4.5%.

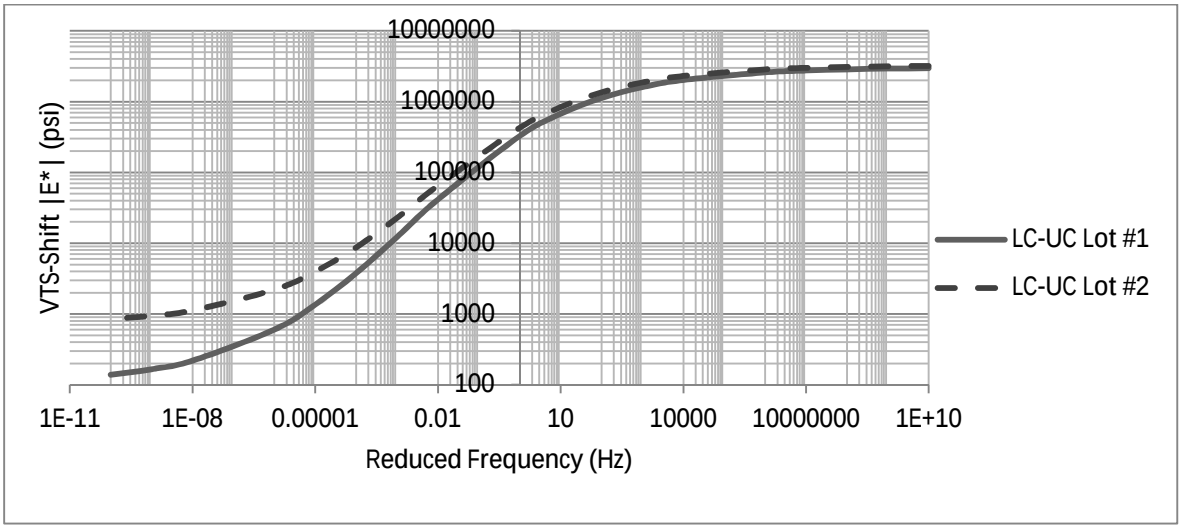

Figure 22. Master Curves for Conventional DGA HMA Surface Lift.

Table 11.Conventional DGA HMA Air Voids and Effective Binder Content by Lot.

	Lot 1	Lot 2
DGA-HMA LC-UC	12.5mm	12.5mm
Air Voids (%)	7.8	4.5
Vbeff (%)	12.7	13.2

2.3.3 Confidence Interval Analysis

An important consideration in the analysis shown earlier is whether or not the data generated using the IDT mode is statistically equal to that of the uniaxial mode. Since the IDT mode was an experimental approach, without a standardized test procedure, differences in pavement analysis using the dynamic modulus may be explained by possible testing error of the IDT test set-up. To evaluate this, the dynamic modulus measured from laboratory compacted specimens

were compared using the uniaxial and IDT testing configurations. Test specimens for each testing configuration were produced in an identical manner and randomly selected for final test specimen preparation. Therefore, if the test specimens were produced under the same conditions (i.e., reheating temperature and time, same method of compaction, etc.), any differences between the measured dynamic modulus would be a resultant of the testing configuration/method itself. Additionally, each data file was review prior to this comparison to ensure the vertical strains were within the recommended range, so as not to result in erroneous and elevated dynamic modulus values.

Figures 23 and 24 are examples of the "confidence intervals" generated for the conventional HMA and SMA mixture produced by DelDOT, respectively. The confidence intervals, shown as the error bars in the dynamic modulus, represents the Acceptable Range for 3 test specimens for Single-Operator precision for dynamic modulus generated in NCHRP Report 702 (Bonaquist, 2011). Although the NCHRP Report 702 only dealt with the uniaxial mode of testing, the same Acceptable Range was used for the IDT mode with the assumption that the precision should most likely be similar to the uniaxial mode.

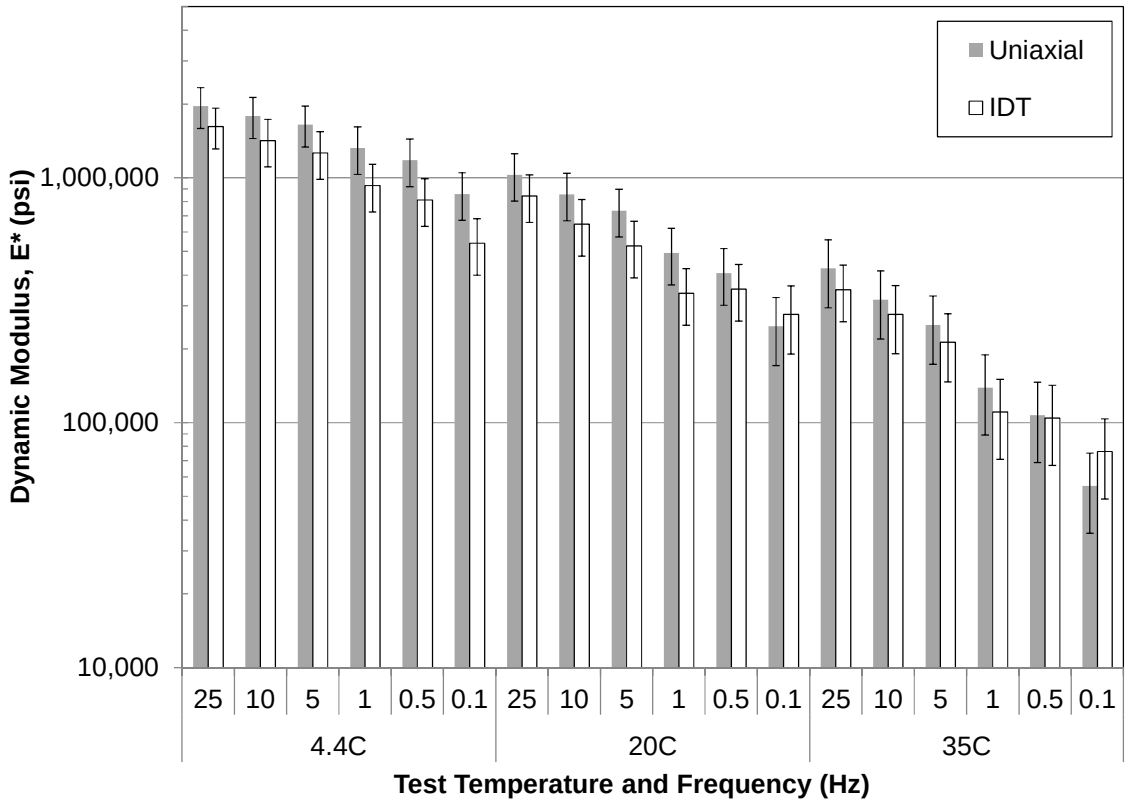

Figure 23. Comparison of IDT and Uniaxial Measured Dynamic Modulus for DelDOT HMA Hi-RAP.

The results shown in Figure 23 and Figure 24 indicate that a good agreement occurs between the IDT and uniaxial dynamic modulus test methods as all of the comparative dynamic modulus values lie within the Acceptable Range bars shown. Therefore, it can be concluded that the IDT mode produces accurate levels of dynamic modulus that is statistically equal to the results generated using AASHTO TP79, *Determining the Dynamic Modulus and Flow Number for Hot Mix Asphalt (HMA) Using the Asphalt Mixture Performance Tester (AMPT).*

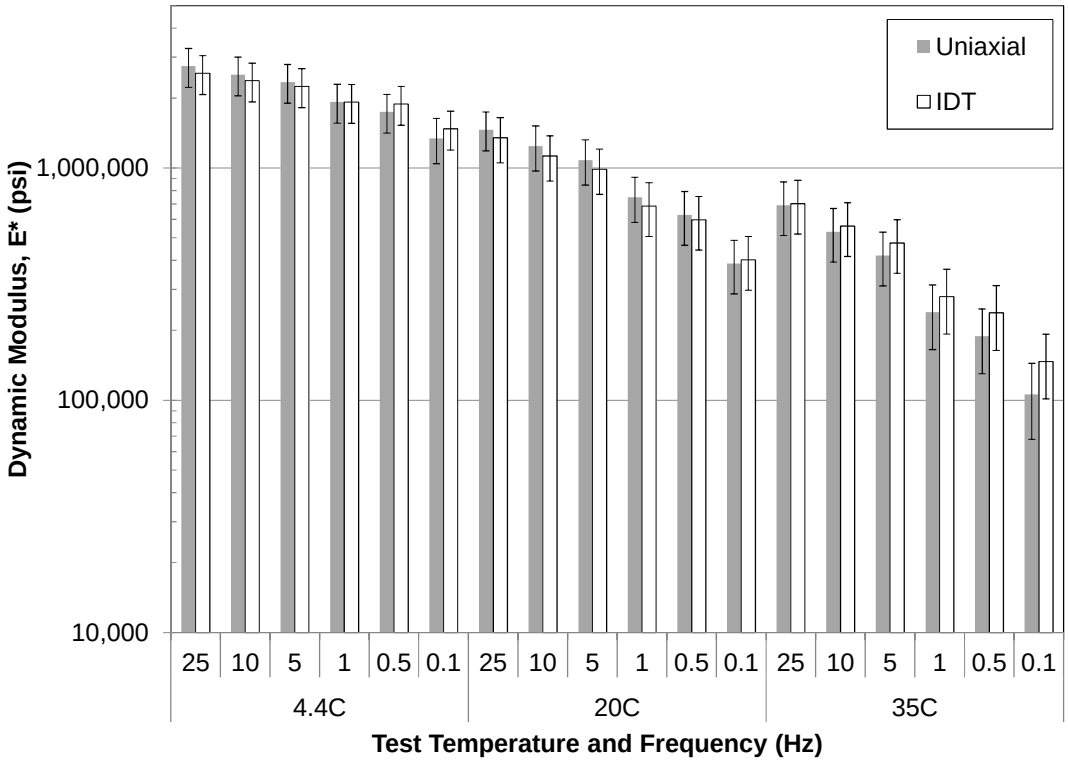

Figure 24. Comparison of IDT and Uniaxial Measured Dynamic Modulus for DelDOT WMA-SMA Mixture.

2.3.4 Summary

The dynamic modulus test results for the DelDOT mixtures resulted in some interesting trends. First, the validation of the IDT test mode by using the Acceptable Ranges established in NCHRP Report 702 indicated that both IDT and uniaxial testing was in reasonable agreement with one another. This finding is important as it validated the IDT approach to testing field cores for E* inputs. However, even though the actual data matched, as shown in the example data of Figures 23 and 24, the resultant forms of the master curves were found to slightly differ from one another. A discussion on how the slight variation in the master curve form influences the pavement response programs (QRSS, SPT Program, and MEPDG) will be included in the next chapter of the report.

Differences in the dynamic modulus between field core and reheated/laboratory compacted was found to be dependent on the mixture type and its origin. For example, the asphalt mixtures from Delaware (WMA-SMA and HMA Hi-RAP) had conflicting findings. For the WMA-SMA mixture, it was found that the dynamic modulus of the field cores was consistently lower than that of the laboratory reheated and compacted specimens. Meanwhile, for the HMA Hi-RAP mixture, it was found that the dynamic modulus of the field cores compared favorably to the laboratory reheated and compacted mixtures. Similar comparisons were also found for the other mixtures.

When plant compacted mixtures were supplied, it was determined that minimal differences were found when comparing the dynamic modulus of plant compacted and laboratory reheated and compacted specimens.

Finally, when comparing the Lot by Lot information, it was determined that the measured dynamic modulus differed slightly. This was attributed mostly to differences in the measured volumetric properties (i.e., effective asphalt content, air voids) of the mixture provided. Additional plots of the data for the remaining lots of both DelDOT mixtures are provided in Appendix D.

CHAPTER 3

FINDINGS AND APPLICATIONS

In order to assess the impacts of specimen type and test configuration, the results from the dynamic modulus testing were input to three different pavement analysis programs: Quality-Related Specification Software (QRSS) from the NCHRP Project 9-22, the Simple Performance Tester (SPT) Program from the NCHRP Project 9-22A, and the AASHTO Mechanistic-Empirical Pavement Design Guide (MEPDG) version1.0 software. All of the programs are based on the flexible pavement distress prediction models developed for use in the AASHTO MEPDG. However, the models from each of the programs are calibrated differently with respect to climate. The MEPDG fatigue cracking model is based upon approximately 850 climatic stations all across the United States; whereas the fatigue damage model used in the QRSS program (NCHRP, 2011) is based upon three climatic locations: Grand Forks, ND (41.6 deg F), Oklahoma City, OK (60.7 deg F), and Key West, FL (77.8 deg F).

The input types vary among the analysis programs and are summarized in Table 12.

Table 12. Summary of Input Types for Analysis Programs.

	Input Type			
Program	**Climate**	**Traffic**	**HMA Inputs**	**Unbound Layers**
MEPDG	LTPP site specific climatic data	Axle Load Spectra	|E*|, G*, and phase angle	Resilient Modulus
NCHRP 9-22A SPT Program	Effective Temperature	Effective Loading Frequency, Daily ESALS	|E*| and $\|E^*\|_{effective}$	Composite Foundation Modulus
QRSS	Effective Temperature	Effective Loading Frequency, Daily ESALs	Volumetric properties, Binder A,VTS	Composite Foundation Modulus

3.1 Mixture Performance Evaluated with Quality-Related Specification Software (QRSS) and NCHRP 9-22A SPT Programs

3.1.1 Surface Rutting Analysis

Interpretation of the surface rutting results indicated that the QRSS is slightly more rewarding of lower-quality paving mix than the SPT Program analysis approach. These results are opposite of what is seen with the WMA-SMA mix where the QRSS produced higher rutting (0.09 inches in the QRSS vs. 0.05 inches in the SPT) than either of the SPT Program analyses. Lot-by-lot comparisons of the predicted life difference (PLD) results for the HMA Hi-RAP and WMA-SMA mixture analyses is presented in Figures 26 and 27.

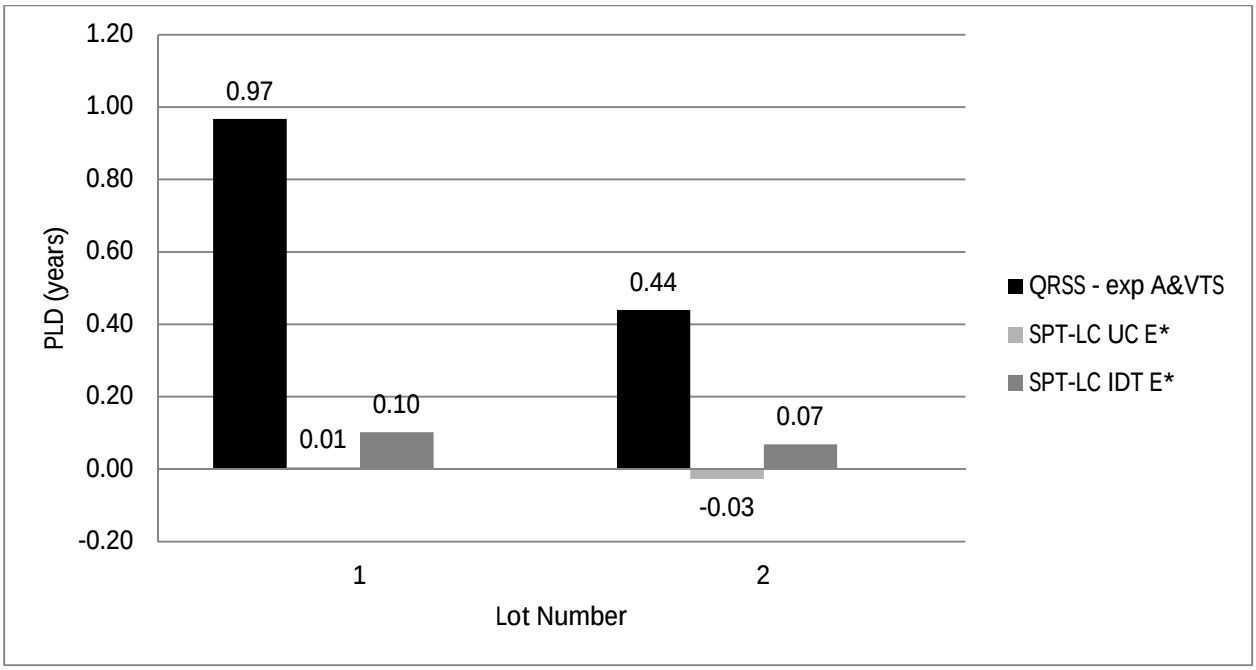

Figure 25. HMA Hi-RAP Lot-by-Lot Surface Rutting PLD Results.

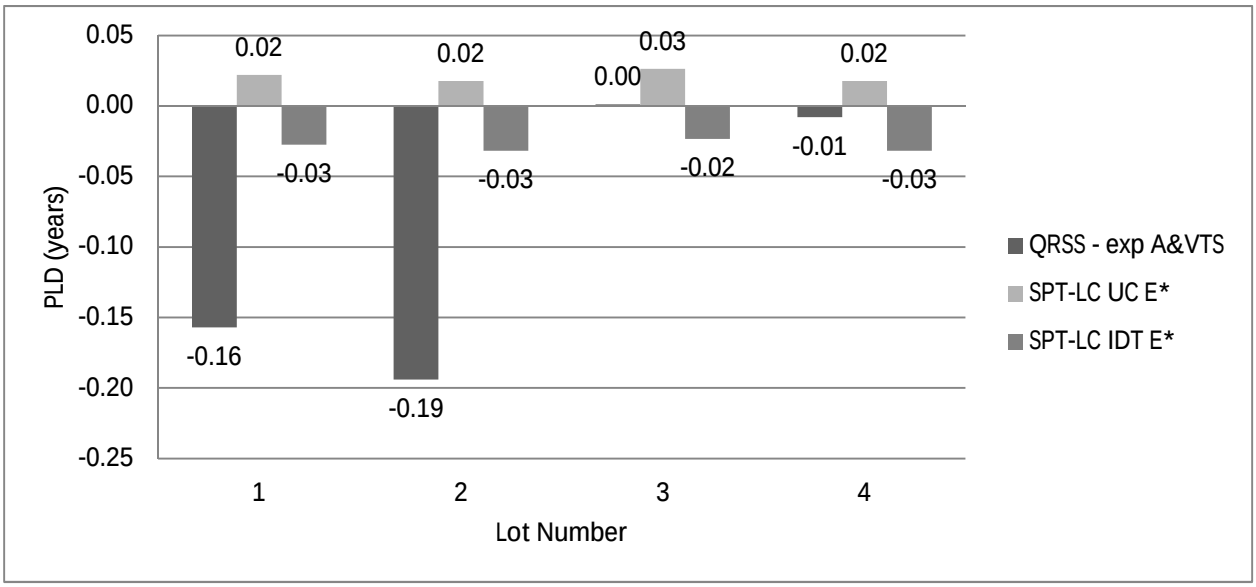

Figure 26. WMA-SMA Lot-by-Lot Surface Rutting PLD Results.

In order to analyze the dense-graded HMA RAP (DGA HMA+RAP) mix, two runs were performed in the QRSS, analyzing the pavement using the standard PG64-28 A and VTS values

and again with the experimental A and VTS values measured in the laboratory on the RAP-modified PG64-28 binder used in construction. Table 13 shows the A & VTS values used for each of the two analysis iterations. The QRSS results are included in Appendix B.

Three analyses runs were created for the DGA HMA+RAP in the SPT Program because Maine DOT was able to send plant-compacted tall samples, in addition to field cores and loose mix buckets. Each of the three runs utilized laboratory-measured |E*| data in the design mix analysis from one of either the plant-compacted uniaxial compression samples (PC-UC), laboratory-compacted uniaxial compression samples (LC-UC), or laboratory-compacted IDT samples (LC-IDT), in addition to standard job-mix formula (JMF), traffic, and volumetric data. The as-designed mix for all three SPT Program iterations was analyzed using the available contractor QA volumetric data, in conjunction with the field core IDT |E*| experimental data.

Table 13. Binder A & VTS Values Used in QRSS Analysis of DGA HMA+RAP.

Binder Data Type	A	VTS
Standard PG64-28	10.312	-3.44
Experimental Lab Results	9.664	-3.224

The two programs were compared for surface and total bituminous layer rutting, and the SPT Program analyses was compared for base rutting and fatigue cracking, excluding the QRSS results due to the QRSS not allowing for the input of the HMA base lift's QA volumetric data in the QA portion of the program. Instead, the HMA base lift volumetric data was approximated with a M_R equal to 200,000 psi. Figure 27 shows the different cross sections used between the QRSS and SPT Program to analyze the DGA HMA+RAP mixture.

9.5mm HMA surface (1.25")
12.5mm HMA binder (1.75")
19.0mm HMA base, M_R = 200,000 psi
Gravel (18") M_R = 50,000 psi

(a) QRSS Software

9.5mm HMA surface (1.25")
12.5mm HMA binder (1.75")
19.0mm HMA base (2")
Gravel (18") M_R = 50,000 psi

(b) SPT Program

Figure 27. Different Cross-Sections Used in QRSS and SPT Program for MEDOT Pavement.

Surface rutting PLD results are plotted in Figure 28. The QRSS resulted in the largest positive surface rutting PLDs at +1.56 years. While this is still 100% payment according to the PLD limits set for the project, a different set of PLD limits would potentially create a pay bonus for the contractor using a QRSS method. This is consistent with the previous results on the HMA Hi-RAP PLD results. The WMA-SMA PLD results showed the opposite result, with the QRSS producing the lowest performance.

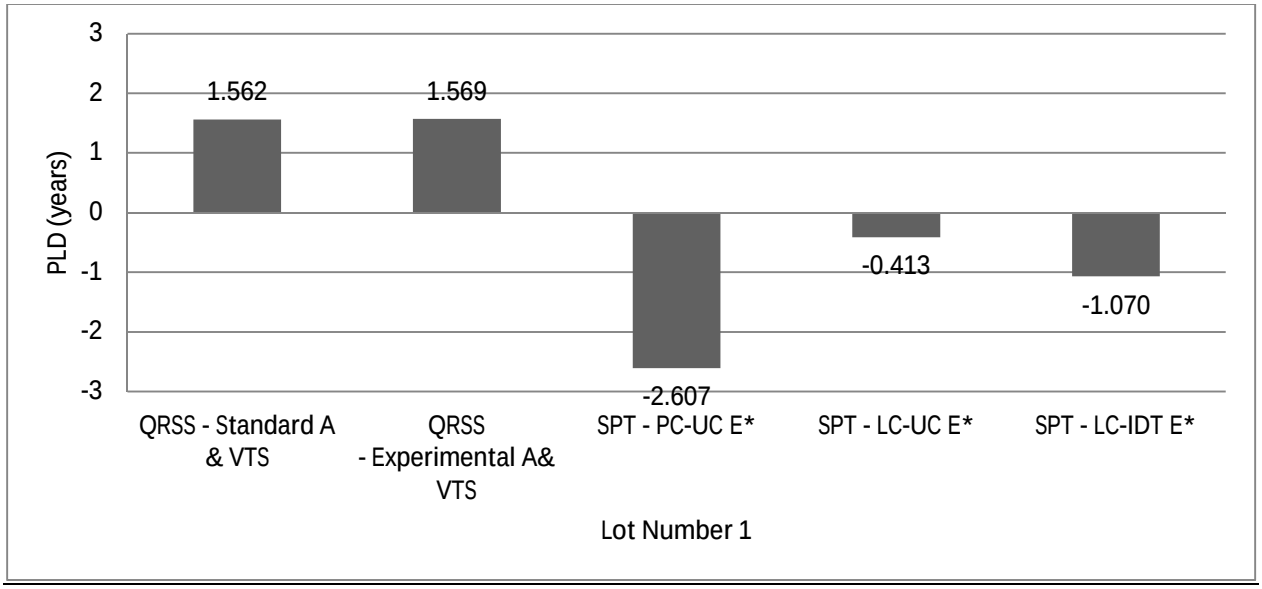

Figure 28. DGA HMA+RAP Surface Layer Rutting Predicted Life Difference Results.

For the conventional DGA HMA mixture, two runs were performed in the QRSS, analyzing the pavement using the standard PG64-28 A and VTS values and the experimental A and VTS values based on laboratory binder testing data. The binder A and VTS values used for a standard PG64-28 were 10.312 and -3.44, respectively. The experimental binder A and VTS values were 9.823 and -3.276, respectively. The full QRSS results are included in Appendix B.

Two lots of surface lift DGA-HMA dynamic modulus data described in Chapter 2 were utilized in the SPT Program analysis; however, due to difficulties with the IDT LVDT apparatus at the conclusion of IDT testing of DGA HMA+RAP samples, only the laboratory-compacted uniaxial compression |E*|data (UC-LC) could be analyzed in the SPT Program. This led to a situation in which both the design mix analysis and the as-built mix analysis portions of the SPT Program were based on the |E*| and $|E^*_{eff}|$ data from the same six LC-UC samples. The expectation from this was that 100% payment would be seen for surface rutting according to the SPT Program.

The surface rutting PLD results are plotted by lot for the DGA=HMA mixture in Figure 29. Since all of these values were within +/- two years of the targeted service life, payment was 100% across all lots for both analysis iterations.

The QRSS results confirm those of the DGA HMA+RAP, indicating that the use of binder values measured in the laboratory in the QRSS analysis has minimal effect on the surface rutting PLD results, making it less variable lot-by-lot. While the experimental values displayed slightly less variation, the scale of Figure 29 shows that the difference between results is on the order of 0.10 years, which is insignificant for payment unless results are very close to the limit for remove and replace. However, across all four candidate projects analyzed in the QRSS, this

situation has not been observed as all projects have displayed 100% payment for surface rutting across all lots.

The SPT Program produced PLD results for 100% payment; however, the variation was much larger than what was seen in the QRSS. While the SPT Program surface rutting PLD values for Lot #1 (-0.64 years) and Lot #2 (+1.25 years) are in the range for 100% payment, they were much closer to the PLD limits for pay disincentive or pay incentive, respectively, than either of the two QRSS analysis results. These rutting results may indicate that the SPT Program is more sensitive to air void levels in the mix since the sample air voids for Lot #1 were significantly higher than those in Lot #2 (7.8% compared to 4.5%, respectively).

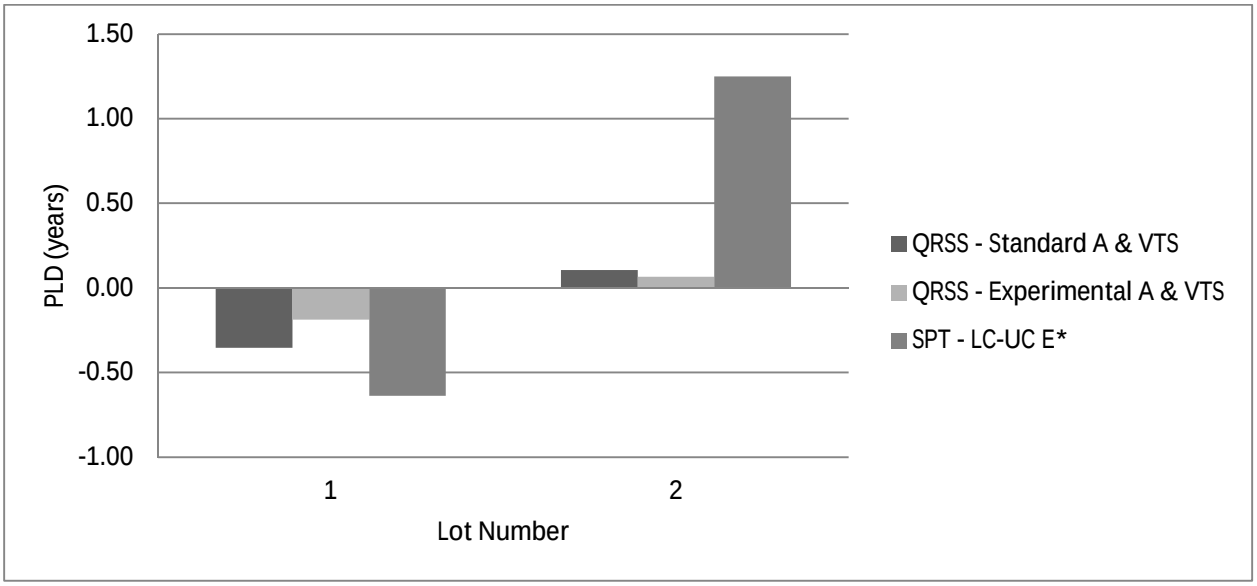

Figure 29. Surface Layer Rutting PLD Results for the DGA HMA Mixture.

3.1.2 Analysis of Total Rutting in Bituminous Layers

Total bituminous layer rutting PLD results for each lot analyzed in the WMA-SMA mixture are plotted in Figure 30 for both mixes and the accompanying pay factor results are plotted in Figures 32. Since the binder layer volumetric and |E*| data is based on results from the Rhode

Island (RI DOT) Route102 in the NCHRP Project 9-22A, it was expected to produce equivalent results regardless of the PRS software used which was not the result.

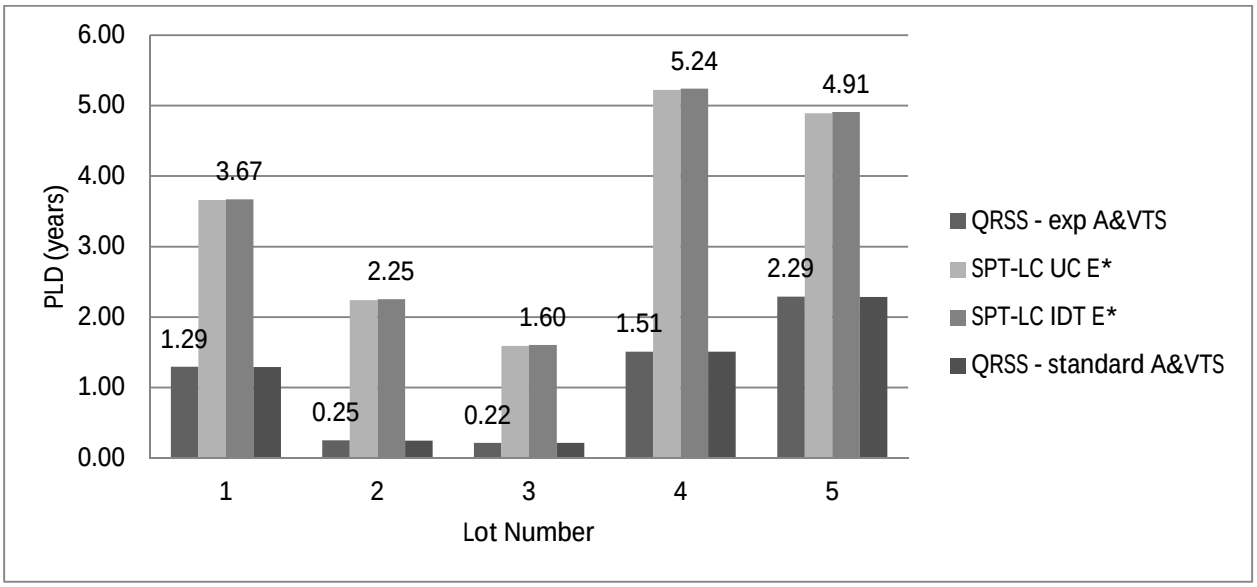

Figure 30. WMA-SMA Lot by Lot Total Bituminous Layer Rutting PLD Results.

As expected based on the equivalent volumetric and |E*|, the two SPT models produced virtually identical binder layer rutting results. The QRSS model generally followed the pattern of the SPT Program models, but the PLD results from the QRSS typically varied by up to approximately two years and as high as four years for Lot #4 of the WMA-SMA mix in the SPT Program results. This was not expected because the SPT Program and QRSS derive analysis from the same contractor QA volumetric and profile data. However, the SPT Program analysis incorporated |E*| and $|E^*_{eff}|$ data compiled by the separate RIDOT QA data, which could account for the variation in results. Additionally, the experimental dynamic modulus data is systematically lower than the predicted dynamic modulus values from the QRSS analysis.

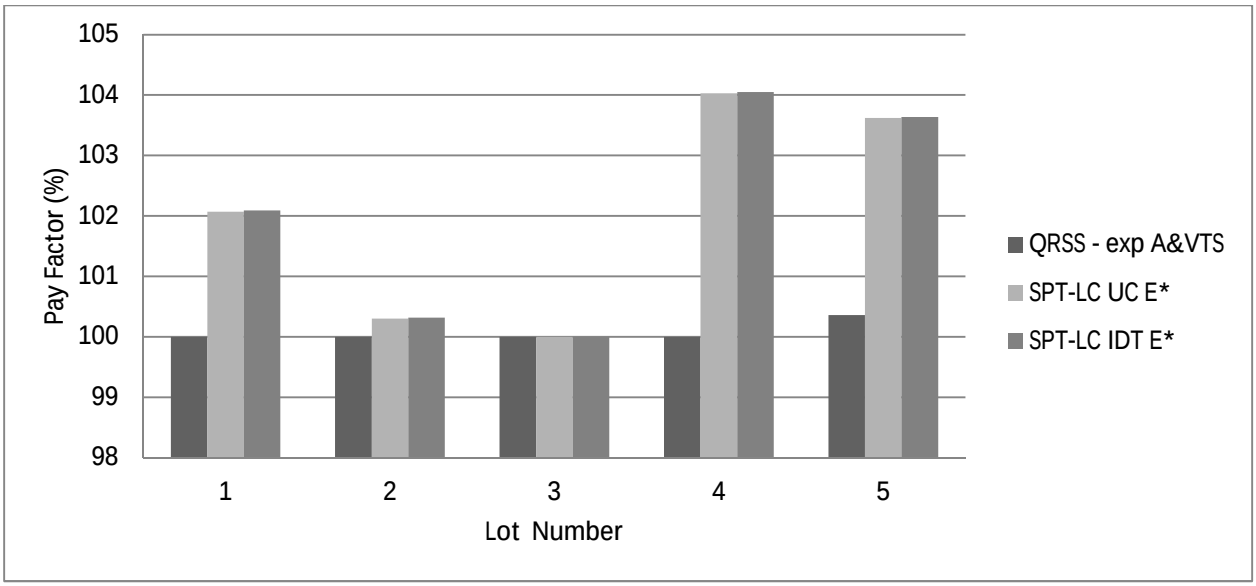

Figure 31. WMA-SMA Mixture Pay Factor for Total Bituminous Layer Rutting.

Contrary to the results found within the surface rutting model, the QRSS analysis is less forgiving in the binder rutting analysis because a softer design mix produces larger positive PLD results. These differences in distress values and PLD ultimately do have a small effect on the contractor's predicted level of payment. The QRSS results showed 100% payment for all five lots analyzed, while the SPT Program typically showed pay incentives between 102% and 104% for the same five lots. While Lot #3 had the same pay factor results between the SPT and QRSS (100% for both), the PLD produced by the SPT Program is still 1.38 years greater than the PLD produced by the QRSS. The equivalent pay factor in this case is merely a result of the arbitrary PLD limits assigned for payment.

Specimen type could not be analyzed for total AC layer rutting analysis due to the use of identical dynamic modulus values from RIDOT Route 102 for every iteration of the SPT analysis for the WMA-SMA and HMA Hi-RAP mixes.

The DGA HMA+RAP mixture was from the only candidate project that provided data and materials from the sub-surface bituminous lifts, which meant that the using the RIDOT Route 102 volumetric and QA data as in the other projects was not necessary. Therefore the experimental binder A and VTS data from Table 13 were also applied to the binder layer of the QRSS model. Total bituminous layer rutting PLD results for the DGA HMA+RAP mixture are plotted by lot in Figure 32.

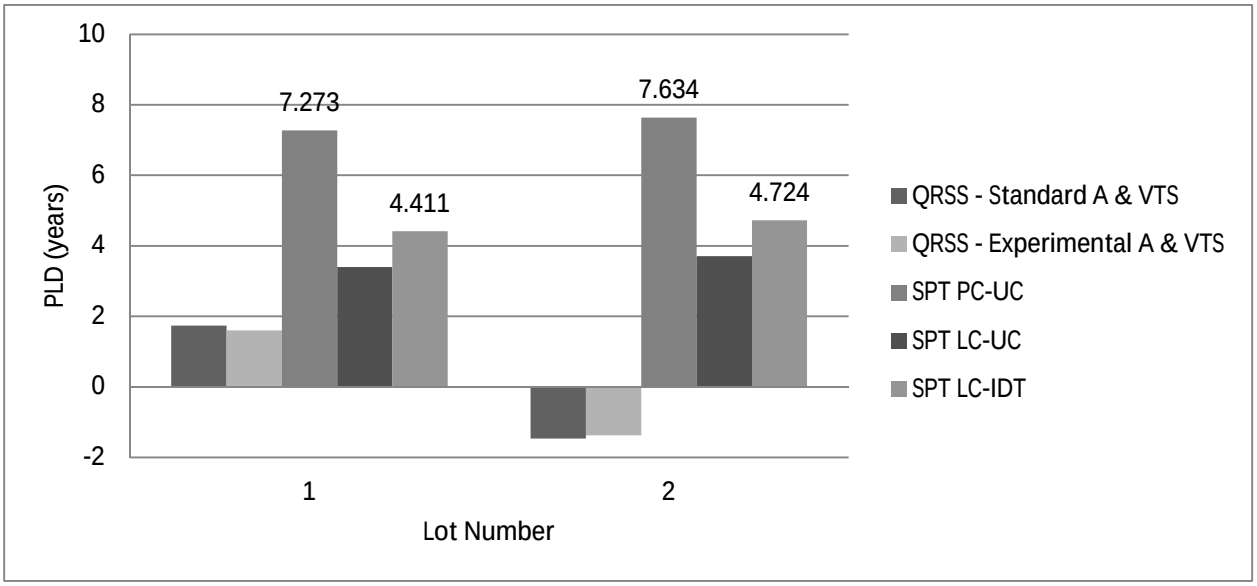

Figure 32. Binder Layer Rutting PLD Results for DGA HMA+RAP Mixture

When the rutting in the base lift was being analyzed for the DGA HMA+RAP mixture in the SPT Program, an apparent programming error was found. Although the PLD values indicated that remove and replace was necessary according to the PLD limits set for the project, the SPT Program assigned a 100% payment or a small pay penalty. These results are presented in Table 14.

Table 14. SPT Program Results for Rutting in Base Lift of DGA HMA+RAP Mix.

Specimen Type	Lot	Design Distress (in)	As Built Distress (in)	Design Service Life (Yrs)	Predicted Service Life (Yrs)	PLD	Pay Factor
SPT - PC-UC E*	1	0.04	0.07	19.99	9.57	-10.43	95.95
SPT - LC-UC E*	1	0.02	0.05	20.00	5.08	-14.92	100.00
SPT - LC-IDT E*	1	0.03	0.05	19.99	6.73	-13.27	100.00

The binder rutting PLD results for the DGA-HMA mixture are plotted by lot in Figure 33. The SPT Program analysis showed a large variation between predicted design mix binder rutting and the predicted as-built binder rutting level. This result may require further exploration since the dynamic modulus data used for both the design mix and as-built mix portion of the analysis was the same.

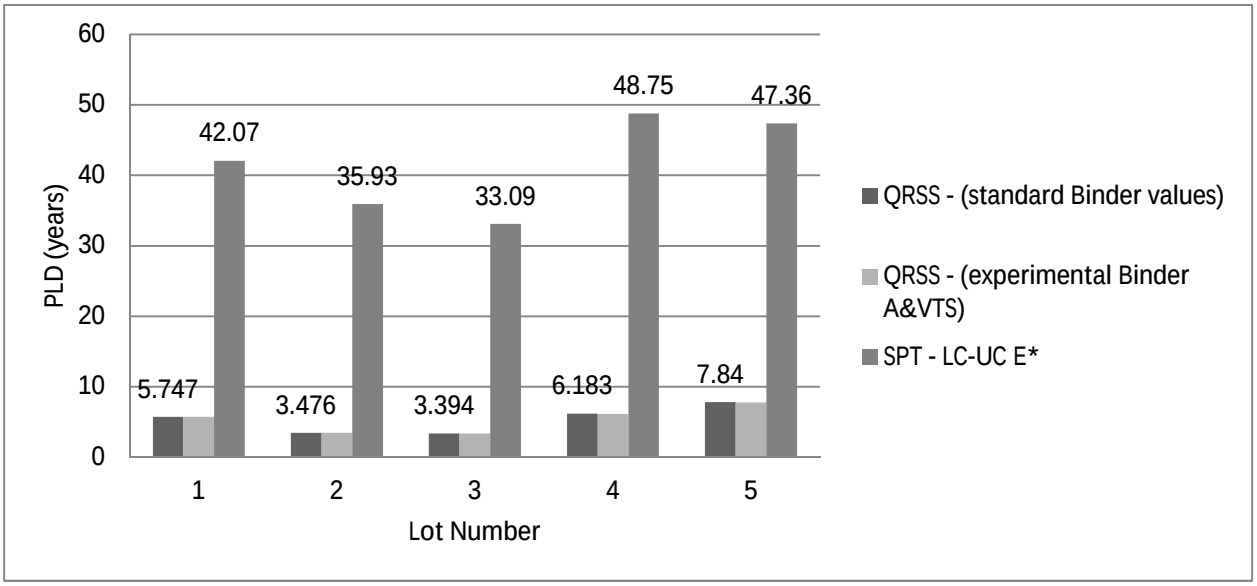

Figure 33. Binder Layer Rutting PLD Results for DGA-HMA Mixture.

3.1.3 Fatigue Cracking Analysis

Fatigue cracking PLD results are plotted lot by lot in Figure 34 for the HMA Hi-RAP mix and in Figure 35 for the WMA-SMA mix. There is significant variation in the predicted life differences between the two models used for each pavement type, to as much as ± nine years in Lot #4 of the WMA-SMA mixture.

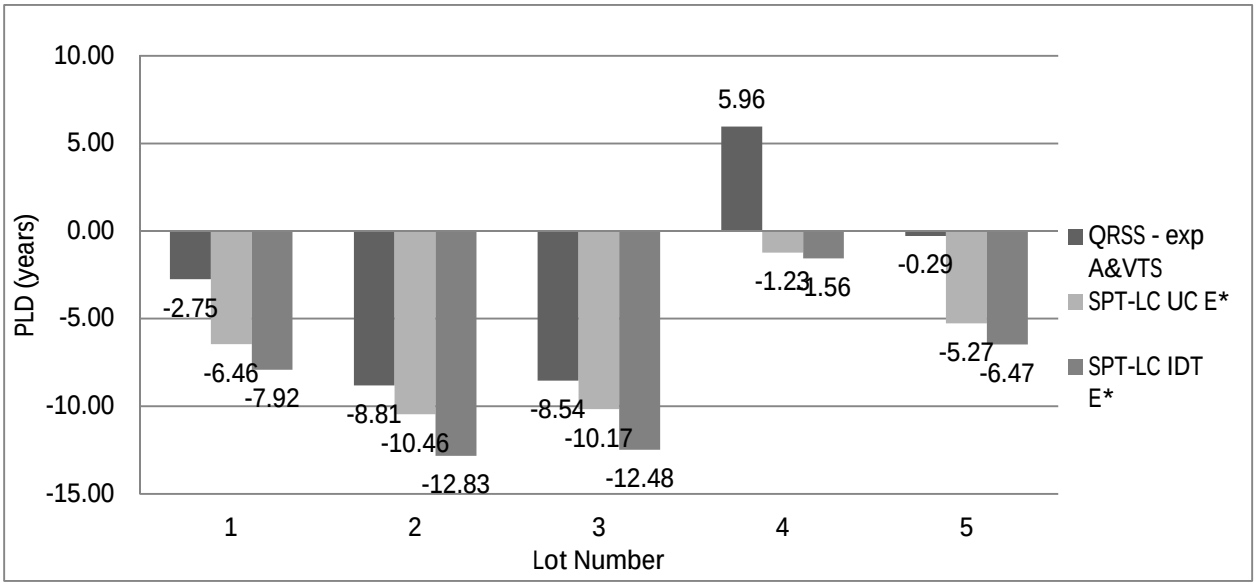

Figure 34. HMA Hi-RAP Fatigue Cracking PLD Results.

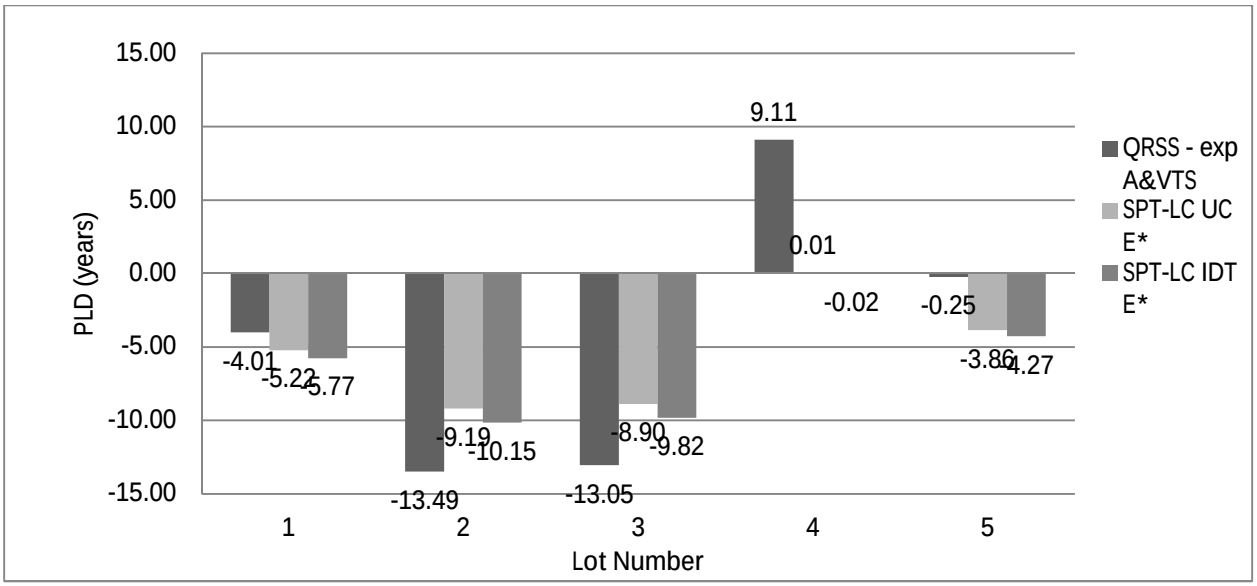

Figure 35. WMA-SMA Fatigue Cracking PLD Results.

The PLD plots show a noticeable trend where, due to the SPT Program analyses producing much higher predicted as-built fatigue cracking results than the QRSS, PLD results for the QRSS are typically longer than the SPT Program analyses in terms of fatigue cracking. The poor fatigue cracking performance in both projects, particularly in Lots 1 through 3 and 5 is attributed to both a low effective binder content and high air void content. Lots #2 and #3 have excessively low effective binder content values, leading to the greater tendency toward early fatigue cracking as there is not enough binder between aggregate allowing cracks to propagate more easily. Table 15 shows that comparatively, Lots #1, #4, and #5 had higher levels of compaction, which could explain the lower negative PLD values observed for those lots. The QRSS results for Lot #4 for both the WMA-SMA and HMA Hi-RAP even show a positive PLD value for fatigue cracking compared to the SPT Program analyses. Additionally, it has been shown that QRSS results were highly sensitive to binder and air void content, leading to the greater variation between lots seen in the QRSS fatigue cracking analysis [Mensching (2011)].

Table 15. NCHRP Project 9-22A RIDOT Route 102 Volumetric Data.

RIDOT Rt 102 Binder QA Data		
Lot #	AV%	V_{beff}
1	4.3	10.213
2	6.5	8.592
3	6.1	8.741
4	2.7	9.058
5	3.2	8.347

Fatigue cracking results of the conventional DGAHMA mixture were significantly more variable, as seen in Figure 36. These results indicate that the pay factor limits for fatigue cracking should be calibrated if the current fatigue cracking model is to be used.

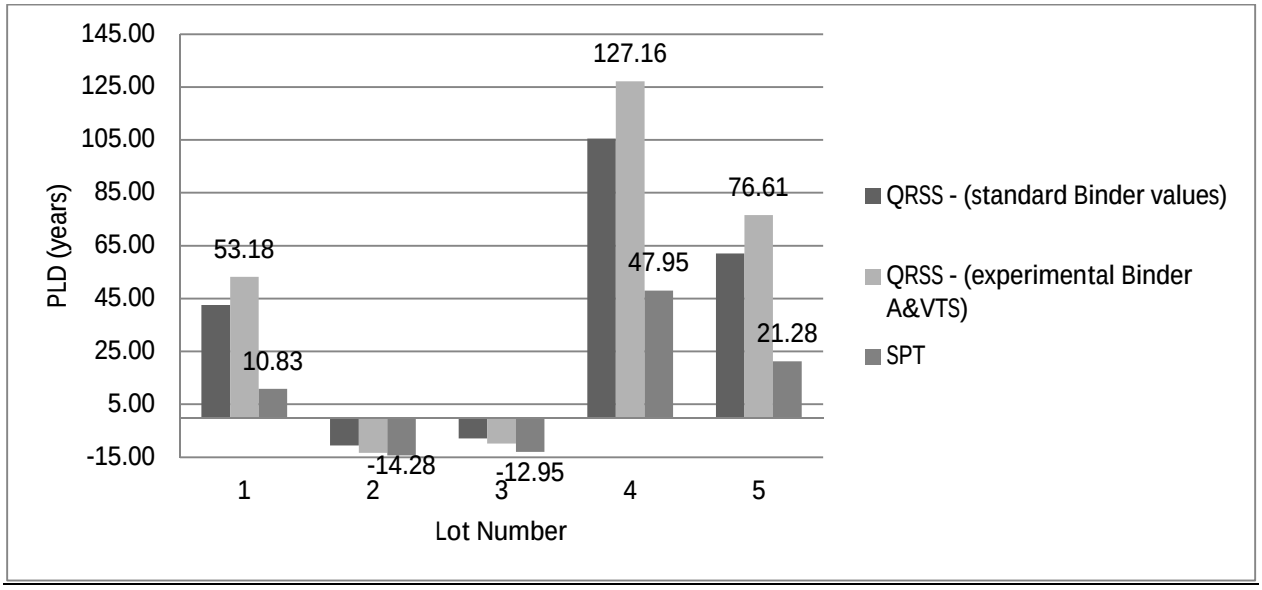

Figure 36. Fatigue Cracking Predicted Life Difference Results for DGA HMA Mixture.

3.1.4 Additional Analysis on Mixture Data from Federal Highway Administration

The Federal Highway Administration (FHWA) Mobile Asphalt Testing Laboratory provided |E*|,mixture volumetric data, pavement profiles, and binder test data for two past projects from

Delaware (DE0883) and Maine (ME0359). The DE0883 mixture was a SMA modified with 30% RAP and the ME0359 was a conventional HMA modified with 10% RAP.

Two analysis runs were performed in the QRSS for each of the two FHWA projects, analyzing the pavement model using the standard PG58-22 A and VTS values, and again with the experimental A and VTS values calculated by the FHWA Mobile Asphalt Mixture Testing Laboratory. Table 16 shows the A and VTS values used for each of the two analysis iterations. An SPT Program analysis was created using dynamic modulus data provided by the FHWA. Similar to the analysis of the DGA HMA mixture, the same dynamic modulus data was used in both the design mix and as-built mix analysis for both of the paving projects provided by FHWA.

Table 16. Binder A and VTS Values Used in Analysis of Mixture Data from FHWA.

Binder Data Type	A	VTS
Standard PG58-22 (DE0883)	11.787	-3.981
FHWA Test Results (DE0883)	10.207	-3.411
Standard PG64-28 (ME0359)	10.312	-3.440
FHWA Test Results (ME0359)	9.976	-3.326

The surface rutting distress results are plotted in Figure 37. The predicted life difference (PLD) results are plotted for the FHWA DE0883 (SMA+30%RAP) and FHWA ME0359 (HMA+10%RAP) projects in Figure 38. Similar to the other candidate projects, both of these mixture analyses confirm that the use of laboratory-measured binder data will modify the rutting distress predicted by the QRSS. However, both the design mix predicted rutting and the as-built mix predicted rutting tend to increase by equivalent amounts, leaving the PLD values from the QRSS analysis mostly unchanged. Comparatively, the SPT Program analysis showed no distinct patterns as compared to the QRSS analysis; however, the overall trend of small variations in

surface rutting distress (e.g., PLD predictions having minimal effect on the resulting pay factors based on the rutting PLD limits defined for this project)was consistent.

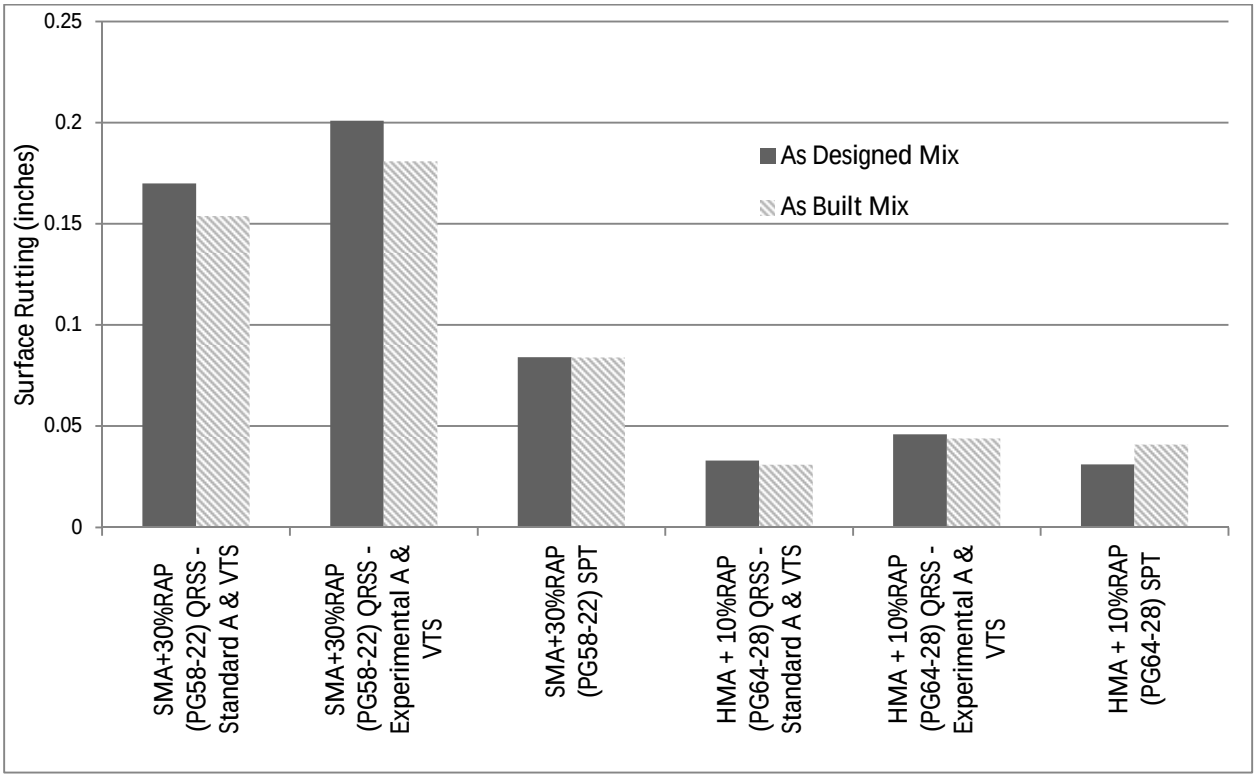

Figure 37. Surface Rutting Distress Results for SMA+30% RAP and HMA+10% RAP Mixtures.

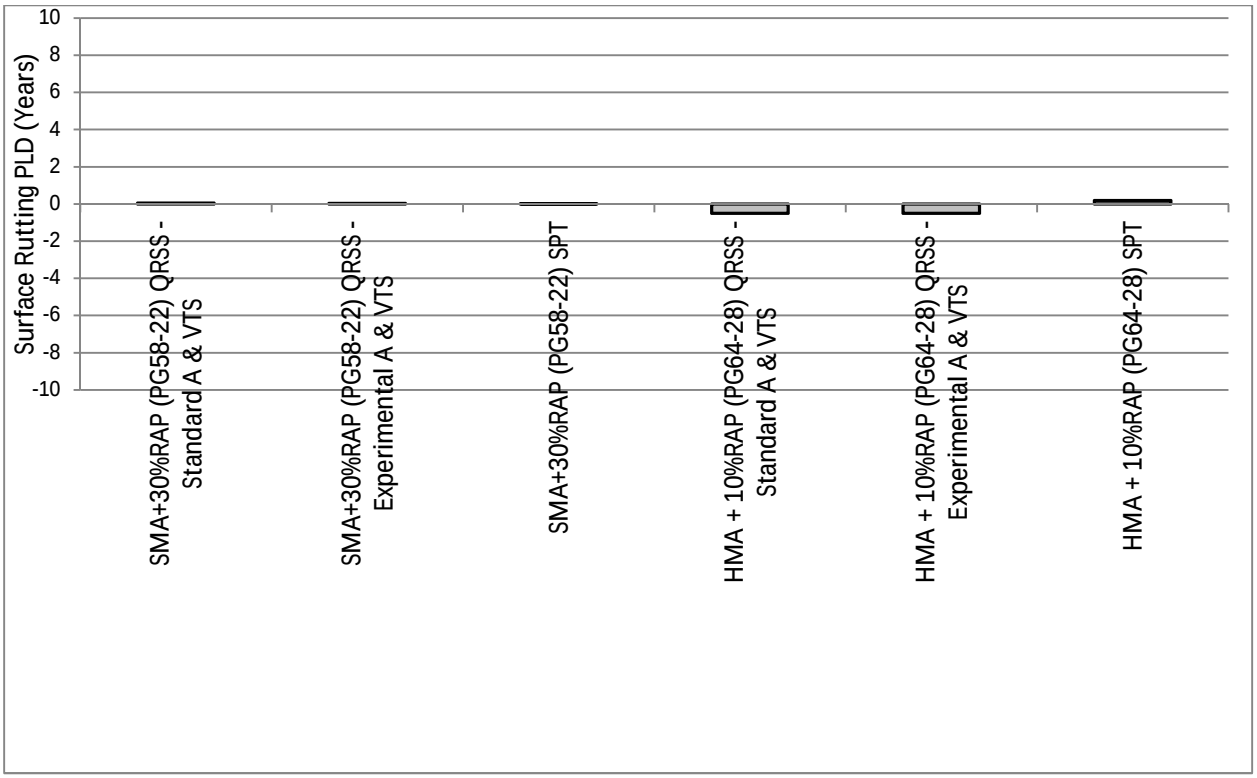

Figure 38. Surface Rutting PLD Results for SMA+30% RAP and HMA+10% RAP Mixtures.

Total bituminous layer rutting distress results are plotted in Figure 39 and the PLD results for the SMA+30% RAP and HMA+10% RAP mixtures from the FHWA paving projects are plotted in Figure 40. Similar to the other project mixes, alteration of the binder data in the QRSS did not affect the resulting total bituminous layer rutting distress or PLD values. For the SMA+30% RAP mixture, the SPT Program was generally consistent with the QRSS analysis in the difference between predicted design mix rutting and predicted as-built rutting, but SPT Program rutting values were approximately 67% of the QRSS values. This led to increased positive PLD values, in two out of five cases over the +2.0 year limit for pay bonuses, as compared to the QRSS analysis results which stayed in the 100% payment range.

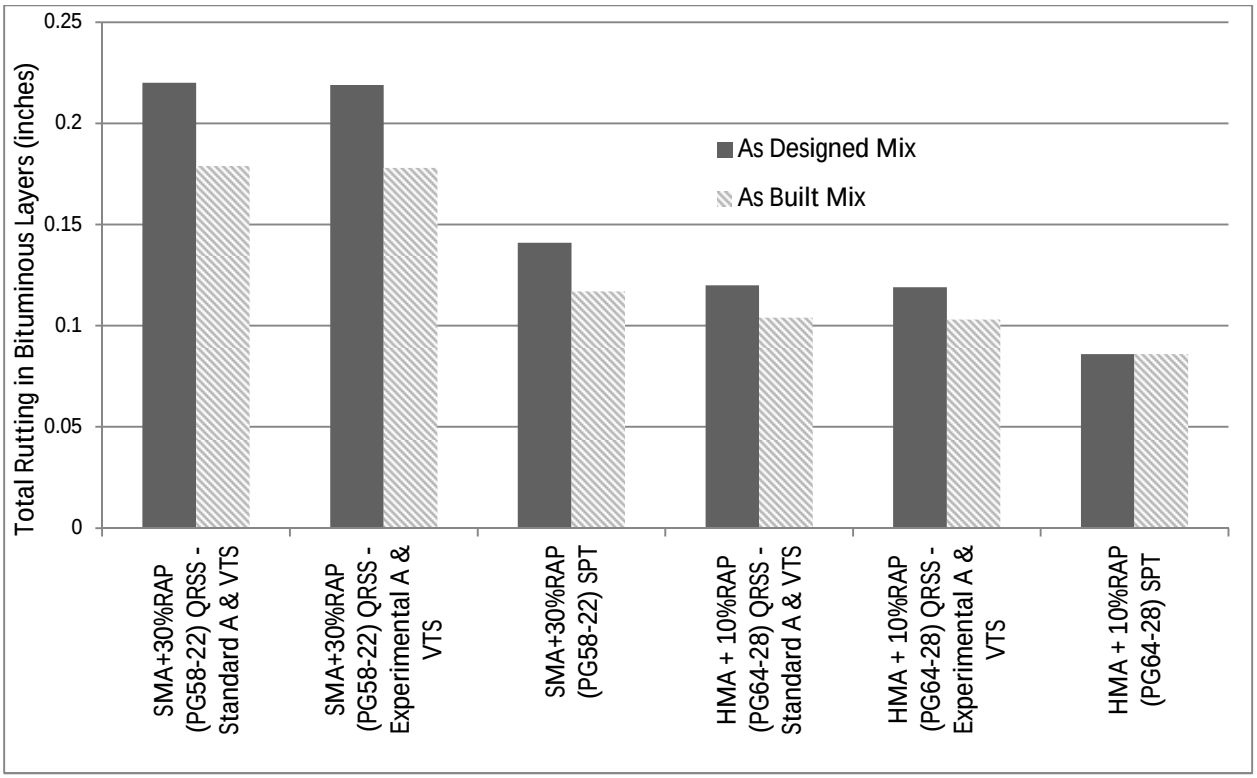

Figure 39. Total Bituminous Layer Rutting Distress Results for SMA+30% RAP and HMA+10% RAP Mixtures.

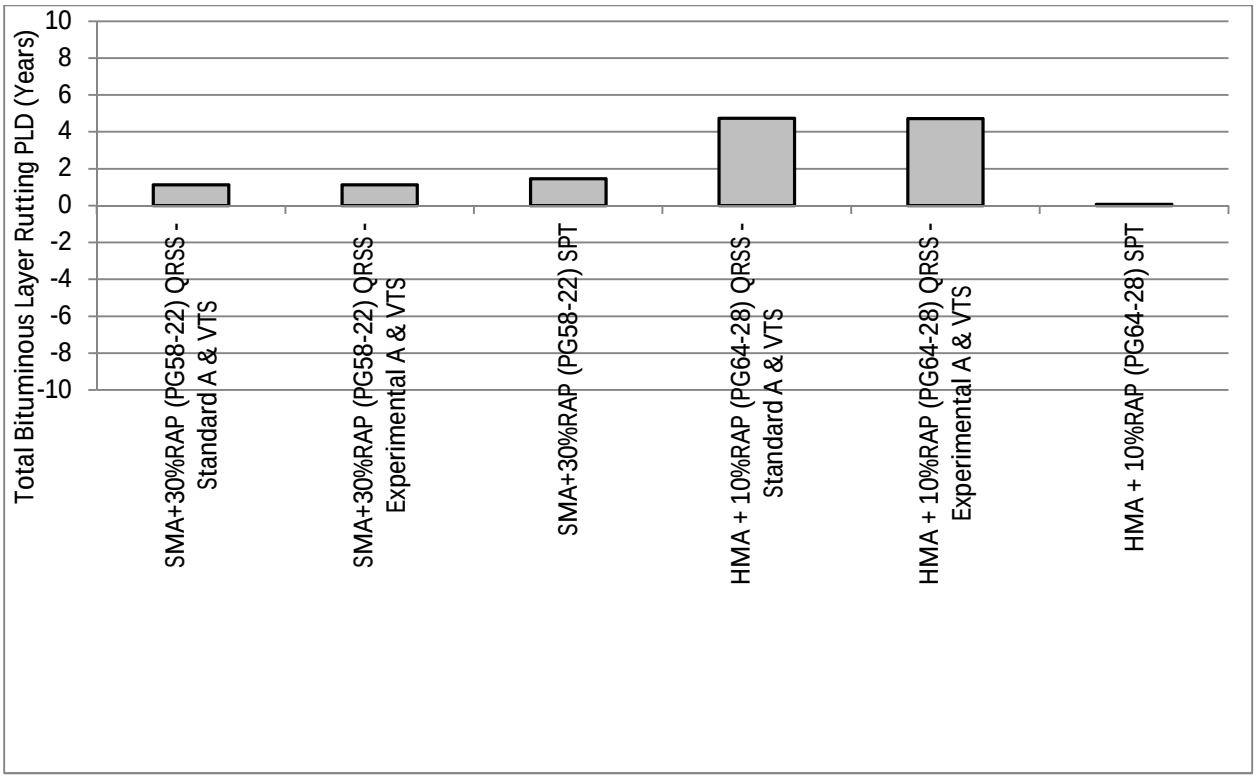

Figure 40. Total Bituminous Layer Rutting PLD Results for SMA+30% RAP and HMA+10% RAP Mixtures.

Fatigue cracking results are plotted in Figure 41 and the PLD results for the FHWA paving projects (SMA+30% RAP and HMA+10% RAP) are plotted in Figure 42. Fatigue cracking results for both FHWA paving projects are remarkably consistent across all three analysis iterations at the macro level; however, the PLD results can vary from as high +41 years to as low as -6 years when analyzed lot by lot. The scale of the PLD values observed indicate that it is likely the fatigue cracking PLD limits for payment that may need to be adjusted to account for the larger scale of variation typically seen between lots in all of the paving mixtures analyzed.

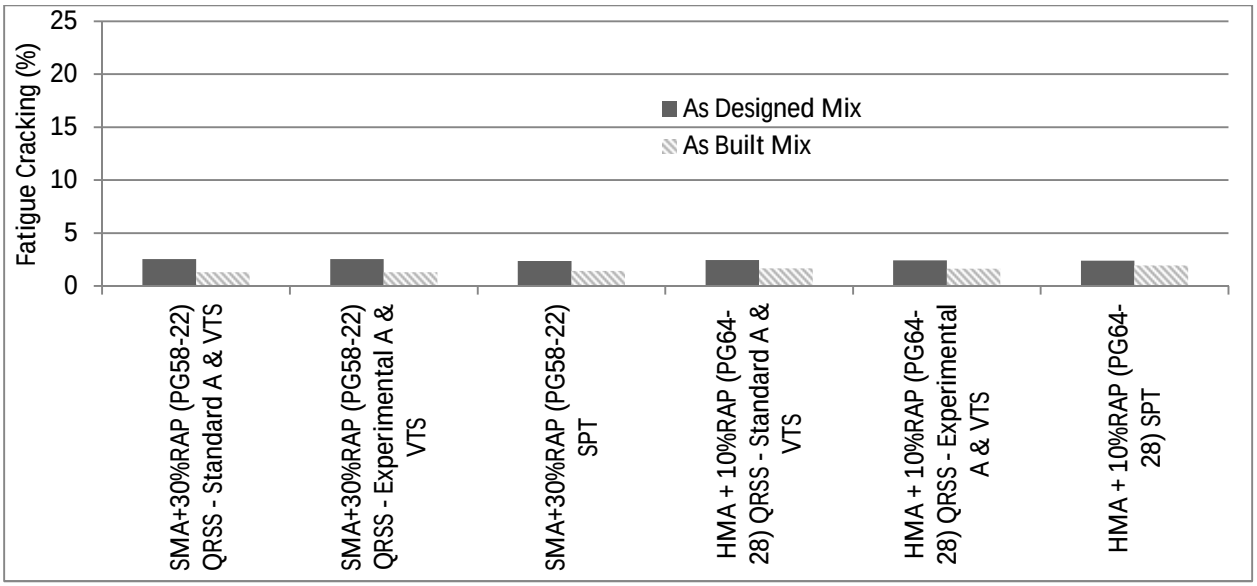

Figure 41. Fatigue Cracking Distress Results for SMA+30% RAP and HMA+10% RAP Mixtures.

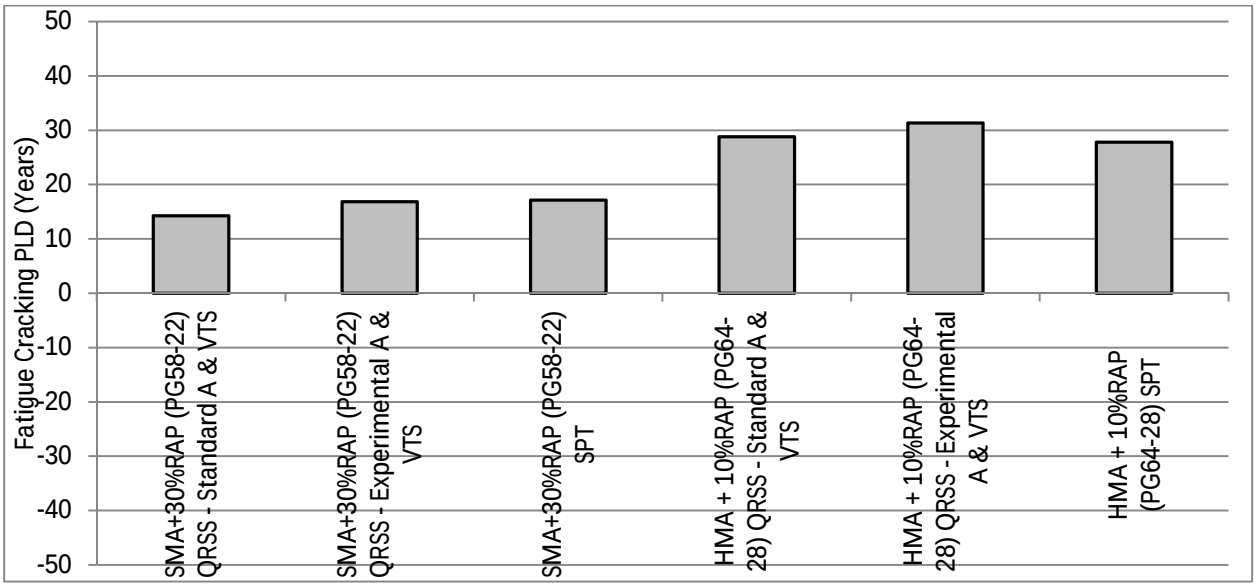

Figure 42. Fatigue Cracking PLD Results for SMA+30% RAP and HMA+10% RAP Mixtures.

3.1.5 Parametric Analysis in SPT Program

A brief parametric analysis was performed to determine the effect of traffic and structural variation on the distress and payment results predicted by the SPT Program. The analysis

followed the matrix shown in Table 17. The ESAL calculations for the traffic variation are presented in Table 18. A modification to the ESAL calculations was made due to a minor variation in the method used by DelDOT. A few of the AADTT values incorporated into the average AADTT calculations were multiplied by a truck factor value (= 1.6 ESALs/truck). As a result, the Year 1 Daily ESAL value DelDOT provided (988 ESALs/Day) was slightly higher than the one calculated by the standard AASHTO method (918 ESALs/Day) in Table 18. The values calculated in Table 18 for the AADTTx2 and AADTTx5 portions of the sensitivity analysis were multiplied by a factor of 988/918 to arrive at the ESAL values used in the analysis.

Table 17. Parametric Analysis Matrix for Analysis of SPT Predictions.

SPT Run		Variable
WMA-SMA LC-IDT		AADTTx2
WMA-SMA LC-UC	X	AADTTx5
HMA Hi-RAP LC-IDT		4-inch Base Thickness
HMA Hi-RAP LC-UC		4-in Base Thickness and4-in Subbase Thickness
		Subgrade M_R = 5,000 psi
		AADTx5, 4-in Base and Subbase, Subgrade M_R = 5,000 psi

Table 18. DelDOT Traffic ESAL Calculations for SPT Program Sensitivity Analysis.

	Mix	ADTT	Tf_i	Design life (yrs)	Growth Rate	GY	D	L	Year 1 Daily ESAL	Yearly ESALs	Total ESALs by AASHTO Method	Year 1 Daily ESAL used in Analysis
Sensitivity Analysis	**DelDOT US-13 HMA & SMA**	1401	1.3	10	0.92%	10.43	63%	80%	**918**	335,046	3,496,879	988 (per calculations provided by DelDOT)
		2802	1.3	10	0.92%	10.43	63%	80%	**1,836**	670,093	6,993,757	x 988/918 = 1976
		7000	1.3	10	0.92%	10.43	63%	80%	**4,586**	1,674,036	17,471,914	x 988/918 = 4936

Surface rutting distress results predicted by the SPT Program are presented in Figure 43for the HMA Hi-RAP mixture and in Figure 44 for the WMA-SMA. Distress levels increased linearly with an increase in AADT, showing approximately a 30% increase in surface rutting

depth at twice the AADT and a 65% increase in surface rutting depth at five times the AADT. Surface rutting was unaffected by changes to the substructure and this result can be explained since the surface rutting is a function of the design traffic inputs, the surface layer mixture volumetrics, and |E*| data only. The worst case scenario (combination of high traffic, thin underlying layers, and a poor subgrade stiffness) produced rutting levels equivalent to the AADTx5 iteration, confirming that only AADT variation affected the surface rutting results significantly for the variables chosen. Pay factors predicted appeared to be insensitive, remaining at 100% pay for all lots and specimen types with each variable change. This finding pointed to the fact that relative distress levels between the design mix and as-built mix corresponded uniformly with each change of variable, leaving the PLD values and resultant pay factors unchanged across all portions of the sensitivity analysis test matrix.

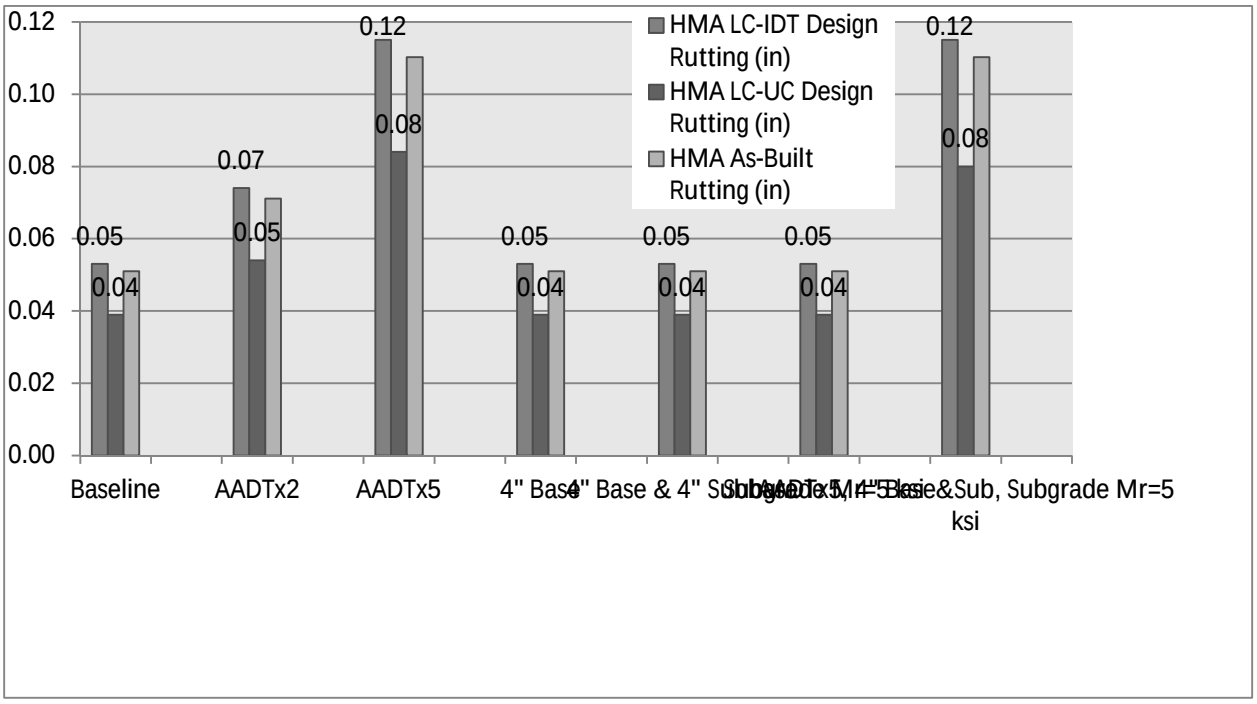

Figure 43. Sensitivity of HMA Hi-RAP Mixture in Surface Rutting.

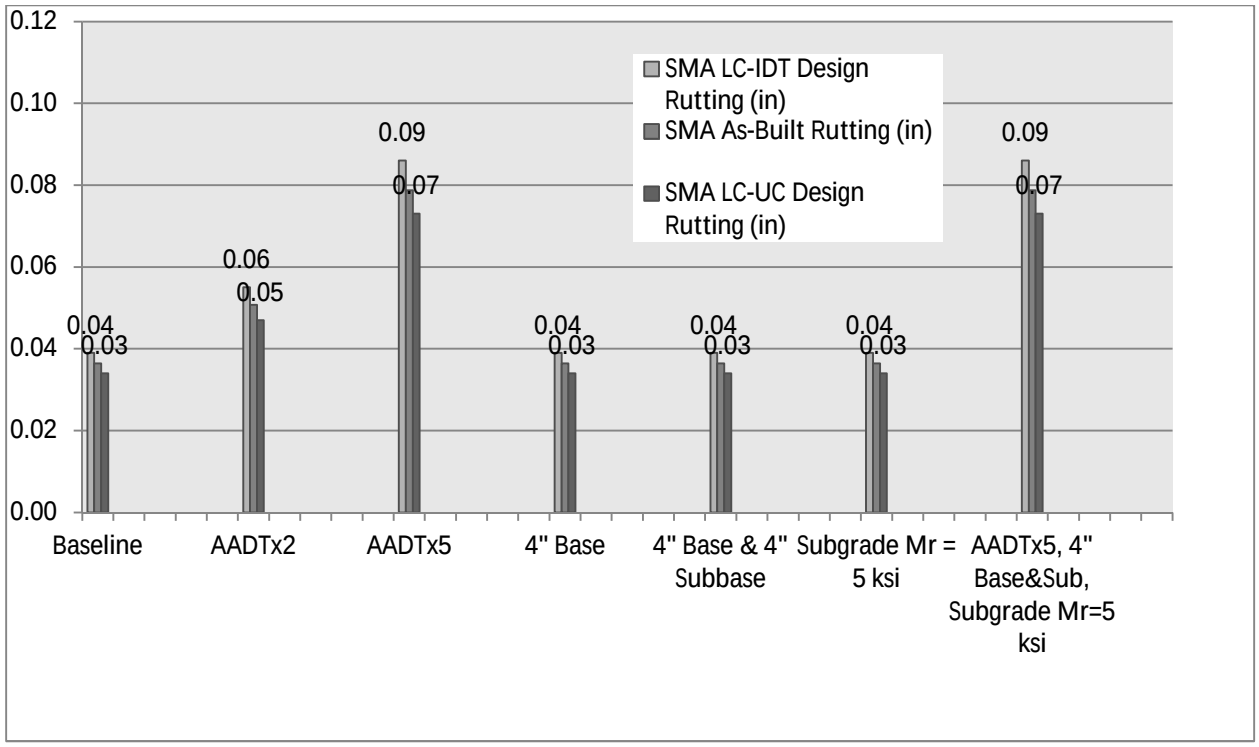

Figure 44. Sensitivity of WMA-SMA Mixture in Surface Rutting.

Overall, trends for the binder rutting were similar to surface rutting and indicated linear variation with traffic. The overall PLD and pay factor values were not affected by the sensitivity analysis, mostly due no change in the relative stiffness between design mix and as-built mix calculated by the SPT Program.

Fatigue cracking results were virtually identical between the HMA Hi-RAP and WMA-SMA mixes, likely due to the use of the RIDOT Route 102 data for the binder lift in the analysis. Fatigue cracking distress showed equivalent linear variation with traffic as in the rutting distress discussed previously. In addition, varying the base thickness, subbase thickness, and subgrade M_R caused an increase in fatigue cracking distress in the binder lift. There was up to a 30% increase in fatigue cracking over the baseline values when the subgrade M_R was reduced to 5,000 psi. The worst case scenario caused a 400% increase (63% from 13% for the as-built mix) in fatigue cracking as compared to baseline values; however, none of this distress variation affected

the PLD values or pay factors. The design mixes and as-built mixes varied linearly with each other across the sensitivity analysis, resulting in no change in relative distress between design mix and as-built mix.

3.1.6 Summary of Findings for QRSS and SPT Program Analysis

Based on comparisons between the two performance-related analysis programs for each of the mixtures evaluated, it is apparent that the use of laboratory-measured binder data inputs versus standard PG-grade binder inputs has minimal effect on the final PLD results. Therefore, it also had a minimal effect on the resultant pay factors produced by the SPT Program. The largest variation is shown in the surface layer rutting PLD at approximately ±0.2 years. This was tested in the surface layer across all projects, and also in the binder layer for the Maine DOT Township D project since it was the only one that involved full-depth reconstruction.

Fatigue cracking was highly variable within each analysis run, with the models which are based partially on the RI Rt 102 data from NCHRP Project 9-22A typically varying between maximum payment bonuses to remove/replace from one lot to the next with no middle ground. It is understood from NCHRP 9-22A that the QA data used from RI for this project contained two lots with higher air void content and lowered effective binder content. MEDOT Township D fatigue cracking values were similar to the DelDOT runs using the RIDOT Rt 102 binder data, with pay factors varying significantly. It is important to consider that while the variation in fatigue cracking results was very inconsistent lot to lot within each analysis iteration, overall both the QRSS and SPT were typically consistent in agreeing which lots. It is possible that the scale of PLD limits for fatigue cracking analysis should be expanded to account for the significant variation typically seen in analysis results for both programs. Table 19 shows a potential modification to the PLD limits which would result in results more friendly to both the

contractor and the state agency (i.e. fewer of both remove/replace and maximum pay incentive results).

Table 19. Potential Modifications to Fatigue Cracking PLD Limits.

Pay Adjustment Parameter	Original PLD Limit	Modified PLD Limit
Minimum for No Penalty	-2	-5
Minimum for Pay Bonus	2	5
Maximum Pay Penalty	-5	-10
Minimum for Remove/Replace	-7	-15
Maximum Pay Bonus	7	10

Surface rutting distress and PLD results across all analysis programs and specimen types showed that despite the different specimen types and binder data sources creating small variations in the surface rutting distress results, the resulting PLDs were typically very precise when considering the scale of PLD values observed. In almost all cases, the difference in surface rutting PLD results was less than ±1.0 year regardless of program or specimen type.

The most variation in surface rutting was seen in the MEDOT Township D HMA paving project. This could be explained by the fact that only one lot of materials for dynamic modulus testing was available for the SPT Program analysis, causing the evaluation of the stiffness of the surface layer to resist rutting to be dependent on a single dynamic modulus curve rather than an average of multiple lots as was done with the DelDOT mixes.

The comparison between QRSS and SPT Program results using the two DelDOT mixes indicates that among the SPT Program analysis, the as-designed models based off the dynamic modulus testing of the stiffer lab compacted samples produced virtually identical rutting distress values compared the as-built analysis using the field core samples for an equivalent lot. This variance between models was consistent across all five lots of the DelDOT SMA+RAP and both lots of the DelDOT HMA+RAP. This produced similar PLD results for the DelDOT mixes for the two SPT runs. The magnitude of variation was very small, on the order of ±0.2 years PLD

between the UC samples and the IDT samples, resulting in identical 100% pay factors regardless of the analysis program.

Comparisons between the surface rutting PLD results from the QRSS and the SPT Program analysis for DelDOT did not show obvious correlation from one lot to the next with variation up to ±1 year PLD between the QRSS and SPT Program for the DelDOT HMA Hi-RAP mix.

Similar to the surface rutting results, binder rutting results from all the candidate projects showed almost no deviation from 100% payment despite minor variations in distress and PLD results between analysis programs and specimen types.

A sensitivity analysis conducted on the DelDOT SPT Program results showed that while design and as-built predicted rutting distress varied linearly with traffic variation, they also tended to vary uniformly with each other meaning the relative distress between the as-designed and as-built mixes did not vary enough to produce appreciably different predicted life difference or pay factor results. These findings were also true of the binder layer rutting and fatigue cracking results.

3.2 Mixture Performance Evaluated with AASHTO MEPDG Program

Analyses of the selected six case study projects (four from the participating DOTs and two from past FHWA MAMTL projects) were conducted with the AASHTO MEPDG version 1.0 software. Based on the availability of data, MEPDG analyses were performed with Level 1, Level 2, and Level 3 inputs for the HMA material properties. Table 20 provides a summary of the selected projects analyzed using the MEPDG version 1.0 software.

Table 20. Projects Analyzed With MEPDG Version 1.0 software.

DOT	PROJECT	MIXTURE TYPE	BINDER TYPE
DE	Rt. 13 Duck Creek Road	WMA-SMA + 10% RAP	PG 76-22
DE	Rt. 13 Duck Creek Road	C/160 HMA + 35% RAP (HMA Hi-RAP)	PG 64-28
DE	FHWA DE0883	SMA + 30% RAP	PG 58-22
ME	Route 17	DGA HMA + 15% RAP	PG 64-28
ME	FHWA ME0359	HMA + 10% RAP	PG 64-28
RI	Dunn's Corner	DGA HMA	PG 64-28

3.2.1 Summary of MEPDG Analyses for Each Project

The MEPDG analyses with Level 3 HMA inputs were performed using only volumetric data. MEPDG analyses with Level 2 HMA inputs used the binder shear modulus (G*) and phase angle (δ) data obtained from laboratory testing. The G* and δ data were also used in conjunction with |E*| values from the three different specimen configurations (plant-produced/QC laboratory-compacted (PP/QC) from uniaxial compression; plant-produced/laboratory-compacted (PP/LC) from IDT; plant-produced/field-compacted (PP/FC) from IDT) to perform MEPDG analysis with Level 1 HMA inputs. Rutting in both the surface lift and the composite of bituminous layers, along with fatigue cracking, were evaluated and compared among each of the specimen/configuration types.

3.2.1.1 WMA-SMA Mixture

The analysis of this mixture was performed on a 2-inch lift of the PG 76-22 9.5mm WMA-SMA overlay, 2.5-inch PG 64-22 19mm binder course, 2.5-inch 19mm HMA, 10-inch cold recycle asphalt pulverized-in-place, a 12-inch layer of A-1-a AASHTO classified soil, and a semi-infinite layer of AASHTO A-1-b classified soil. The soil modulus was taken from a nearby climatic site in southern New Jersey since there was information on soil moduli for Delaware

[NCHRP (2007)]. Figure 45 illustrates the cross-sectional profile of Route 13 Duck Creek Road based on the information provided by DelDOT.

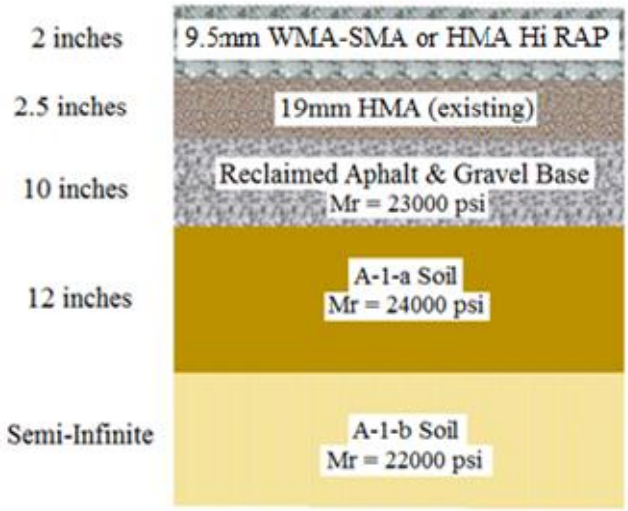

Figure 45. Route 13 Duck Creek Road Cross-Section (Analyzed with WMA-SMA and HMA Hi-RAP Mixtures).

Table 21 summarizes the experimental binder data (G* and δ) inputted from laboratory testing for Levels 1 and 2 in the MEPDG software.

Table 21. WMA-SMA Mixture Binder Data.

WMA-SMA + 10% RAP,PG76-22		
Temperature (°F)	**at 10 rad/sec**	
	G* (Pa)	d
10	303,256,923	21.46
40	41,723,691	36.02
70	3,985,928	49.71
100	342,394	59.98
130	38,817	67.02

Binder data from the 10^{o} F test temperature were not inputted to the analysis because the MEPDG software allowed only inputs for temperatures between 40^{o} F and 130^{o} F. A summary of the |E*| data were obtained from three different sources are presented in the following tables as:

- Uniaxial Compression testing of plant-produced and laboratory-compacted samples (Table 22);
- IDT testing of plant-produced and laboratory-compacted samples (Table 23); and,
- IDT testing of plant-produced and field-compacted samples (Table 24).

Table 22. LC-UC |E*| Data Used in Analysis of WMA-SMA Mixture.

Temperature (^{o}F)	Uniaxial Compression Laboratory-Compacted |E*|for WMA-SMA (psi)					
	0.1 Hz	0.5 Hz	1.0 Hz	5.0 Hz	10.0 Hz	25.0 Hz
10	1,584,383	1,934,496	2,070,127	2,342,296	2,440,666	2,554,079
40	1,369,197	1738608	1887038	2193432	2306896	2,439,459
70	331,744	560,334	684,755	1,022,248	1,181,406	1,396,107
100	73,141	132,813	172,395	310,365	393,641	527,999
130	26,844	43,124	54,245	96,467	124,983	176,295

Table 23. LC IDT |E*| Data Used in Analysis of WMA-SMA Mixture.

Temperature (^{o}F)	IDT Laboratory-Compacted |E*|for WMA-SMA (psi)					
	0.1 Hz	0.5 Hz	1.0 Hz	5.0 Hz	10.0 Hz	25.0 Hz
10	1,436,815	1,710,935	1,823,735	2,065,707	2,159,685	2,273,588
40	1,263,044	1,544,148	1,662,866	1,923,346	2,026,594	2,153,251
70	372,773	560,498	656,994	912,537	1,033,158	1,198,487
100	85,762	146,609	183,612	301,791	368,551	472,621
130	27,548	45,089	56,504	96,930	122,454	166,122

Table 24. FC IDT |E*| Data Used in Analysis of WMA-SMA Mixture.

Temperature (°F)	IDT Field-Compacted |E*|for WMA-SMA (psi)					
	0.1 Hz	0.5 Hz	1.0 Hz	5.0 Hz	10.0 Hz	25.0 Hz
10	769,486	1,097,010	1,245,777	1,588,188	1,728,398	1,902,549
40	613,325	917,138	1,061,551	1,407,533	1,554,293	1,740,434
70	101,970	192,894	250,342	436,031	539,715	697,338
100	22,872	41,505	54,538	104,444	137,958	197,427
130	9,412	14,661	18,253	32,182	41,935	60,258

Since version 1.0 of the MEPDG software did not accept |E*| values below 10,000 psi, the |E*| value obtained at a temperature of 130^{o} F and at a frequency of 0.1 Hz (9,412 psi) was changed to 10,000 psi in order to allow the software to perform the analysis. Predicted fatigue cracking and rutting values obtained from analysis with Level 1, Level 2 and Level 3 HMA inputs are presented in Table 25. The distress targets were selected by the DOT along with a pavement life of ten years. All distress predictions fell below the targets set by DelDOT. The predicted distresses show that the structure was more susceptible to rutting but performed well in fatigue. The rutting predictions for the surface may be biased in that the MEPDG version 1.0 software was not calibrated to unconventional gradations or highly modified mixtures. Therefore, it could be that the rutting predictions are higher than what may actually occur in the field. In addition, the artificial stiffening which has been presumed to occur with laboratory-compacted samples can be seen in the surface rutting predictions, with the uniaxial compression specimen type resulting in the lowest level of rutting.

Table 25. Distress Predictions for Structure with WMA-SMA Surface.

Performance Criteria	Distress Target	MEPDG Predicted Distresses				
		Level 3	Level 2	Level 1		
				Uniaxial Compression	IDT Lab Compacted	IDT Field Compacted
AC Bottom Up Cracking (Alligator Cracking) (%):	20	0.1	0	0.3	0.2	0
Permanent Deformation (AC Only) (in):	0.5	0.42	0.43	0.39	0.4	0.45
Permanent Deformation (Total Pavement) (in):	1	0.84	0.84	0.79	0.8	0.87

3.2.1.2 HMA High-RAP Mixture

Analysis of the PG 64-28 HMA mixture produced with 35% RAP (designated the HMA Hi-RAP mixture) consisted of the same cross-section illustrated previously in Figure 45, with replacement of the surface lift with the HMA Hi-RAP mix. Details on the experimental binder data (G* and δ) used as Levels 1 and 2 inputs in the MEPDG software are included in Appendix C. Once again, values tested at 10^{o} F were not used since the software only allowed inputs for temperatures between 40^{o} F and 130^{o} F. The Level 1 |E*| inputs for this project from the three different specimen types and test procedures are presented in Appendix C.

Predicted fatigue cracking and rutting values obtained with Level 1, Level 2 and Level 3 HMA inputs are presented in Table 26. As in the previous mixture, all distress predictions fell below the targets set by DelDOT. The findings are similar to the WMA-SMA mixture in terms of the slight artificial stiffening of laboratory-compacted mixtures and the additional stiffness added by the high RAP percentage may not be accurately reflected in the default calibration factors in the MEPDG software. The amount of variation between predictions using Levels 1 and 2 inputs is relatively low. This finding may indicate that use of experimental binder data (Level 2 inputs) in the analysis is adequate for the prediction of pavement distresses.

Table 26. Distress Predictions for Structure with HMA Hi-RAP Surface.

Performance Criteria	Distress Target	MEPDG Predicted Distresses				
		Level 3	Level 2	Level 1		
				Uniaxial Compression	IDT Lab Compacted	IDT Field Compacted
AC Bottom Up Cracking (Alligator Cracking) (%):	20	0.2	0.2	0.4	0.1	0
Permanent Deformation (AC Only) (in):	0.5	0.43	0.43	0.4	0.42	0.45
Permanent Deformation (Total Pavement) (in):	1	0.84	0.84	0.8	0.84	0.88

3.2.1.3 Conventional Dense-Graded HMA+RAP Mixture

This project consisted of a full-depth reconstruction of a section of two-lane roadway in northern Maine. The pavement's cross-section is shown in Figure 46 and featured a 1.25-inch PG 64-28 9.5mm HMA surface produced with 15% RAP, a 1.75-inch PG 64-28 12.5mm HMA binder lift, a 2-inch 64-28 19mm HMA base courses, a 18-inch crushed gravel subbase, and a semi-infinite layer of A-7-6 AASHTO classified soil.

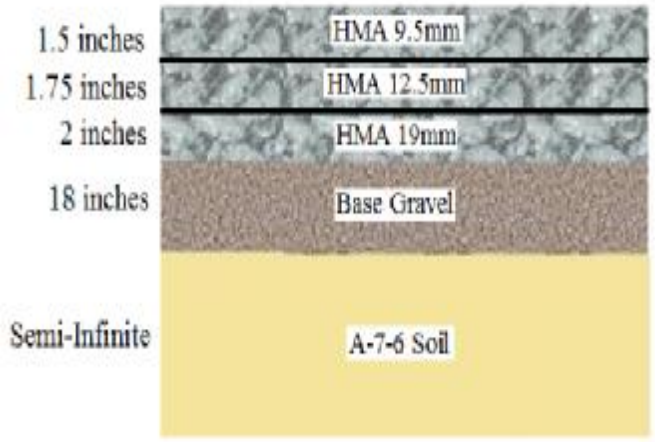

Figure 46. Township D Road Cross-Section (Analyzed with HMA+RAP Mixture).

Tables included in Appendix C present the experimental binder data. For this project, the |E*| data were obtained from four different conditions for specimen type and test procedure:

- Uniaxial Compression testing of plant-produced and contractor QC laboratory-compacted samples,
- Uniaxial Compression testing of plant-produced and laboratory-compacted samples,
- IDT testing of plant-produced and contractor QC laboratory-compacted samples,
- IDT testing of plant-produced and field-compacted samples.

The following tables (Tables 28 through 31) summarize the |E*| values used as Level 1 inputs for the various specimen and test configurations for the HMA surface lift. Corresponding tables for the binder lift and bituminous base lift are presented in Appendix C.

Table 27. LC-UC |E*| Data Used in Analysis of HMA+RAP Surface Mixture.

Temperature (°F)	Uniaxial Compression Laboratory-Compacted |E*|for 9.5mm HMA+RAP (psi)					
	0.1 Hz	0.5 Hz	1.0 Hz	5.0 Hz	10.0 Hz	25.0 Hz
10	1,951,100	2,214,854	2,315,590	2,519,146	2,594,218	2,682,630
40	733,087	1,035,547	1,174,430	1,501,182	1,638,949	1,814,356
70	154,894	282,215	356,218	574,775	687,740	851,505
100	29,161	60,487	82,026	159,981	208,823	290,305
130	7,435	15,091	20,679	43,155	58,956	88,104

Table 28. QC Plant-Compacted UC |E*| Data Used in Analysis of HMA+RAP Surface Mixture.

Temperature (°F)	Uniaxial Compression QC Plant-Compacted |E*|for 9.5mm HMA+RAP (psi)					
	0.1 Hz	0.5 Hz	1.0 Hz	5.0 Hz	10.0 Hz	25.0 Hz
10	1,685,839	1,957,240	2,063,042	2,280,428	2,361,817	2,458,522
40	573,377	839,826	966,289	127,2911	1,405,756	1,577,781
70	114,153	213,792	273,448	455,551	552,622	696,413
100	21,763	45,397	61,881	122,820	161,844	228,124
130	5,802	11,687	15,992	33,428	45,803	68,857

Table 29. Laboratory-Compacted IDT |E*| Data Used in Analysis of HMA+RAP Surface Mixture.

Temperature (°F)	IDT Laboratory-Compacted |E*|for 9.5mm HMA+RAP (psi)					
	0.1 Hz	0.5 Hz	1.0 Hz	5.0 Hz	10.0 Hz	25.0 Hz
10	1,426,030	1,812,206	1,967,984	2,289,101	2,407,404	2,544,809
40	414,713	660,112	792,246	1,148,102	1,314,866	1,538,674
70	127,338	203,490	251,702	413,094	507,699	657,791
100	62,094	87,191	103,353	160,924	197,838	262,045
130	42,790	53,546	60,299	84,013	99,268	126,320

Table 30. Field-Compacted IDT |E*| Data Used in Analysis of HMA+RAP Surface Mixture.

Temperature (°F)	IDT Field-Compacted |E*|for 9.5mm HMA+RAP (psi)					
	0.1 Hz	0.5 Hz	1.0 Hz	5.0 Hz	10.0 Hz	25.0 Hz
10	1,367,071	1,702,748	1,840,745	2,135,729	2,249,803	2,387,634
40	342,483	556,772	669,441	969,677	1,110,943	1,303,261
70	62,262	119,414	156,392	281,014	354,121	470,248
100	15,141	28,351	37,563	72,742	96,387	13,8567
130	5,876	9,839	12,569	23,173	30,581	44,454

Tables summarizing the |E*| data from all three bituminous layers for the plant-compacted and field-compacted specimens are included in Appendix C. Once again, the |E*| values for 130^{o}F at 0.1Hz and 0.5 Hz were changed to 10,000 psi in order to perform the MEPDG analysis. The same change was applied to the |E*| value at 130^{o}F and 0.1Hz and the |E*| values for 130^{o}F at

0.1Hz, 0.5 Hz, and 1.0 Hz. When using the data as Level 1 HMA inputs for the analysis, the MEPDG software would not function properly and crashed, despite many attempts. Results from the MEPDG analyses are summarized in the following table, excepting the IDT field-compacted which could not be generated due to software issues. Table 31 shows that there is very little impact of the HMA input level on the distresses predicted. A slight variation is observed among specimen types, which could again be explained by the calibration of the MEPDG version 1.0 models (that do not include a significant number of mixtures produced with RAP) and the additional stiffness due to reheating (for laboratory-compacted samples).

Table 31. Distress Predictions for Structure with HMA+RAP Mixture Used in Full-Depth Reconstruction.

Performance Criteria	Distress Target	MEPDG Predicted Distresses					
				Level 1			
		Level 3	Level 2	Uniaxial Compression LC	Uniaxial Compression PC	IDT Lab Compacted	IDT Field Compacted
AC Bottom Up Cracking (Alligator Cracking) (%):	25	0.6	0.6	0.5	0.6	0.6	-
Permanent Deformation (AC Only) (in):	0.25	0.1	0.1	0.08	0.11	0.1	-
Permanent Deformation (Total Pavement) (in):	0.5	0.69	0.7	0.66	0.72	0.7	-

3.2.1.4 Conventional Dense-Graded Asphalt HMA

The project mix evaluated was the conventional dense-graded asphalt (DGA HMA) with no modification and no RAP. The pavement cross-section for Dunn's Corner Road in Rhode Island is shown in Figure 47.

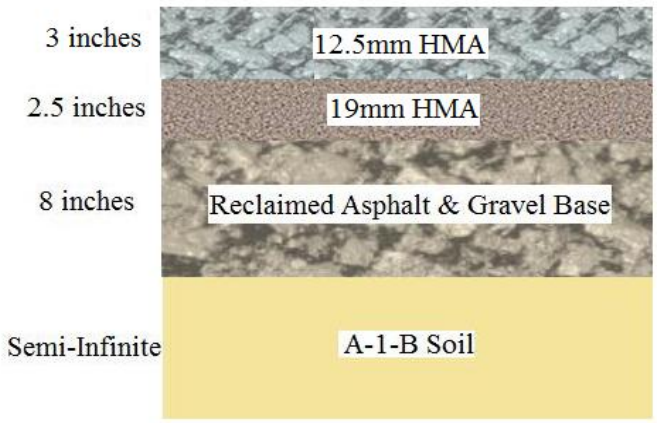

Figure 47. Dunn's Corner Road Cross-Section (Analyzed with DGA HMA Mixture).

Tables included in Appendix C present the experimental binder data and the |E*| data obtained from uniaxial compression testing of plant-produced laboratory-compacted samples which was used as Level 1 and 2 inputs in the MEPDG analysis. Results from the MEPDG analysis of the Dunn's Corner Road project are summarized in Table 32 and the trends observed reflect those in the other mixtures discussed previously.

Table 32. Distress Predictions for Structure with DGA HMA Mixture.

Performance Criteria	Distress Target	MEPDG Predicted Distresses		
		Level 3	Level 2	Level 1
				Uniaxial Compression LC
AC Bottom Up Cracking (Alligator Cracking) (%):	25	0.1	0.1	0.1
Permanent Deformation (AC Only) (in):	0.25	0.17	0.19	0.15
Permanent Deformation (Total Pavement) (in):	0.5	0.43	0.44	0.4

3.2.1.5 FHWA DE0883 SMA + 30 % RAP Mixture

As discussed previously, the researchers coordinated with FHWA Office of Pavement Technology and Turner-Fairbanks Highway Research Center to obtain critical asphalt material property data (G*, delta, |E*|, VMA, air voids, binder grade, aggregate gradation, etc.) for two completed projects that exhibited similar geographic conditions, mixture characteristics, and traffic levels in Delaware and Maine. This data was used in the MEPDG simulations as additional inputs for pavement performance predictions. Corresponding general traffic data and underlying pavement layer inputs (Level 3) were based on the characteristics of the projects from which the FHWA asphalt data (Level 1) was obtained.

The FHWA DE0883 project consisted of a2-inch PG58-22 9.5mm HMA overlay, 6-inch PG 64-22 19mm binder course, 12-inch granular base, 12-inch granular subbase, and a semi-infinite layer of A-2-4 AASHTO classified soil shown in Figure 48.

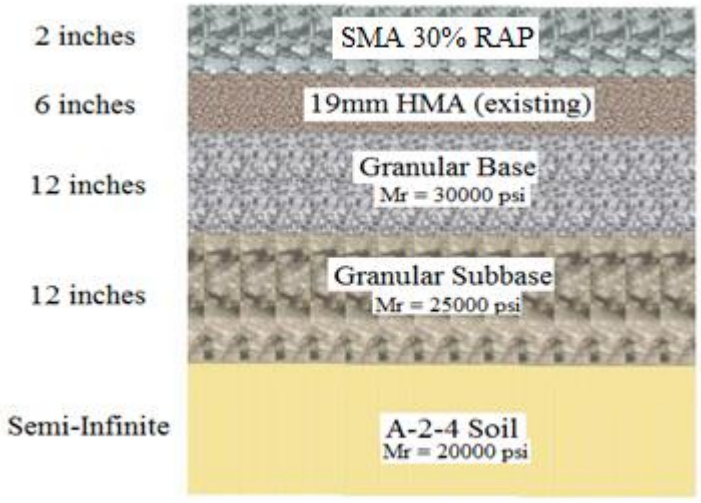

Figure 48. FHWA DE0883 Cross-Section (Analyzed with SMA+30%RAP Mixture).

Tables in Appendix D summarize the binder and |E*| input data (G* and δ) obtained by the FHWA MAMTL testing. Results from the MEPDG analyses of the SMA + 30% RAP are summarized in Table 33. In this analysis, there appears to be more variation in the predictions between the various HMA input levels and the level of distress may be inflated due to the predictive models not properly implementing the characteristics of a modified mixture gradation with RAP.

Table 33. Distress Predictions for Structure with SMA+30%RAPMixture.

Performance Criteria	Distress Target	MEPDG Predicted Distresses		
		Level 3	Level 2	Level 1
				Uniaxial Compression LC
AC Bottom Up Cracking (Alligator Cracking) (%):	20	1.2	0.9	4.9
Permanent Deformation (AC Only) (in):	0.5	1.06	1.12	0.89
Permanent Deformation (Total Pavement) (in):	1	1.42	1.48	1.23

3.2.1.6 FHWA ME0359 HMA + 10 % RAP 64-28

This surface mixture came from FHWA ME0359 project which was a full-depth reconstruction with the cross-section shown in Figure 49 and featured a 9.5mm PG 64-28 HMA produced with 10% RAP. Results of the MEPDG analyses are provided in Table 34. Because this mixture had characteristics that were closer to the conventional designs that the MEPDG predictive models were based upon, the variation in distress among the various input levels was insignificant.

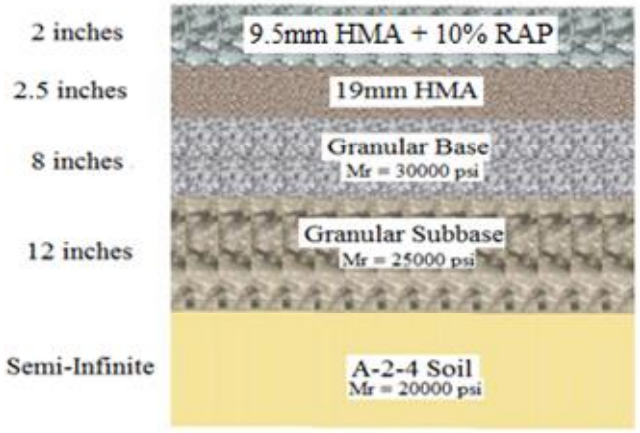

Figure 49. FHWA ME0359 Cross-Section (Analyzed with HMA+10%RAP Mixture).

Table 34. Distress Predictions for Structure with HMA + 10% RAP.

Performance Criteria	Distress Target	MEPDG Predicted Distresses		
		Level 3	Level 2	Level 1
				Uniaxial Compression
AC Bottom Up Cracking (Alligator Cracking) (%):	25	0.1	0.1	0.1
Permanent Deformation (AC Only) (in):	0.25	0.54	0.53	0.53
Permanent Deformation (Total Pavement) (in):	0.5	0.94	0.94	0.93

3.2.2 Parametric Analysis in AASHTO MEPDG 1.0 Software

As previously discussed in section 3.1.5, a brief parametric analysis was performed to determine the impacts of traffic and structural variation on the distress levels predicted by the SPT Program, as well as in the AASHTO MEPDG version 1.0 software. The analysis followed the matrix shown in Tables 18 and 19.MEPDG analyses were run with Level 1 HMA inputs for the WMA-SMA and HMA Hi-RAP project mixtures based on |E*| data measured from each specimen type and test configuration. The following list represents the parameters changed in the six different scenarios used to perform the sensitivity analysis in the MEPDG:

- Increase AADTT (from 1,401 vehicles per day (vpd) to 2,802 vpd);
- Increase AADTT (from 1,401vpd to 7,000 vpd);
- Decrease base layer thickness (from 10 inches to 4 inches);
- Decrease base layer thickness (from 10 inches to 4 inches) and decrease subbase layer thickness (from 12 inches to 4 inches);
- Decrease subgrade modulus (from AASHTO A-2-4 with M_R= 22,000psi to AASHTO A-6-7 with M_R = 5,000psi);
- Combined previous five scenarios to create the worst case scenario (AADTT = 7,000vpd, base thickness = 4 inches, subbase thickness = 4 inches, and subgrade A-7-6, M_R = 5,000psi)

A total of thirty six MEPDG analyses were conducted with Level 1 HMA inputs to test the scenarios listed for each specimen type and test configuration. The results of the analyses were compared to those of the original baseline structure. The baseline structure is the pavement cross-section from the DelDOT Route 13 Duck Creek Road shown previously in Figure 45. The results of the analyses and the related predicted performance distresses (fatigue cracking and

permanent deformation) are included in Table 35for the WMA-SMA mixture and in Table 36 for HMA Hi-RAP mixture. The shaded boxes in the tables indicate where the pavement damage that exceeded the threshold level for that distress type.

Table 35. Sensitivity Analysis of WMA-SMA Mixture in MEPDG Software.

	MEPDG Predicted Pavement Distresses								
	Uniaxial Compression - E*			IDT Lab Compacted - E*			IDT Field Compacted - E*		
VARIABLE	Fatigue Cracking (%)	AC Rutting (in)	Total Rutting (in)	Alligator Cracking (%)	AC Rutting (in)	Total Rutting (in)	Alligator Cracking (%)	AC Rutting (in)	Total Rutting (in)
Baseline	0.3	0.39	0.79	0.2	0.4	0.8	0	0.45	0.87
AADTT x 2 (2,802 vpd)	0.6	0.54	0.98	0.4	0.55	0.99	0.1	0.62	1.08
AADTT x 5 (7,000 vpd)	1.8	0.84	1.32	1.3	0.86	1.34	0.2	0.96	1.47
Base 4 in	0.3	0.39	0.78	0.2	0.4	0.79	0	0.44	0.85
Base 4 in; Subbase 4 in	0.3	0.39	0.76	0.2	0.4	0.77	0	0.44	0.84
Subgrade A-7-6 M_R=5,000psi	0.3	0.4	1.05	0.2	0.4	1.06	0	0.44	1.11
Worst Case	2.9	0.96	2	1.9	0.96	2.01	0.2	0.96	2.05

Table 36. Sensitivity Analysis of HMA Hi-RAP Mixture in MEPDG Software.

	MEPDG Predicted Pavement Distresses								
	Uniaxial Compression - E*			IDT Lab Compacted - E*			IDT Field Compacted - E*		
VARIABLE	Fatigue Cracking (%)	AC Rutting (in)	Total Rutting (in)	Alligator Cracking (%)	AC Rutting (in)	Total Rutting (in)	Alligator Cracking (%)	AC Rutting (in)	Total Rutting (in)
Baseline	0.4	0.4	0.8	0.1	0.42	0.84	0	0.45	0.88
AADTT x 2 (2,802 vpd)	1	0.55	0.99	0.3	0.58	1.04	0.1	0.63	1.09
AADTT x 5 (7,000 vpd)	2.9	0.85	1.34	0.9	0.9	1.4	0.3	0.98	1.49
Base 4 in	0.4	0.4	0.79	0.1	0.41	0.82	0	0.45	0.86
Base 4 in; Subbase 4 in	0.5	0.4	0.77	0.1	0.42	0.81	0	0.45	0.85
Subgrade A-7-6 M_R=5,000psi	0.4	0.41	1.06	0.1	0.41	1.09	0	0.44	1.13
Worst Case	4.4	0.96	2.02	0.9	0.95	2.04	0.2	0.97	2.07

A number of plots were generated to compare the baseline design with the various parameters altered for both projects and for the three testing types. These 54 plots are included in Appendix C. A similar trend was observed in terms of the amount of fatigue cracking and rutting predicted for both mixtures and for all specimen types.

Traffic modifications to the baseline structure resulted in the same trend in terms of pavement distress for all conditions. As shown in Figures 50 through 55,the amount of fatigue cracking and rutting increase accordingly with increases in truck traffic volumes, regardless of specimen type or mixture. The same finding was true of modifications to the pavement structure. As shown in Figures 51 and 54, permanent deformation in the surface layer had very little variation when the base and subbase thicknesses were decreased. The same minimal variation was predicted when the subgrade strength was decreased. Total rutting was affected minimally when base and subbase thicknesses were decreased, but increased as expected when the subgrade strength was decreased. Fatigue cracking was minimally affected by any of the parametric changes to the baseline structure.

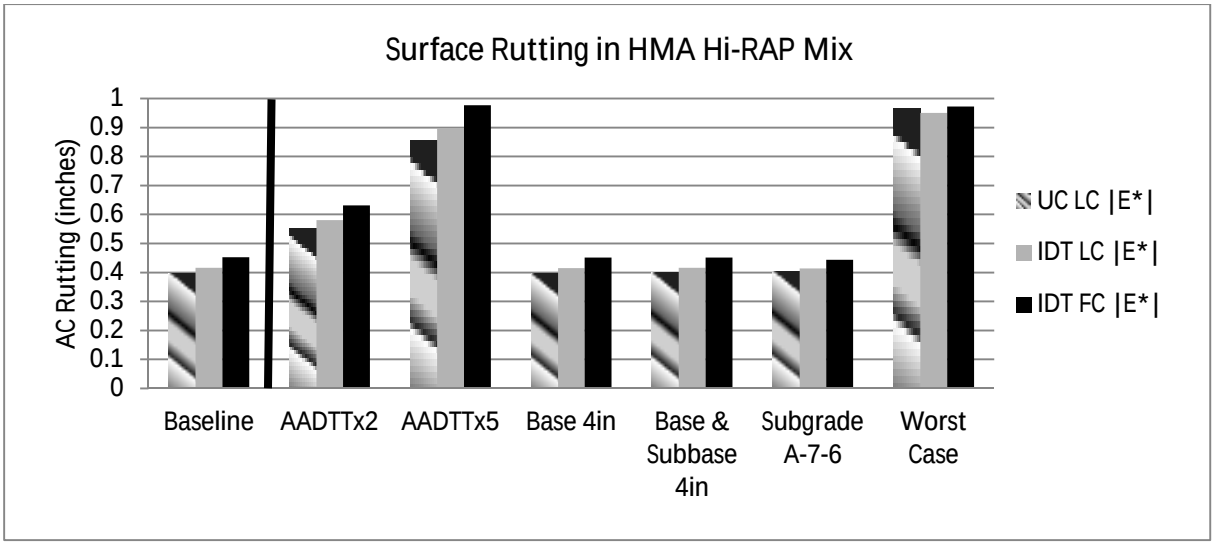

Figure 50. Parametric Analysis of HMA Hi-RAP Mixture Impact on Surface Rutting.

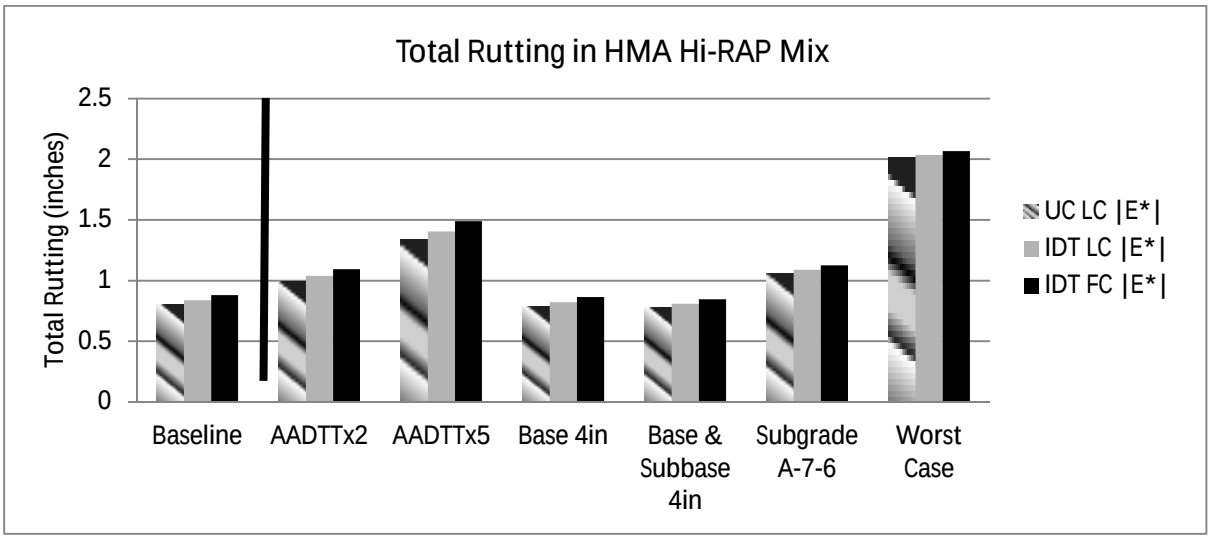

Figure 51. Parametric Analysis of HMA Hi-RAP Mixture Impact on Total Permanent Deformation.

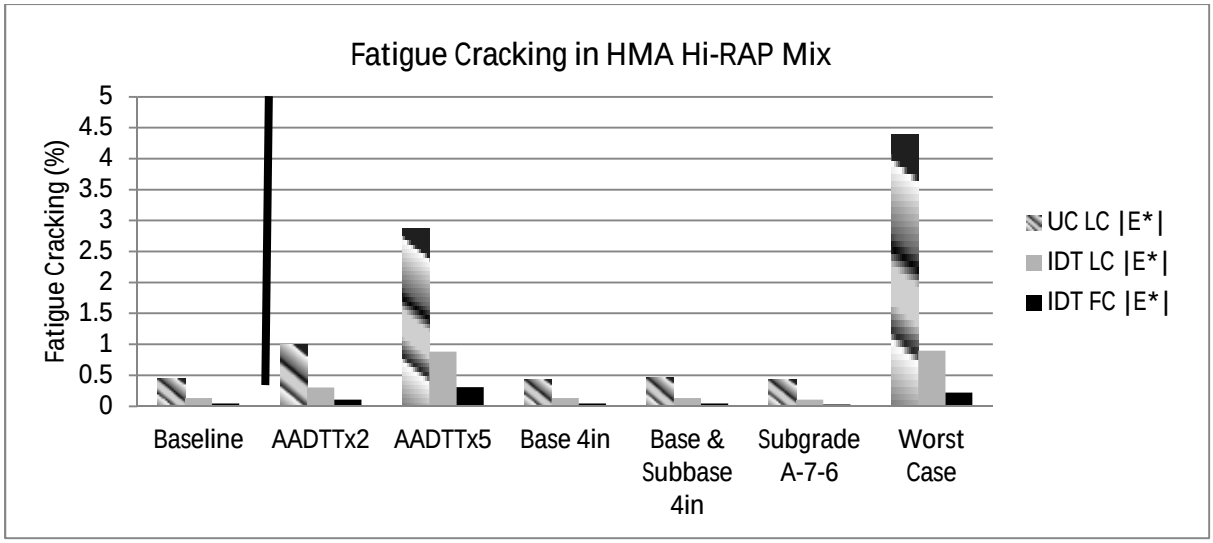

Figure 52. Parametric Analysis of HMA Hi-RAP Mixture Impact on Fatigue Cracking.

When comparing output from the modified design in which all parameters were altered (designated as the worst case scenario) from the baseline structure conditions, it was noted that fatigue cracking and rutting predictions increased amongst all of the testing types for both mixes. The figures indicate that all pavement distresses increased accordingly. Again, the same trends were observed regardless of specimen type for both the WMA-SMA and HMA Hi-RAP mixtures.

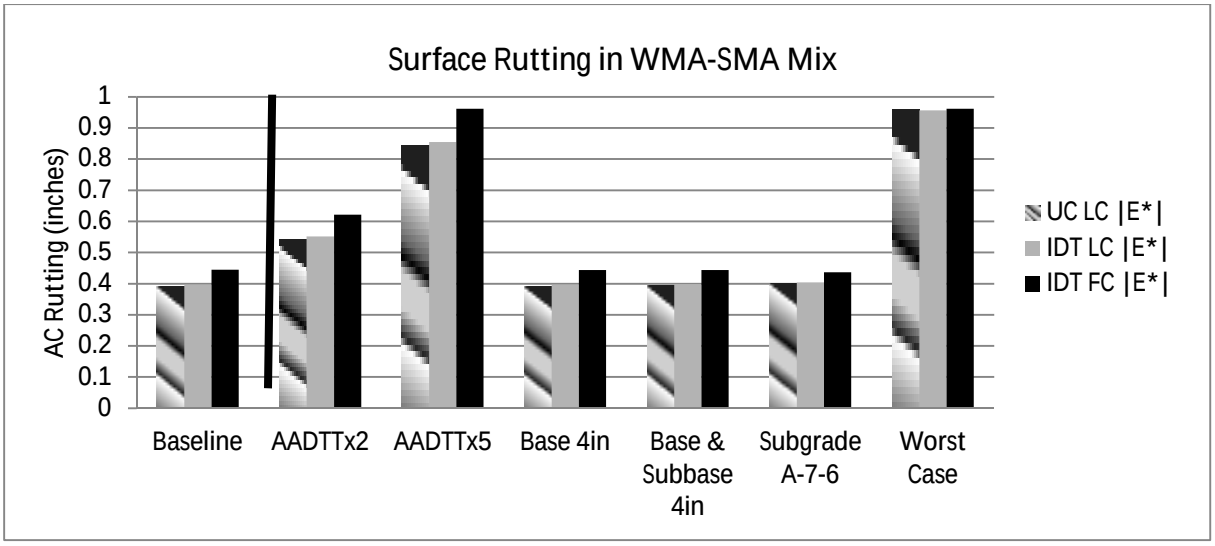

Figure 53. Parametric Analysis of WMA-SMA Mixture Impact on Surface Rutting.

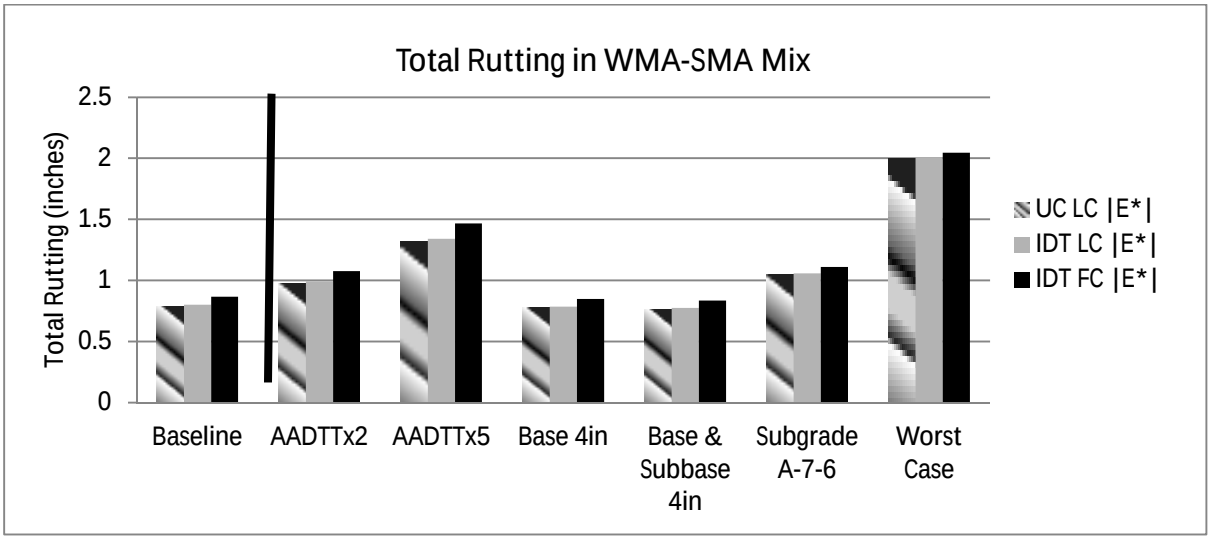

Figure 54. Parametric Analysis of WMA-SMA Mixture Impact on Total Permanent Deformation.

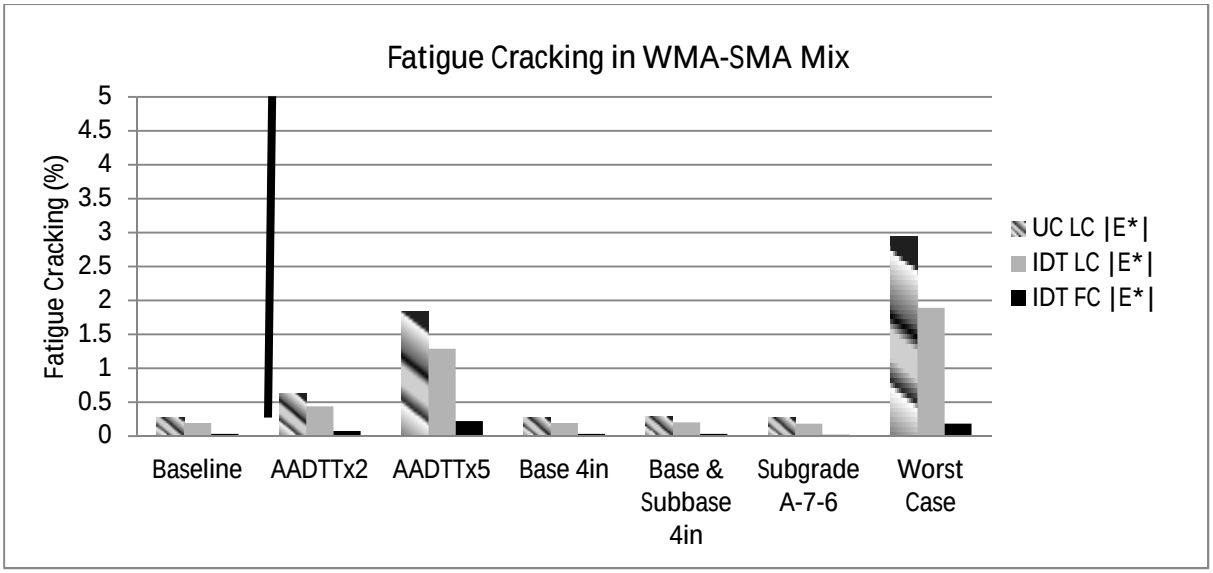

Figure 55. Parametric Analysis of WMA-SMA Mixture Impact on Fatigue Cracking.

As in the complementary analysis discussed in section 3.1.5, the amount of pavement distress produced by the MEPDG software for the baseline structure appears to be reasonable, as proven by the relative differences in distress amount verified in the parametric study.

3.3 Summary on the Impacts of Specimen Type

In order to assess the impacts of specimen type and test configuration on pavement performance, differences were identified through the three analysis programs (QRSS, SPT Program, and MEPDG). The data in the following sections is organized by specimen type: laboratory-compacted and field-compacted, as well as plant-compacted where applicable. In addition, the test configuration, uniaxial compression (UC) and indirect tension (IDT), is noted for each comparison. As mentioned in previous discussion, the three distress types of interest in this

study were rutting in the surface lift, total rutting in the bituminous layers (commonly called binder rutting), and fatigue cracking.

3.3.1 Rutting in the Surface Lift

Table 37 summarizes the surface rutting predictions generated by the three analysis programs for the mixtures tested in this project, as well as for the two mixes tested by the Federal Highway Administration. The table shows that overall there was minimal impact of specimen type or test procedure on the amount of rutting predicted in the surface lift. This is especially true given the magnitude of the rutting when compared to the ultimate threshold of 0.25 inch, as seen in Figure 56. In addition, all of the MEPDG analysis levels predicted close to the same amount of rutting.

Table 37. Summary of Surface Rutting Levels Predicted by Analysis Programs.

Rutting in Surface Lift (inches)											
Project	MEPDG Level 3	MEPDG Level 2	MEPDG Level 1 UC - LC	MEPDG Level 1 UC - PC	MEPDG Level 1 IDT-LC	MEPDG Level 1 IDT - FC	SPT UC - LC	SPT UC-PC	SPT IDT-LC	SPT IDT-FC	QRSS
WMA-SMA PG 76-22	0.11	0.11	0.09	-	0.09	0.14	0.03	-	0.04	0.04	0.09
HMA Hi-RAP PG 64-28	0.12	0.14	0.09	-	0.11	0.14	0.04	-	0.05	0.05	0.10
DGA HMA+RAP PG 64-28	0.01	0.01	0.01	0.01	0.01	Software Crashed	0.01	0.02	0.01	0.01	0.00
DGA HMA PG 64-28	0.11	0.12	0.09	-	-	-	0.18 Design	-	-	-	0.06 Design
							0.18 As Built				0.06 As Built
SMA + 30% RAP PG 58-22 (FHWA DE0883)	0.37	0.42	0.22	-	-	-	-	-	-	-	0.20 Design
											0.18 As Built
HMA + 10% RAP PG 64-28 (FHWA ME0359)	0.15	0.15	0.14	-	-	-	-	-	-	-	0.05Design
											0.04 As Built

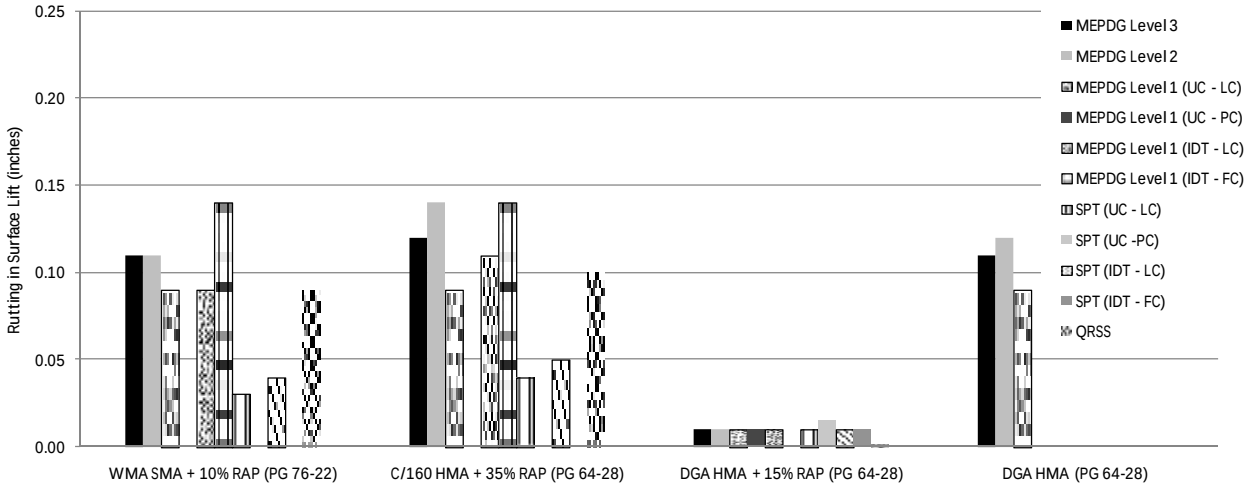

Figure 56. Surface Rutting Predicted for all Mixtures and Specimen Types.

Figure 57 presents a comparison between outputs from the QRSS and SPT Program, based on dynamic modulus data collected from the multiple different specimen types (laboratory-compacted tall and IDT samples, plant-compacted tall samples, and field cores).The surface layer rutting results from the SPT Program analysis displayed the stiffest mix design when analyzed using the LC-UC |E*| values. When compared to as-design mix data from either of the other two specimen types, the results are consistent with the stiffer |E*| master curve reported previously.

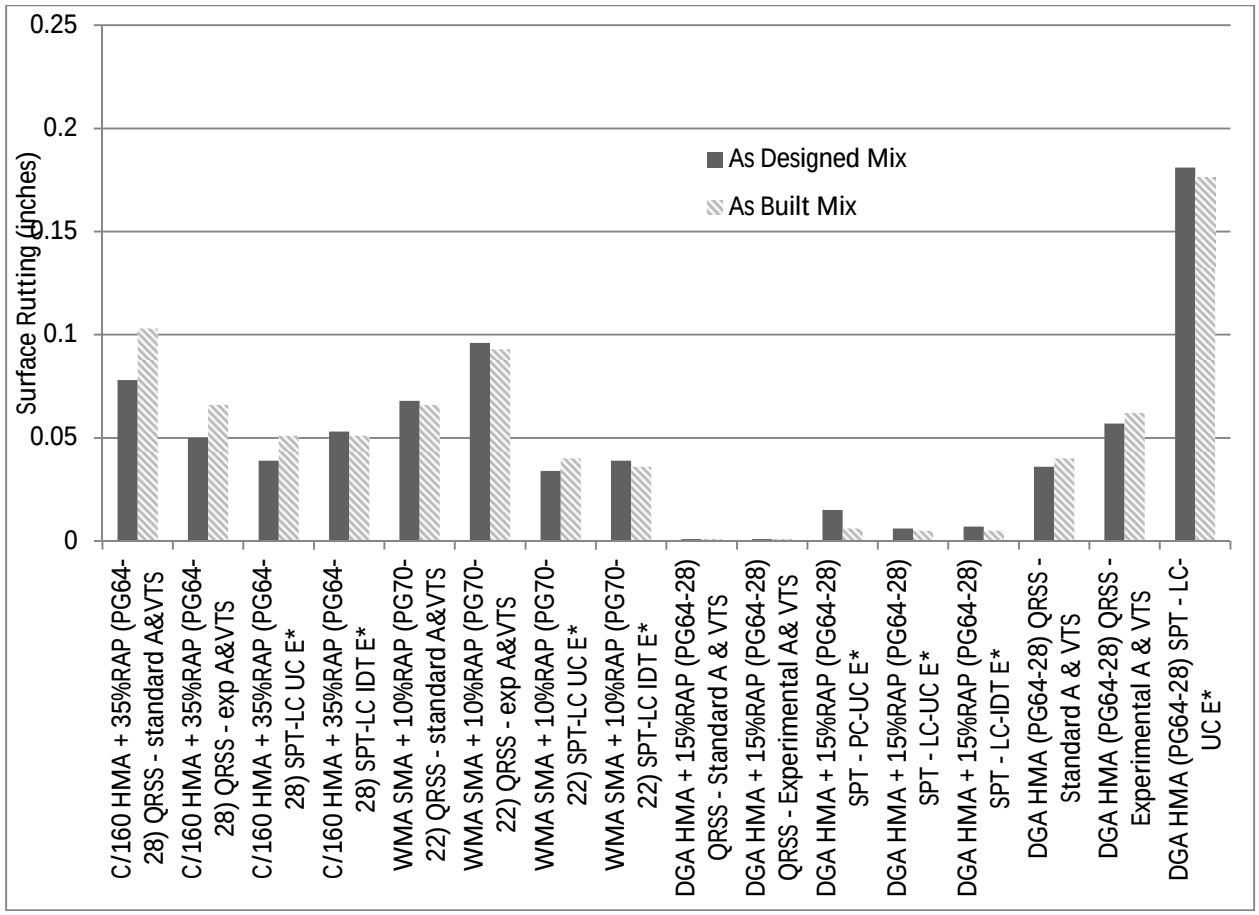

Figure 57. Comparison of Surface Rutting from Design and As-Built Mixes Analyzed with QRSS and SPT Programs.

The as-built mix surface rutting distress results, based on the IDT dynamic modulus results for the HMA Hi-RAP and WMA-SMA mixture field core samples (FC-IDT),are comparable between the LC-IDT (as designed rutting) and FC-IDT(as-built Rutting) when analyzed in the SPT Program. Comparatively the FC-IDT samples produced slightly higher as-built rutting values compared to the as designed rutting values from the LC-UC samples from both mixes. These results are both consistent with the trends observed in the dynamic master curve analysis discussed in Chapter 2. Likewise, the DGA HMA+RAP PC-UC samples which proved to be the

softest of the three gyratory samples tested and resulted in a higher level of rutting based on the design mix (0.015 inches).

Contrary to the fact that the LC-IDT samples were tested to be the stiffest at the high temperatures at which rutting generally occurs, the dynamic modulus data from the LC-UC samples resulted in the lowest predicted design mix surface rutting (0.006 inches). The LC-IDT sample E* data resulted in an equivalent predicted rutting value (0.007 inches). The FC-IDT samples resulted in a 0.005 inch predicted as built rutting value, equivalent to the LC-IDT and LC-UC design mix results.

Comparisons between the SPT Program, which utilizes laboratory measured |E*| data, and the QRSS program, which operates based exclusively on volumetric and structural inputs, displayed no explicit correlation. This indicated that the tendency of the QRSS to under- or over-predict surface rutting distress values relative to the SPT Program output is dependent on the |E*| from laboratory tests.

3.3.2 Total Rutting in Bituminous Layers

The total rutting in bituminous layers (designated as binder rutting in the SPT and QRSS programs) was generated by each of the analysis programs. A summary of the binder rutting predictions is presented in Table 38. The analyses showed that the total rutting in the bituminous layers for all mixtures evaluated did not exceed 0.3 inches, which is under the typical total rutting threshold of 0.5 to 0.75 inch. All of the input levels to MEPDG predicted the same amount of binder rutting.

Table 38. Summary of Total Rutting in Bituminous Layers Predicted by Analysis Programs.

Total Rutting in Bituminous Layers (inches)											
Project	MEPDG Level 3	MEPDG Level 2	MEPDG Level 1 UC - LC	MEPDG Level 1 UC - PC	MEPDG Level 1 IDT-LC	MEPDG Level 1 IDT - FC	SPT UC - LC	SPT UC -PC	SPT IDT-LC	SPT IDT-FC	QRSS
WMA-SMA PG 76-22	0.31	0.31	0.30	-	0.31	0.31	0.17	-	0.17	0.14	0.21
HMA Hi-RAP PG 64-28	0.31	0.31	0.31	-	0.31	0.31	0.17	-	0.17	0.14	0.2
DGA HMA+RAP PG 64-28	0.06	0.06	0.05	0.07	0.06	Software Crashed	0.04	0.08	0.04	0.02	0.21
DGA HMA PG 64-28	0.06	0.07	0.07	-	-	-	0.07 Design 0.03 As Built	-	-	-	0.03 Design 0.03 As Built
SMA + 30% RAP PG 58-22 (FHWA DE0883)	0.69	0.70	0.67	-	-	-	-	-	-	-	0.22 Design 0.18 As Built
HMA + 10% RAP PG 64-28 (FHWA ME0359)	0.39	0.39	0.39	-	-	-	-	-	-	-	0.12 Design 0.10 As Built

The variation of specimen type was only analyzed for the DGA HMA+RAP mix from Maine since it was the only candidate project to have provided loose mix, field cores, and plant compacted samples from the HMA binder lift. The different specimen types produced similar relative distress results as in the surface layer rutting. Plant-compacted samples (PC-UC) which did not undergo extra age hardening in the lab through reheating and compaction and produced the softest dynamic modulus master curves of the specimens analyzed. Figure 58 presents the binder rutting data from the QRSS and SPT Program all specimen types based on both design and as-built mix values.

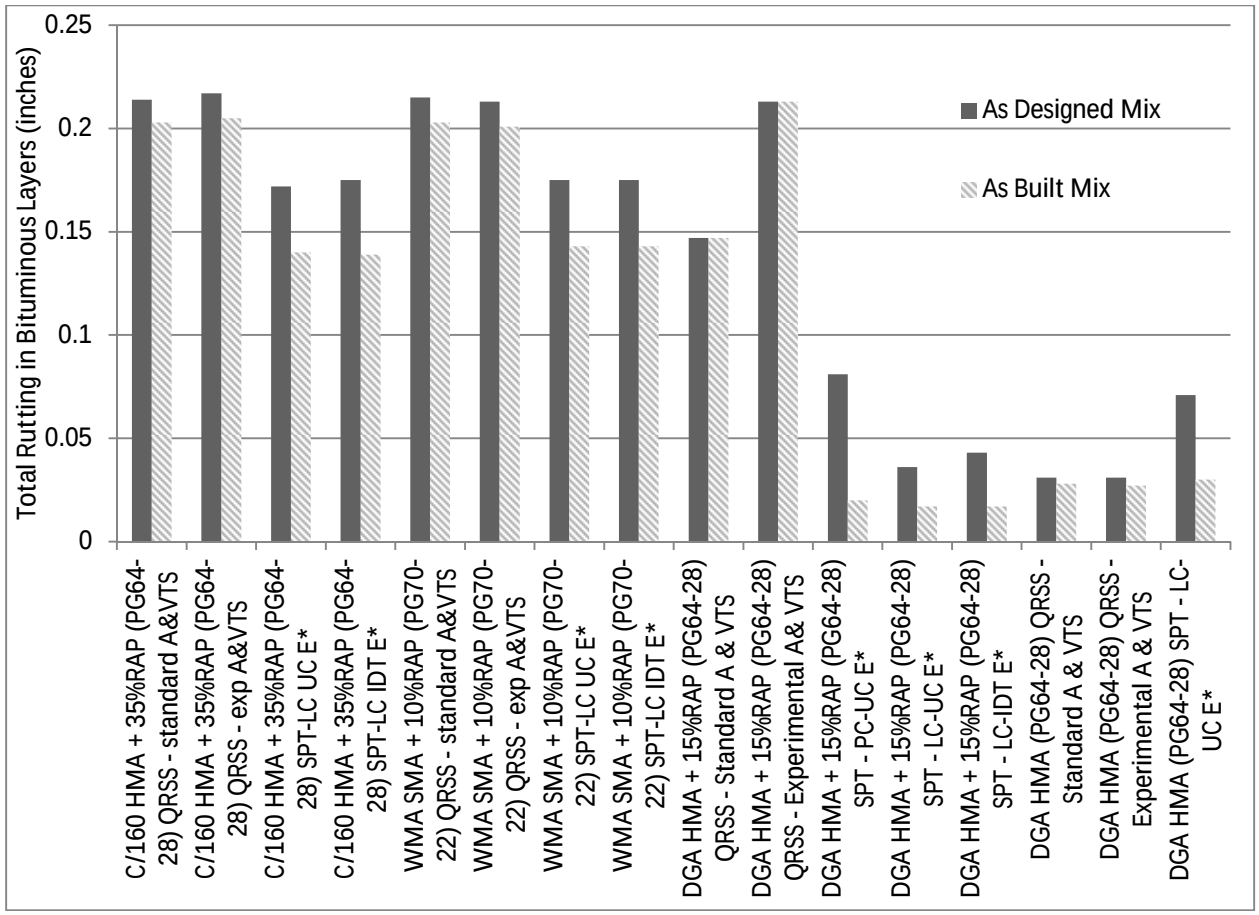

Figure 58. Comparison of Binder Rutting from Design and As-Built Mixes Analyzed with QRSS and SPT Programs.

Despite the higher LC-IDT |E*| results at high temperatures for the DGA HMA+RAP mix, the laboratory-compacted uniaxial compression samples produced the lowest amount of binder rutting in the as designed mix analysis. The field core IDT (FC-IDT) samples produced the lowest amount of binder rutting overall, as can be observed in the as-built mix analysis.

The comparison between two sets of QRSS results for each mix show that the difference between predicted design distresses was more pronounced when using the laboratory-measured binder values in the binder lift than it was in the surface lift. However, it appears to have negligible effect on the resulting PLD values since the predicted as-built distresses were almost identical whether using the experimental binder values or the standard values preprogrammed in

the QRSS program. It should be noted that the QRSS program cannot differentiate between binders used in design versus those used in the field mix analysis.

Results for mixes other than the DGA HMA+RAP were based on the asphalt binder layer's volumetric data and laboratory-compacted uniaxial compression dynamic modulus results collected in NCHRP Project 9-22A. The only dynamic modulus data available for this project was from reheated laboratory-compacted mix tested in the established method (LC-UC). The different SPT Program models for the WMA-SMA and HMA Hi-RAP mixtures represent the only changes in dynamic modulus data of the laboratory-measured samples from the surface lift. The results show that variation of the surface layer dynamic modulus results based on specimen type from these two projects had no effect on total bituminous layer rutting.

3.3.3 Fatigue Cracking in Bituminous Layer

The amount of fatigue cracking predicted was another distress included in the investigation and the results are summarized in Table 39.The results showed that the most variation out of the different distresses examined occurred with fatigue cracking predictions. However, Figure 59 shows that the amount of distress predicted was minimal when compared to the threshold of 25% lane area cracked. The most variation was predicted for analyses of the unconventional mixtures (WMA-SMA and HMA Hi-RAP), whereas the fatigue cracking predictions for the dense-graded mixtures compared well among the different analysis programs. The other explanation for the variation between the MEPDG output and results from the QRSS and SPT Program may be due to the climatic model calibration, as discussed previously. The fatigue cracking model for QRSS was validated using only ten climatic locations, none of which were in

the northeastern US. Among these locations Washington D.C. is the closest location to Delaware which is where the two highly modified unconventional (WMA-SMA and HMA Hi-RAP) mixes were placed. Even though the two locations are relatively close, the climatic conditions may not be the same.

Table 39. Summary of Fatigue Cracking Levels Predicted by Analysis Programs.

Fatigue Cracking (% of lane area cracked)											
Project	MEPDG Level 3	MEPDG Level 2	MEPDG Level 1 UC - LC	MEPDG Level 1 UC - PC	MEPDG Level 1 IDT-LC	MEPDG Level 1 IDT - FC	SPT UC - LC	SPT UC -PC	SPT IDT-LC	SPT IDT-FC	QRSS
WMA-SMA PG 76-22	0.05	0.04	0.30	-	0.20	0.03	1.95	-	1.93	-	2.72
HMA Hi-RAP PG 64-28	0.17	0.21	0.40	-	0.10	0.05	2.57	-	2.49	13	2.50
DGA HMA+RAP PG 64-28	0.57	0.60	0.46	0.63	0.61	Software Crashed	0.60	0.59	0.81	0.53	N/A
DGA HMA PG 64-28	0.07	0.08	0.14	-	-	-	0.15 Design	-	-	-	0.34 Design
							0.25 As Built				0.21 As Built
SMA + 30% RAP PG 58-22 FHWA DE0883	1.21	0.91	4.90	-	-	-	-	-	-	-	2.55 Design
											1.31 As Built
HMA + 10% RAP PG 64-28 FHWA ME0359	0.12	0.12	0.12	-	-	-	-	-	-	-	2.42 Design
											1.64 As Built

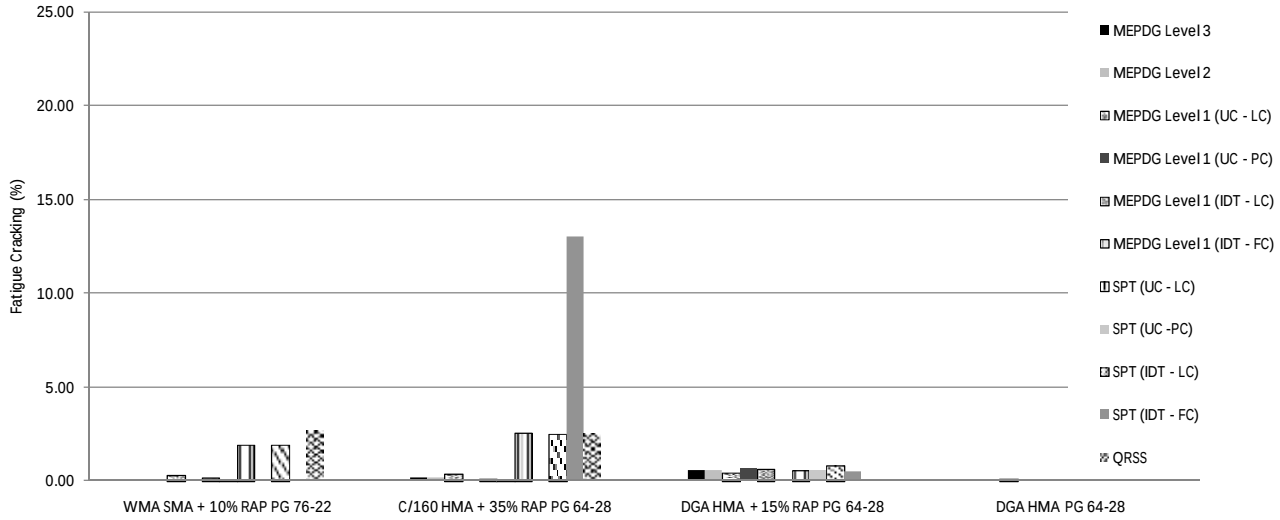

Figure 59. Fatigue Cracking Predicted for all Mixtures and Specimen Types.

Figure 60 shows that the variation of specimen type was only analyzed for fatigue cracking for the DGA HMA+RAP mix, since it was the only candidate project to provide loose mix, field cores, and plant compacted samples from the bottom AC layer (in this case the HMA base lift) where fatigue cracking initiates. Variation of the surface layer dynamic modulus data did not appear to have any effect on the fatigue cracking results. Results indicated that the different specimen types produce roughly equivalent levels of fatigue cracking, with only minor variation observed. As the stiffest specimens tested, the LC-IDT samples resulted in the highest fatigue cracking in the design mix (0.80% cracked), while the softer PC-UC samples resulted in the least amount of fatigue cracking in the design mix (0.589% cracked). Despite the scale of the fatigue cracking distress results, the discrepancies ranging between 0.80% cracked from the LC-IDT design mix analysis to 0.518% cracked from the FC-IDT as built mix analysis, are not as insignificant when compared to the predicted life difference. The 0.29% disparity in fatigue cracking distresses between the design and as-built mixes resulted in predicted life difference up approximately 0.75 years, discussed in Section 3.3.5.

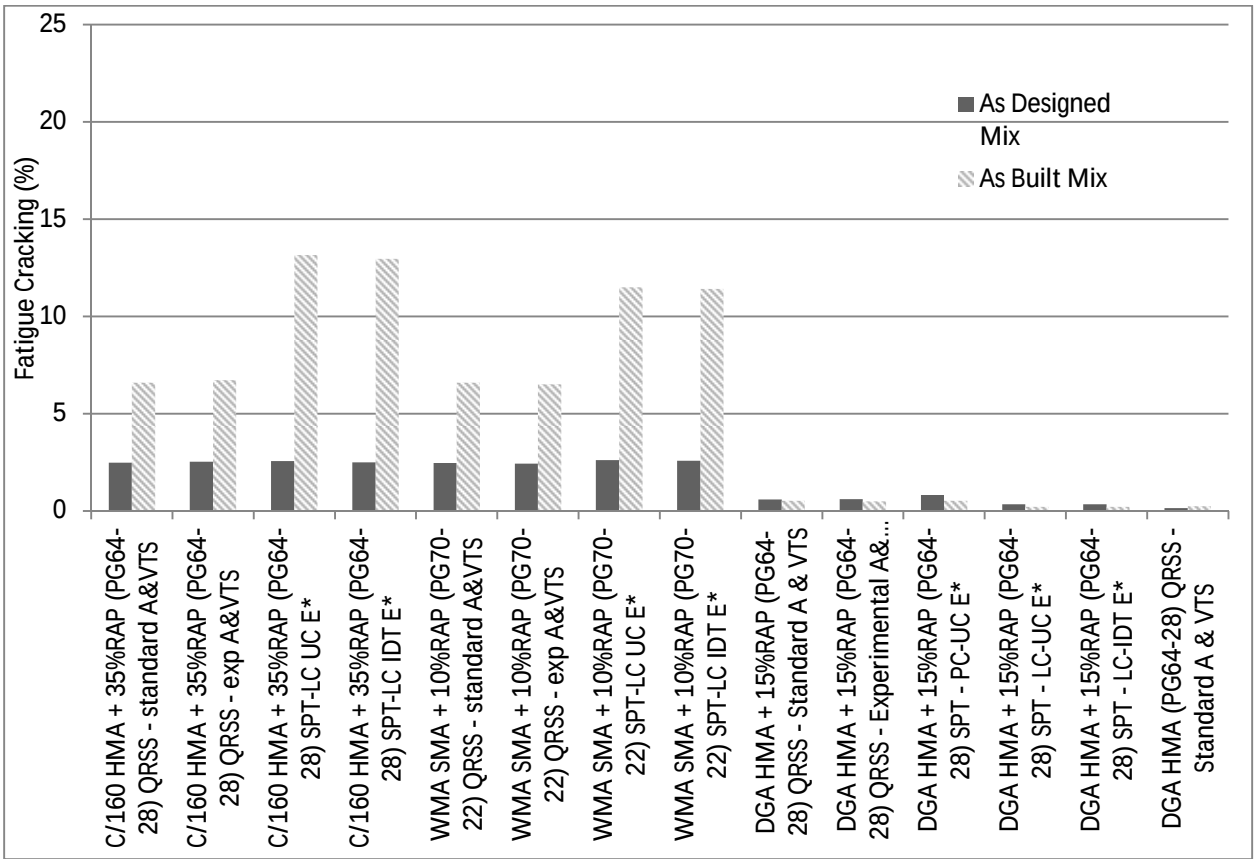

Figure 60. Comparison of Fatigue Cracking from Design and As-Built Mixes Analyzed with QRSS and SPT Programs.

3.3.4 Analysis of Lot-by-Lot Impact on MEPDG Level 1 and Level 2 Inputs

As discussed in the last three sections, the outputs from MEPDG are different compared to the outputs provided by both the SPT Program and the QRSS software. The research team investigated possible sources of discrepancy by performing a lot-by-lot analysis of the Level 1 and Level 2 HMA inputs of two of the projects: the WMA-SMA and HMA Hi-RAP mixtures. The intent of the lot-by-lot analysis was to determine whether using the average |E*| value across lots influenced the output of the predicted distresses from the MEPDG and whether that is the source of variation when compared to the other two analysis programs. The following

tables(Tables 41 through 44) summarize the predicted distresses for both projects when analyzed by lot.

The fact that average |E*| values across all lots were used as input in the MEPDG software raised the question of whether the difference in values between MEPDG predicted distresses and QRSS- and SPT Program-predicted distresses are generated by the use of average |E*|data. As shown in Tables 41 and 43, using average |E*| data did not make a difference in how the Level 1 MEPDG results compared to the predicted distresses from SPT Program. The greatest difference was noted in the prediction of fatigue cracking, whereas rutting predictions were all relatively uniform.

Table 40. MEPDG Analysis of WMA-SMA Mixture Using Level 1 |E*|By Lot.

MEPDG, SPT Program, and QRSS Predicted Distress Levels								
Distress Type	**Test Type**	**Lot 1**	**Lot 2**	**Lot 3**	**Lot 4**	**Lot 5**	**SPT Program**	**QRSS**
Fatigue Cracking (%)	Uniaxial Compression	0.17	0.32	0.34	0.28	0.28	1.95	2.72
	IDT Lab Compacted	0.07	-	0.36	0.18	0.19	1.93	
	IDT Field Compacted	-	0.03	0.07	0.03	0.02	-	
Surface Rutting (inches)	Uniaxial Compression	0.10	0.08	0.08	0.08	0.09	0.03	0.09
	IDT Lab Compacted	0.11	-	0.08	0.10	0.09	0.04	
	IDT Field Compacted	-	0.15	0.12	0.13	0.15	0.04	
Binder Rutting (inches)	Uniaxial Compression	0.31	0.30	0.30	0.30	0.31	0.17	0.21
	IDT Lab Compacted	0.31	-	0.30	0.31	0.31	0.17	
	IDT Field Compacted	-	0.31	0.31	0.31	0.31	0.14	

Table 41. MEPDG Analysis of WMA-SMA Mixture Using Level 2Volumetric Data By Lot.

MEPDG, SPT Program, and QRSS Predicted Distress Levels							
Distress Type	**Lot 1**	**Lot 2**	**Lot 3**	**Lot 4**	**Lot 5**	**SPT Program**	**QRSS**
Fatigue Cracking (%)	-	0.04	0.03	0.04	0.04	1.95	2.72
						1.93	
						-	
Surface Rutting (inches)	-	0.11	0.11	0.11	0.11	0.03	0.09
						0.04	
						0.04	
Binder Rutting (inches)	-	0.31	0.31	0.31	0.31	0.17	0.21
						0.17	
						0.14	

Table 42. MEPDG Analysis of HMA Hi-RAP Mixture Using Level 1 |E*| Data By Lot.

MEPDG, SPT Program, and QRSS Predicted Distress Levels					
Distress Type	**Test Type**	**Lot 1**	**Lot 2**	**SPT Program**	**QRSS**
Fatigue Cracking (%)	Uniaxial Compression	0.32	0.57	2.57	2.5
	IDT Lab Compacted	0.11	0.16	2.49	
	IDT Field Compacted	0.01	0.14	13	
Surface Rutting (inches)	Uniaxial Compression	0.10	0.08	0.04	0.10
	IDT Lab Compacted	0.11	0.10	0.05	
	IDT Field Compacted	0.18	0.12	0.05	
Binder Rutting (inches)	Uniaxial Compression	0.31	0.30	0.17	0.20
	IDT Lab Compacted	0.31	0.31	0.17	
	IDT Field Compacted	0.30	0.31	0.14	

Table 43.MEPDG Analysis of HMA Hi-RAP Mixture Using Level 2Volumetric Data By Lot.

MEPDG, SPT Program, and QRSS Predicted Distress Levels				
Distress Type	**Lot 1**	**Lot 2**	**SPT Program**	**QRSS**
Fatigue Cracking (%)	0.21	0.21	2.57	2.5
			2.49	
			13	
Surface Rutting (inches)	0.14	0.15	0.04	0.10
			0.05	
			0.05	
Binder Rutting (inches)	0.31	0.31	0.17	0.20
			0.17	
			0.14	

Tables 41 and 43 illustrate that fatigue cracking values for any of the lots is quite different when comparing outputs from the MEPDG and other programs. However, it should be noted that these terminal fatigue cracking values are well below the threshold limit of 20% lane area cracked. When comparing predicted rutting values for Level 1 HMA inputs, there is only a small difference noted between using lot-by-lot data as opposed to average |E*| data.

Tables 42 and 44 indicate that using lot-by-lot |E*| data did not impact how the results from the analysis with MEPDG Level 2 HMA inputs compared to the QRSS-predicted distresses. Once again, the largest difference was noted in the fatigue cracking predictions. For example, the amount of fatigue cracking predicted in the WMA-SMA mix was calculated by the QRSS to be 2.72% and by the SPT Program to be 1.93% or 1.95%. However, the lot-by-lot analysis in the MEPDG predicted fatigue cracking levels less than 0.04% lane area cracked. The same trend is true of the HMA Hi-RAP mix.

Therefore, it can be concluded by this analysis that using average |E*| data across lots did not affect the outcome of the MEPDG analysis, as compared to predictions from QRSS and SPT Programs which are based on data from independent lots.

3.3.5 Predicted Life Difference (PLD)

One of the features of the QRSS and SPT Program is a calculation of the predicted life difference (PLD) between the as-designed and as-built mixes in a project. The surface rutting distress and PLD results from both analysis programs are presented in Figure 61, plotted for the various specimen types, and showed that although binder data sources created small variations in the surface rutting distress results, the resulting PLDs appeared to be consistent when considering the scale of PLD values observed. In almost all cases, the variation in the lift predicted was less than ±1.0 year regardless of analysis program or specimen type.

Based on comparisons between the two QRSS models for each of the paving projects, it is apparent that the use of laboratory-measured binder data inputs versus the standard PG-grade binder inputs has a minimal effect on the final PLD results. Therefore, it also had a minimal effect on the resultant pay factors generated by the programs. This finding was verified in the surface layer prediction for all projects and also in the binder layer predictions for the DGA HMA+RAP mix.

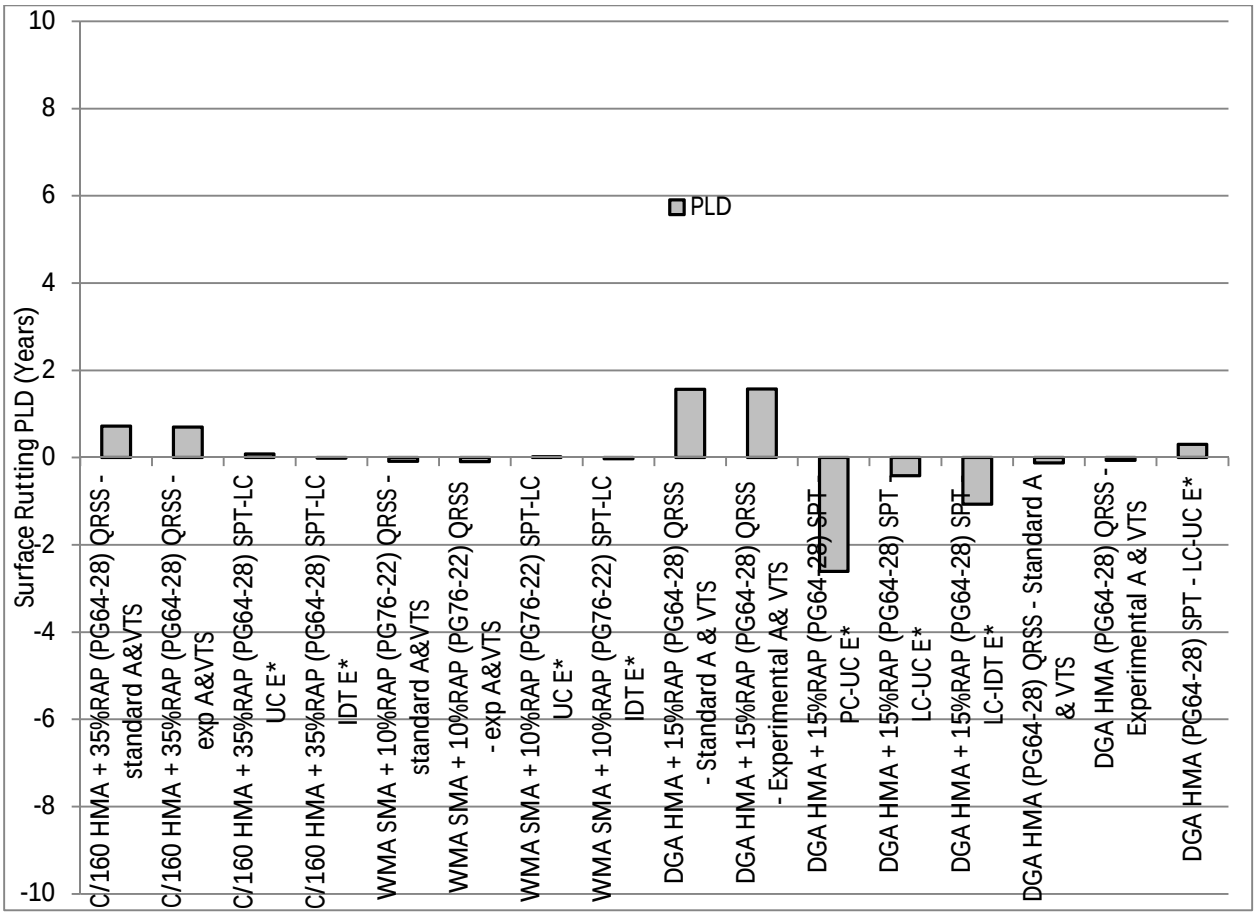

Figure 61. Surface Rutting Predicted Life Differences from QRSS and SPT Program.

A comparison of total bituminous layer PLD results is shown in Figure 62. Based on variation of test specimen types for the DGA HMA+RAP mix, the figure shows that while the PC-UC binder lift samples had the lowest stiffness, it produced the highest positive PLD values. The PLD values generated were even larger than those produced for the LC-IDT samples, which had the highest stiffness of all the specimen types. Considering the fact that the use of PC-UC dynamic modulus data in the design mix analysis only softens the predicted design mix rutting compared to the as-built rutting, which is a positive if the aim is to extend the projected PLD on a paving project.

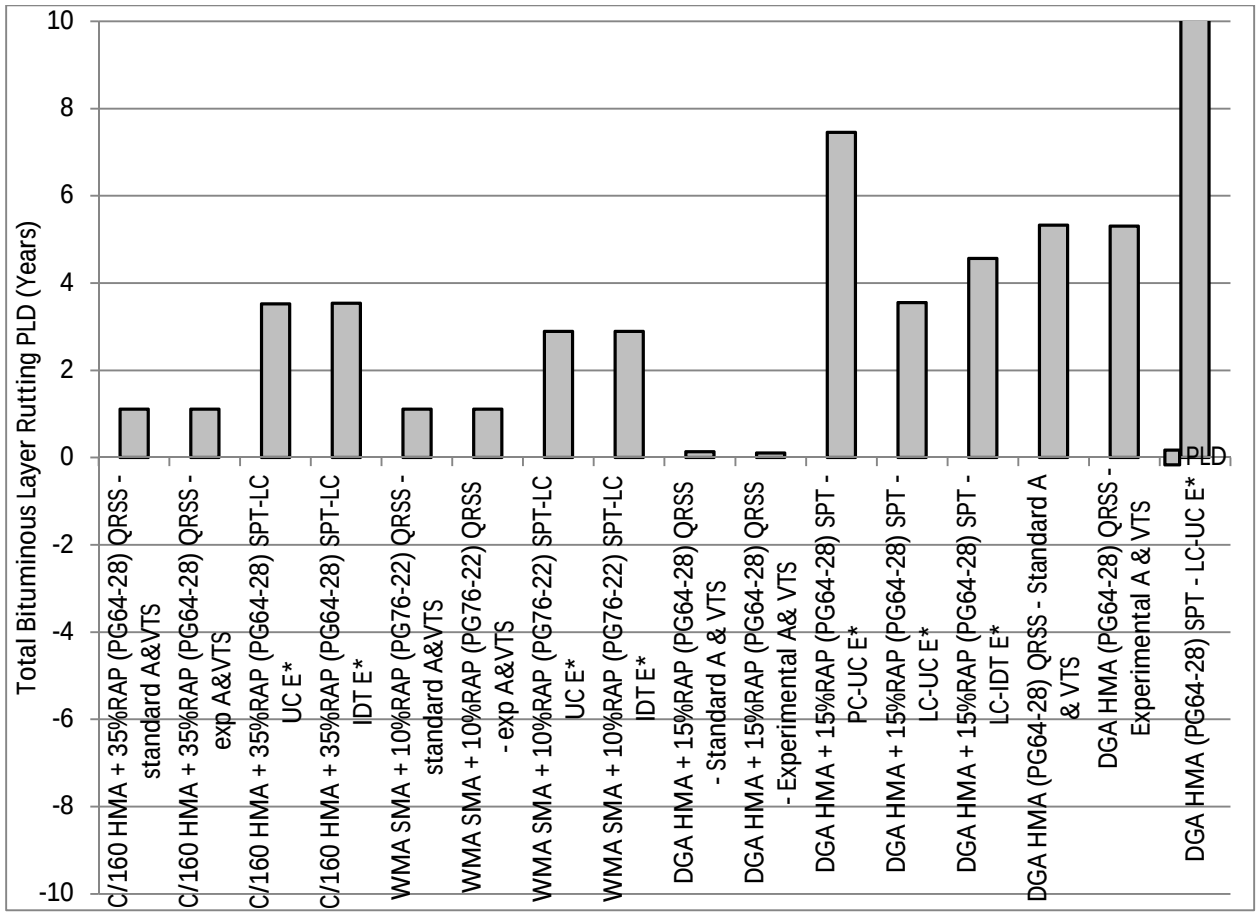

Figure 62. Total Bituminous Layer Rutting Predicted Life Differences QRSS and SPT programs.

The PLD values in Figure 63 show that virtually no variation with surface AC layer specimen type in the SPT Program for the WMA-SMA and HMA Hi-RAP mixes. Variation of the |E*| data from the HMA base lift by specimen type showed that the LC-IDT samples (as-designed mix analysis in the SPT) when compared with FC-IDT sample data (as-built mix analysis in the SPT) produce the most positive PLD results indicative of a longer service life. The tall samples compacted during production at the plant (PC-UC) produced the most negative PLD results (shortened pavement life) when compared with the higher stiffness FC-IDT samples.

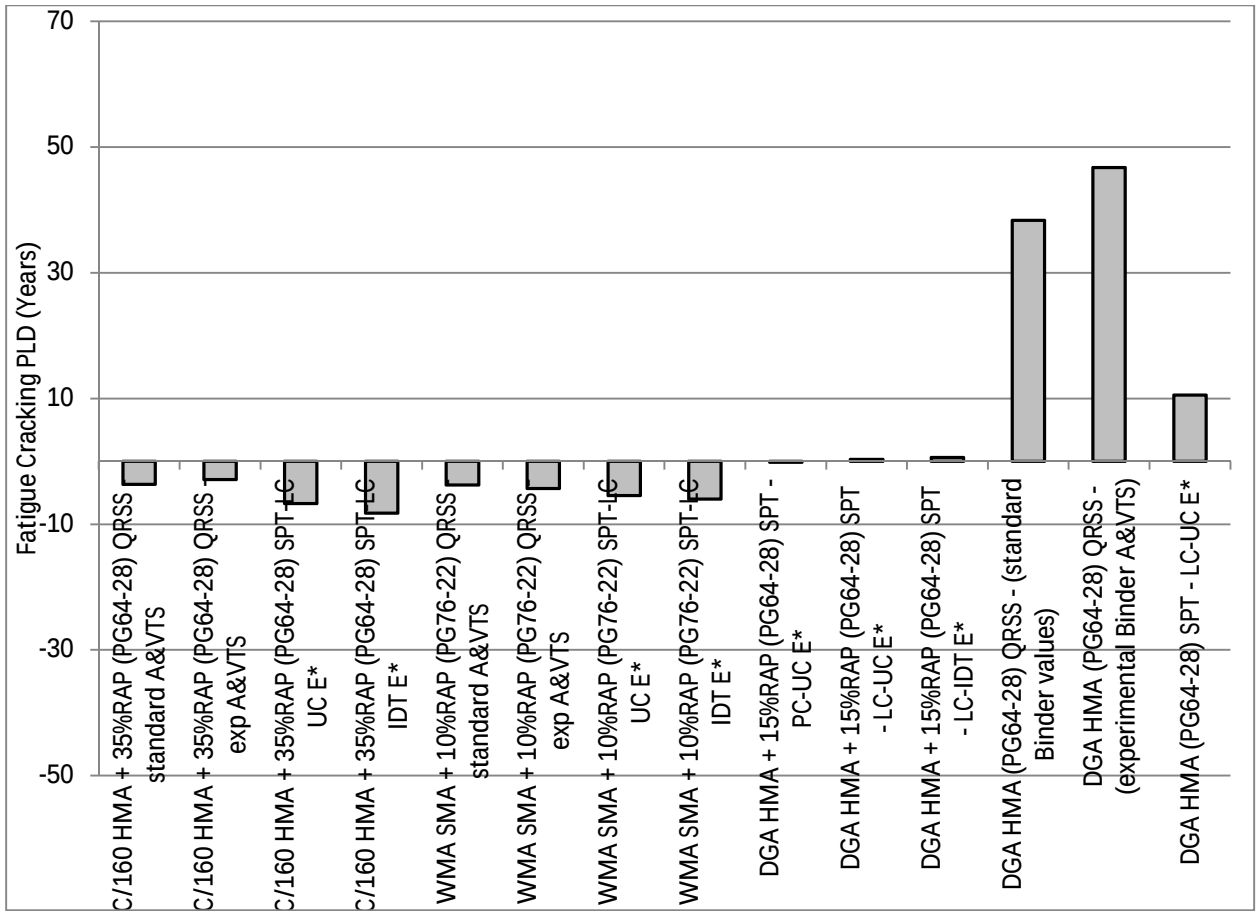

Figure 63. Fatigue Cracking Predicted Life Differences QRSS and SPT Programs.

Based on the analysis, it appears that the PLD limits may require adjusting when specifically addressing binder rutting for the small difference when comparing levels between the QRSS and SPT Program.

3.3.6 Predicted Pay Factors

The QRSS and SPT Program also both predict a pay factor for each distress type as part of the analysis. Surface rutting pay factors were all 100% for PRS analysis of all specimen types and mixes, except for one instance. The DGA HMA+RAP mix PC-UC samples produced 95% payment to the contractor. The plant-compacted specimens produced the softest |E*| and as a result was the only specimen type to produce a pay penalty for surface rutting.

Conversely, despite producing the most negative pay factor results for surface rutting, pay factor results for binder rutting shown in Figure 64were highest when using the PC-UC specimen |E*| data. This represents a strange incongruity in the way the SPT Program is analyzing the results for payment between the rutting in the surface lift and the total rutting in the bituminous layers.

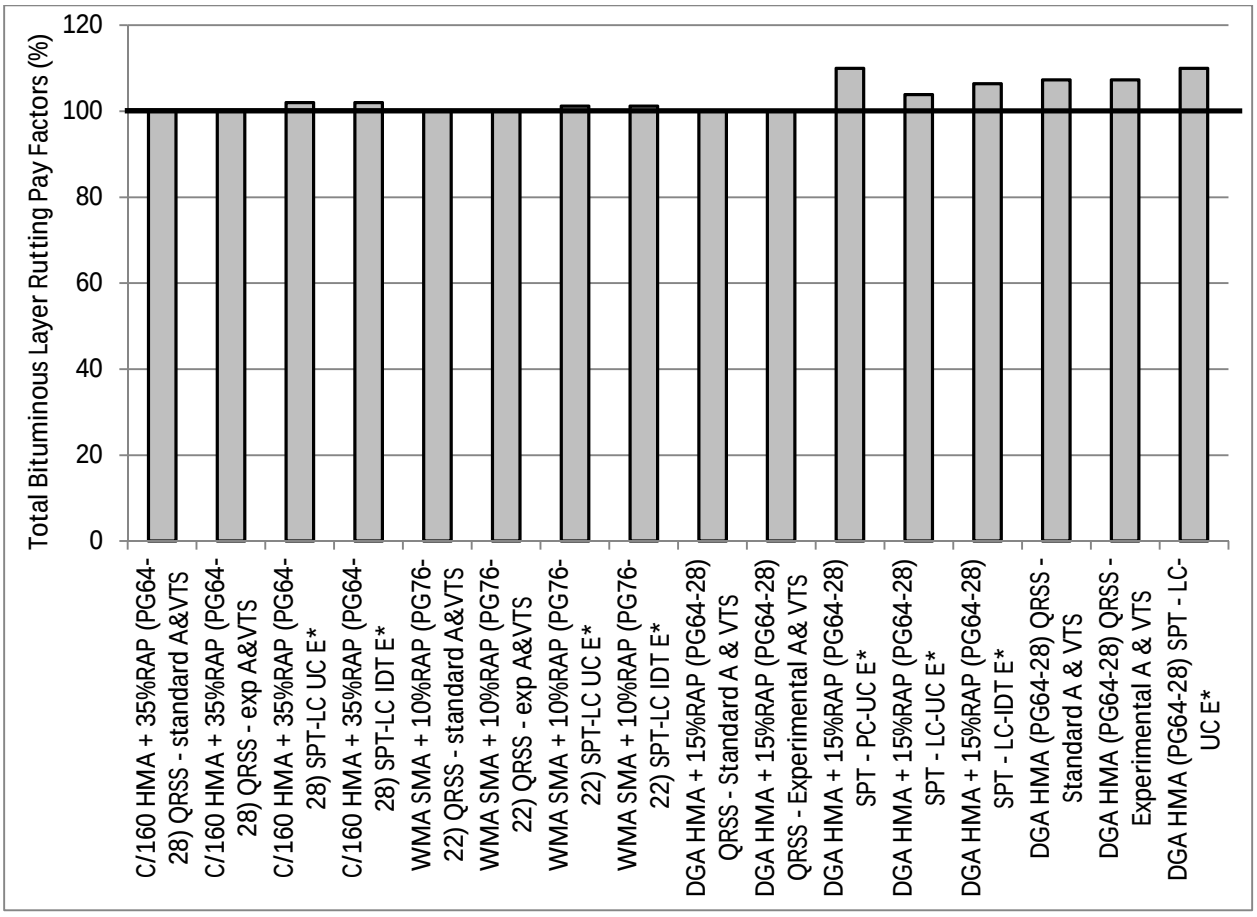

Figure 64. Pay Factors Based on Total Rutting in Bituminous Layers from QRSS and SPT Programs.

The fatigue cracking pay factor results were highly variable within each analysis run. It should be again noted that the models are based on the Rhode Island Route 102 data from the NCHRP Project 9-22A, except for the DGA HMA+RAP analysis. The pay factors typically varied between maximum pay incentives to a remove and replace recommendation from one lot

of specimens to the next. The QA data from the RI Route 102 project contained two lots with higher air void contents and lower effective binder contents, which likely produced these results in the QRSS and SPT Program.

Consistent with the PLD results, fatigue cracking pay factor results for the DGA HMA+RAP mix were 100% for all specimen types tested. The best correlation for fatigue cracking in the SPT Program appeared to be when testing in uniaxial compression. It is should be considered that while the variation in the fatigue cracking results was very inconsistent lot-to-lot within each analysis iteration, the QRSS and SPT were typically consistent overall in terms of which mixes and individual production lots of material were worthy of pay incentives and which required remove and replace. It is possible that the scale of PLD limits for fatigue cracking analysis should be expanded to account for the significant variation typically seen in analysis results for both programs.

CHAPTER 4

CONCLUSIONS AND SUGGESTED RESEARCH

4.1 Conclusions

Based on the comprehensive analysis of mixtures from four paving projects, some key preliminary conclusions can be drawn from this scoping study.

4.1.1 The data appears to support that IDT testing can be used as a suitable alternate for uniaxial compression testing.

Analysis by three different programs indicated that testing procedure did not impact the levels of distress predicted, except at the highest temperature and lowest frequency. In order to ultimately use field core samples for dynamic modulus testing, the only current option available for analyzing pavement performance is the MEPDG software. This is because the SPT Program analysis requires either the use of only plant-compacted or laboratory-compacted sample dynamic modulus in the design mix and either plant-compacted sample or field core effective |E*| in the as-built mixture analysis, or the use two different samples (e.g., plant-compacted or laboratory-compacted samples dynamic modulus master curves in the design mix analysis and effective |E*| from field cores in the as-built mix analysis). The use of only field cores is not possible in the SPT Program as it currently exists because it is necessary to have dynamic modulus sample data to input in the design mix analysis portion of the program [Jeong 2009]. It appears that the only way to make the SPT Program work exclusively for field core sample analysis would be to remove the dynamic modulus as a design mix input, in a format similar to

the QRSS program in which the design mix is based off of available structural and mixture volumetric data.

4.1.2 On the whole, the data appears to support that it is not necessary to require plant-compacted or field-compacted mix to get the most accurate results for predicted pavement performance.

Results from the three analysis programs appear to indicate that rutting predictions from laboratory-compacted samples are consistent with those of plant-compacted and field-compacted samples. However, in terms of fatigue cracking, the plant-compacted samples produced the best results by not inducing the artificial hardening observed in the laboratory-compacted samples. The recommendation is that a DOT should consider the type of specimen based on the type of distress that it most wants to design against.

4.1.3 The data appears to indicate that the MEPDG software can be used effectively to predict the life expectancy of a pavement.

The results of the study showed that there was much more consistency among specimen types when analyzed with the MEPDG as compared to the other analysis methods, QRSS and SPT Program. It was found that the predictions from the MEPDG matched either the QRSS or the SPT Program output, but rarely was consistent with both.

4.1.4 The data appears to indicate that the MEPDG software can be used effectively with Level 2 inputs in lieu of requiring Level 1 inputs to predict the life expectancy of a pavement.

Evidence from the analyses supports the use of MEPDG Level 2 inputs in lieu of Level 1 inputs for the HMA mixture. The MEPDG Level 1 and 2 inputs produced the same level of distress across all projects. The predictions with MEPDG Level 2 inputs were comparable to those of the QRSS program.

4.2 Suggested Research

During IDT testing of WMA SMA and HMA specimens from DelDOT, a deterioration of the LVDTs was witnessed that likely led to some of the errors in dynamic modulus results witnessed in Chapter 2. The LVDTs used for IDT testing are flimsy and do not stand up well to repeated use, as pictured in Figure 65. If the IDT test mode is to serve as a suitable replacement for the standard uniaxial dynamic modulus testing mode, consideration should be given to designing a more durable LVDT.

(a) **(b)**

Figure 65. LVDTs from IDT testing in various states of distress (a) Broken LVDT (b) Bent LVDTs.

PRS software analysis showed that fatigue cracking PLD results typically varied significantly. Consideration should be given to performing a sensitivity analysis to calibrate proper PLD limits for payment if the QRSS or SPT QA are to be suitable for use by contractors and state agencies for payment determination. Table 44 shows a potential modification to the PLD limits which may result in more reasonable pay adjustments (i.e., fewer of both the remove/replace and the maximum pay incentive results).

Table 44. Possible Modifications to the Fatigue Cracking PLD Limits for QRSS and SPT Analysis.

Pay Adjustment Type	Original PLD Limit (Rutting and Fatigue Cracking)	Modified PLD Limit (Fatigue Cracking)
Minimum for No Disincentive	-2	-5
Minimum for Pay Incentive	2	5
Maximum Pay Disincentive	-5	-10
Minimum for Remove/Replace	-7	-15
Maximum Pay Incentive	7	10

Overall, the user friendliness of both the QRSS and the NCHRP 9-22A SPT programs was inconsistent. A list of issues which should be considered in future research on both of the programs follows:

a) QRSS showed a capacity to erase previously saved structural and volumetric design data during a save overwrite when the user is attempting to use the direct input binder data feature (as used in the project to input the laboratory recorded A and VTS binder values).
b) Comparison between differing design and as-built binders is impossible in the QRSS due to a glitch in the software that automatically changes the design binder previously input to match the binder entered into the contractor QA portion of the program. To avoid this

issue, once a design binder was directly entered into the QRSS, the binder tab of the contractor QA data input portion had to be avoided.

c) The SPT Program base rutting model results were unusable due to inconsistencies shown between the PLD results and the resulting pay factors calculated by the program.

d) A glitch in QRSS base rutting model of the QA Data portion did not allow the user to manually enter AC base layer contractor QA in order to analyze the AC base layer for distress. This made comparison of base rutting and fatigue cracking results for the MEDOT Township D project impossible.

e) If the predicted life difference calculated by the SPT Program fatigue cracking model resulted in values larger than approximately +50 to +75 years, the cells containing the PLD values in the fatigue cracking detail tab of the program sometimes disappeared. This needs to be fixed or it could have an effect on the total average payment calculated by the program when lot tonnage and weighted average pay factors are considered (they were not analyzed in this project due to insufficient data provided by the DOTs).

f) The SPT Program had a tendency to freeze or crash often during use. In some cases, work was lost and had to be re-entered. The Microsoft Excel auto-recover feature was helpful in some cases to manage this issue.

REFERENCES

Bennert, T., Colley, L.A., Daniel, J.S., Schmitt, R., and Kandhal, P., 2008, *Research Proposal for NCHRP Project 9-48, Field versus Laboratory Volumetrics and Mechanical Properties*, Rutgers University, Center for Advanced Infrastructure and Transportation (CAIT), 63 pp.

Bennert, T., and Williams, S.G., 2009, "Precision of AASHTO TP62-07 for Use in Mechanistic-Empirical Pavement Design Guide for Flexible Pavements", *Transportation Research Record: Journal of the Transportation Research Board No. 2127*, p. 115-126,

Bonaquist, R., 2009, *Wisconsin Mixture Characterization Using the Asphalt Mixture Performance Tester (AMPT) on Historical Aggregate Structures*, SPR #0092-08-06, Wisconsin Highway Research Program (WHRP), 123 pp.

Bonaquist, R., 2011, *Precision of the Dynamic Modulus and Flow Number Tests Conducted with the Asphalt Mixture Performance Tester, NCHRP Report 702*, National Cooperative Highway Research Program, NCHRP 9-29 Final Report, 211 pp.

Bonaquist, R., and Christensen, D.W., 2005, "Practical Procedure for Developing Dynamic Modulus Master Curves for Pavement Structural Design", *Transportation Research Record: Journal of the Transportation Research Board No. 1929*, p. 208-217.

Christensen, D.W., Pellinen, T.K., and Bonaquist, R., 2003, "Hirsch Model for Estimating the Modulus of Asphalt Concrete", *Journal of the Association of Asphalt Paving Technologists*, Vol. 72, p. 97-121.

Dongre, R., Myers, L., D'Angelo, J., and C. Paugh, "Field Evaluation of Witczak and Hirsch Models for Predicting Dynamic Modulus of Hot-Mix Asphalt," *Journal of the Association of Asphalt Paving Technologists* (AAPT), Vol. 74, 2005.

Kim, Y. R., Y. Seo, M. King, and M. Momen, 2004, Dynamic Modulus Testing of Asphalt Concrete in Indirect Tension Mode", *Transportation Research Record No. 1891*, p. 163 – 173.

Kim, Y.R., E. Dukatz, and K. Hall, 2009, *Ruggedness Testing for IDT |E*| Specification*, Presented at the February 2009 Meeting of the FHWA Asphalt Mixture and Construction Expert Task Group.

Jeong, M. G. "Implementation of a Simple Performance Test Procedure in a Hot Mix Asphalt Quality". Ph.D. Dissertation. Arizona State University, 2010.

Mensching, D. "Applicability of Implementing Quality Related Specification-Based Pay Factors in Rhode Island ". Master's Thesis. Villanova University, 2011

Moulthrop, J., and M. Witzcak, 2011, *Performance-Related Specification for Hot-Mixed Asphalt*, National Cooperative Highway Research Program, NCHRP Report 704, National Research Council, 199 pp.

Peterson, R.L., Mahboub, K.C., Anderson, and R.M., Tashman, L.,2004, ”Comparing Superpave Gyratory Compactor Data to Field Cores”, *Journal of Materials in Civil Engineering,* p. 78-83.

Witczak, M., El-Basyouny, M., Jeong, M. G., and S. El-Badawy, 2007, *Final Revised Section Calibration Data For Asphalt Surfaced Pavement Recalibration Under NCHRP 1-40D,* National Cooperative Highway Research Program, NCHRP 1-40D Final Report, 320 pp.

ABBREVIATIONS AND ACRONYMS

A - Intercept of temperature susceptibility relationship (related to VTS) of Asphalt Binder

AADT - Annual Average Daily Traffic

AADTT – Annual Average Daily Truck Traffic

AASHTO – American Association of State Highway and Transportation Officials

AC – Asphalt Concrete Layer of Pavement Cross Section

AMPT –Asphalt Mixture Performance Tester

COV – Statistical Coefficient of Variation

DE0883 - Project ID of FHWA Mobile Asphalt Testing Laboratory Analysis Project

DELDOT – Delaware Department of Transportation

δ – Phase Angle

DGA – Conventional Dense-Graded Asphalt Mixture

DOT – State Department of Transportation (state highway agency)

$|E^*|$ – Dynamic Modulus Estimate of Asphalt Mixture Stiffness

ESAL – Equivalent Single Axle Load

ETG – Expert Task Group

FHWA – Federal Highway Administration

FC – Field Compacted Asphalt Core Sample

G^* – Asphalt Binder Shear Modulus

HMA – Hot Mix Asphalt

IDT – Indirect Tension Testing Mode for Asphalt Mixtures

JMF – Job Mix Formula of an Asphalt Mixture

LC – Laboratory Compacted Asphalt Mixture Sample

LVDT – Linear Variable Displacement Transducer

MAMTL – FHWA Mobile Asphalt Mixture Testing Laboratory

ME0359 – Project ID of FHWA Mobile Asphalt Testing Laboratory Analysis Project

MEDOT – Maine Department of Transportation

MEPDG – Mechanistic Empirical Pavement Design Guide

M_R – Resilient Modulus of Unbound Materials

NCHRP – National Cooperative Highway Research Program

PC – Contractor Laboratory Plant Compacted Asphalt Mixture Sample

PG – Asphalt Binder Superpave Performance Grade

PLD – Predicted Life Difference

PP/FC – Plant-produced mix compacted during construction and extracted as a field core

PP/LC – Plant-produced loose mix reheated and compacted at the research laboratory

PP/QC – Plant-produced loose mix compacted at the contractor's QC laboratory at the plant

PSI – Pounds Per Squared Inch

PRS – Performance Related Specification

QA – Quality Assurance

QC – Quality Control

QLC – Quality Lab Compacted Asphalt Mixture Sample

QRSS – Quality-Related Specification Software

RAP – Reclaimed Asphalt Pavement

RIDOT – Rhode Island Department of Transportation

SGC – Superpave Gyratory Compactor

SPT – Simple Performance Tester

SPT Program – Simple Performance Tester PRS Software created in NCHRP 9-22 and 9-22A

SMA – Stone Matrix Asphalt

UC – Uniaxial Compression Testing Mode for Asphalt Mixtures

VPD – Vehicles Per Day

VTS – Viscosity Temperature Susceptibility of Asphalt Binder

WMA – Warm Mix Asphalt

WPE - Witczak Predictive Equation To Calculate the Dynamic Modulus of Asphalt

APPENDIX C
AASHTO MEDPG DETAILED OUTPUT

HMA Hi-RAP Mixture |E*| and Binder Data

WMA-SMA + 10% RAP, PG64-28 Binder Data		
Temperature (°F)	**at 10 rad/sec**	
	G* (Pa)	d
10	141,299,994	22.92
40	25,939,999	43.57
70	1,881,000	57.66
100	143,300	68.2
130	14,130	74.33

Temperature (°F)	**Uniaxial Compression Laboratory-Compacted |E*|for HMA Hi-RAP (psi)**					
	0.1 Hz	**0.5 Hz**	**1.0 Hz**	**5.0 Hz**	**10.0 Hz**	**25.0 Hz**
10	1,281,548	1,585,385	1,709,485	1,973,331	2,074,868	2,197,200
40	1,108,019	1,417,259	1,547,286	1,830,372	1,941,607	2,077,244
70	294,065	482,907	583,188	852,864	980,736	1,155,628
100	63,995	121,807	158,907	282,526	354,192	466,950
130	18,385	34,577	45,796	88,027	115,909	164,792

Temperature (°F)	**IDT Laboratory-Compacted |E*|for HMA Hi-RAP (psi)**					
	0.1 Hz	**0.5 Hz**	**1.0 Hz**	**5.0 Hz**	**10.0 Hz**	**25.0 Hz**
10	636,480	867,677	974,975	1,231,988	1,342,713	1,486,081
40	542,883	759,098	862,073	1,114,762	1,226,045	1,372,142
70	173,365	276,614	334,106	499,868	584,742	707,984
100	62,951	104,142	129,243	210,379	256,984	330,799
130	29,487	47,384	58,645	97,127	120,692	160,166

Temperature (°F)	**IDT Field-Compacted |E*|for HMA Hi-RAP (psi)**					
	0.1 Hz	**0.5 Hz**	**1.0 Hz**	**5.0 Hz**	**10.0 Hz**	**25.0 Hz**
10	612,335	874,033	996,291	1,288,764	1,414,042	1,575,178
40	492,280	732,019	848,304	1,135,921	1,262,789	1,428,916
70	93,813	169,189	215,792	364,200	446,565	572,051
100	24,885	42,574	54,513	98,536	127,216	177,123
130	11,421	17,080	20,807	34,634	43,949	60,963

DGA HMA + 15% RAP Mixture |E*| and Binder Data

DGA HMA + 15% RAP PG 64-28 Binder Data		
Temperature (°F)	at 10 rad/sec	
	G* (Pa)	d
40	19,392,000	41.41
70	1,596,900	54.94
100	102,282	65.76
130	9,289	72.38

Temperature (°F)	Uniaxial Compression Laboratory-Compacted |E*|for 9.5mm HMA + RAP (psi)					
	0.1 Hz	0.5 Hz	1.0 Hz	5.0 Hz	10.0 Hz	25.0 Hz
10	1,951,100	2,214,854	2,315,590	2,519,146	2,594,218	2,682,630
40	733,087	1,035,547	1,174,430	1,501,182	1,638,949	1,814,356
70	154,894	282,215	356,218	574,775	687,740	851,505
100	29,161	60,487	82,026	159,981	208,823	290,305
130	7,435	15,091	20,679	43,155	58,956	88,104

Temperature (°F)	Uniaxial Compression Laboratory-Compacted |E*|for 12.5mm HMA + RAP (psi)					
	0.1 Hz	0.5 Hz	1.0 Hz	5.0 Hz	10.0 Hz	25.0 Hz
10	2,066,513	2,314,182	2,408,122	2,597,159	2,666,689	2,748,510
40	823,334	1,133,126	1,272,606	1,595,662	1,730,152	1,900,230
70	178,891	319,485	399,429	630,331	747,387	915,019
100	31,999	66,887	90,672	175,560	227,987	314,465
130	7,366	15,454	21,401	45,371	62,189	93,089

Temperature (°F)	Uniaxial Compression Laboratory-Compacted |E*|for 19mm HMA + RAP (psi)					
	0.1 Hz	0.5 Hz	1.0 Hz	5.0 Hz	10.0 Hz	25.0 Hz
10	2,066,513	2,314,182	2,408,122	2,597,159	2,666,689	2,748,510
40	823,334	1,133,126	1,272,606	1,595,662	1,730,152	1,900,230
70	178,891	319,485	399,429	630,331	747,387	915,019
100	31,999	66,887	90,672	175,560	227,987	314,465
130	7,366	15,454	21,401	45,371	62,189	93,089

Temperature (°F)	Uniaxial Compression Plant-Compacted |E*|for 9.5mm HMA + RAP (psi)					
	0.1 Hz	0.5 Hz	1.0 Hz	5.0 Hz	10.0 Hz	25.0 Hz
10	1,685,839	1,957,240	2,063,042	2,280,428	2,361,817	2,458,522
40	573,377	839,826	966,289	1,272,911	1,405,756	1,577,781
70	114,153	213,792	273,448	455,551	552,622	696,413
100	21,763	45,397	61,881	122,820	161,844	228,124
130	5,802	11,687	15,992	33,428	45,803	68,857

Temperature (°F)	Uniaxial Compression Plant-Compacted |E*|for 12.5mm HMA + RAP (psi)					
	0.1 Hz	0.5 Hz	1.0 Hz	5.0 Hz	10.0 Hz	25.0 Hz
10	1,556,477	1,842,332	1,956,006	2,193,634	2,284,068	2,392,624
40	522,887	778,083	900,999	1,203,416	1,336,300	1,510,021
70	110,464	208,224	266,812	445,838	541,396	683,152
100	22,428	47,620	65,172	129,671	170,657	239,792
130	6,042	12,714	17,648	37,697	51,885	78,144

Temperature (°F)	Uniaxial Compression Plant-Compacted |E*|for 19mm HMA + RAP (psi)					
	0.1 Hz	0.5 Hz	1.0 Hz	5.0 Hz	10.0 Hz	25.0 Hz
10	1,722,200	2,011,732	2,124,401	2,355,149	2,441,176	2,543,046
40	617,961	906,653	1,042,733	1,369,733	1,510,013	1,690,329
70	136,247	255,778	326,550	538,933	650,054	812,232
100	28,101	59,981	82,174	163,208	214,196	299,301
130	7,631	16,162	22,501	48,334	66,605	100,311

Temperature (°F)	IDT Lab-Compacted |E*|for 9.5mm HMA+RAP (psi)					
	0.1 Hz	0.5 Hz	1.0 Hz	5.0 Hz	10.0 Hz	25.0 Hz
10	1,426,030	1,812,206	1,967,984	2,289,101	2,407,404	2,544,809
40	414,713	660,112	792,246	1,148,102	1,314,866	1,538,674
70	127,338	203,490	251,702	413,094	507,699	657,791
100	62,094	87,191	103,353	160,924	197,838	262,045
130	42,790	53,546	60,299	84,013	99,268	126,320

Temperature (°F)	IDT Lab-Compacted |E*|for 12.5mm HMA+RAP (psi)					
	0.1 Hz	0.5 Hz	1.0 Hz	5.0 Hz	10.0 Hz	25.0 Hz
10	1,769,288	2,137,337	2,273,048	2,534,707	2,626,127	2,729,731
40	476,690	784,468	950,695	1,382,257	1,572,461	1,813,872
70	138,624	213,529	263,026	438,361	546,563	723,559
100	77,547	99,095	113,308	165,400	199,825	261,465
130	61,518	70,007	75,477	95,182	108,124	131,420

Temperature (°F)	IDT Lab-Compacted |E*|for 19mm HMA+RAP (psi)					
	0.1 Hz	0.5 Hz	1.0 Hz	5.0 Hz	10.0 Hz	25.0 Hz
10	1,300,348	1,720,192	1,893,983	2,256,819	2,391,126	2,546,825
40	420,688	678,697	819,775	1,202,801	1,382,454	1,622,465
70	153,964	246,747	305,778	502,895	617,332	796,468
100	82,882	118,233	141,298	224,096	277,155	368,695
130	59,172	75,812	86,485	124,764	149,751	194,295

Temperature (°F)	IDT Field-Compacted |E*|for 9.5mm HMA+RAP (psi)					
	0.1 Hz	0.5 Hz	1.0 Hz	5.0 Hz	10.0 Hz	25.0 Hz
10	1,367,071	1,702,748	1,840,745	2,135,729	2,249,803	2,387,634
40	342,483	556,772	669,441	969,677	1,110,943	1,303,261
70	62,262	119,414	156,392	281,014	354,121	470,248
100	15,141	28,351	37,563	72,742	96,387	138,567
130	5,876	9,839	12,569	23,173	30,581	44,454

Temperature (°F)	IDT Field-Compacted |E*|for 12.5mm HMA+RAP (psi)					
	0.1 Hz	0.5 Hz	1.0 Hz	5.0 Hz	10.0 Hz	25.0 Hz
10	933,813	1,247,225	1,384,664	1,694,129	1,819,197	1,974,036
40	186,947	318,341	393,582	613,661	726,607	889,550
70	38,890	68,044	87,196	154,852	196,996	267,704
100	13,810	21,417	26,425	44,828	57,044	79,012
130	7,686	10,515	12,304	18,680	22,855	30,391

Temperature	IDT Field-Compacted |E*|for 19mm HMA+RAP (psi)

(°F)	0.1 Hz	0.5 Hz	1.0 Hz	5.0 Hz	10.0 Hz	25.0 Hz
10	1,097,979	1,429,157	1,570,548	1,882,518	2,006,624	2,159,110
40	247,695	422,928	519,040	786,103	916,597	1,098,674
70	44,104	87,652	116,666	217,829	279,055	378,558
100	10,821	20,914	28,102	56,245	75,592	110,702
130	4,183	7,254	9,412	17,990	24,106	35,733

DGA HMA Mixture |E*| and Binder Data

DGA HMA PG 64-28 Binder Data		
Temperature (°F)	at 10 rad/sec	
	G* (Pa)	d
10	206,621,992	19.1
40	29,948,699	38.2
70	2,515,360	55.4
100	84,153	69.9
130	6,012	76.8

Temperature (°F)	Uniaxial Compression Laboratory-Compacted |E*|for DGA HMA (psi)					
	0.1 Hz	0.5 Hz	1.0 Hz	5.0 Hz	10.0 Hz	25.0 Hz
10	2,147,412	2,388,064	2,476,218	2,647,609	2,708,406	2,778,212
40	827,223	1,167,399	1,319,569	1,666,263	1,807,378	1,982,466
70	152,516	291,969	374,889	622,370	750,300	934,527
100	24,373	53,004	73,671	152,442	203,821	291,598
130	6,012	12,088	16,670	36,036	50,320	77,685

SMA + 30% RAP Mixture |E*| and Binder Data

SMA + 30% RAP PG 58-22 Binder Data		
Temperature (°F)	at 10 rad/sec	
	G* (Pa)	d
10	127,300,000	28.27
40	22,300,000	47.4
70	1,100,000	65.7
100	61,500	75.4
130	4,470	82.4

Temperature (°F)	Uniaxial Compression Laboratory-Compacted |E*|for SMA + 30% RAP (psi)					
	0.1 Hz	0.5 Hz	1.0 Hz	5.0 Hz	10.0 Hz	25.0 Hz
10	2,782,193	2,915,514	2,960,522	3,042,263	3,069,406	3,099,329
40	1,353,046	1,764,173	1,939,241	2,335,680	2,499,768	2,706,422
70	271,874	475,223	582,928	898,922	1,054,453	1,276,462
100	37,951	77,569	106,527	215,615	288,188	414,927
130	11,036	18,644	24,272	48,183	68,820	109,736

HMA + 19% RAP Mixture |E*| and Binder Data

HMA + 10% RAP PG 64-28 Binder Data		
Temperature (°F)	at 10 rad/sec	
	G* (Pa)	d
41	15,100,000	39.24
64	2,420,000	39.24
75	1,390,000	56.69
100	126,000	63.24
111	43,900	69.3
113	35,328	67.33

Temperature (°F)	Uniaxial Compression Laboratory-Compacted |E*|for HMA + 10% RAP (psi)					
	0.1 Hz	0.5 Hz	1.0 Hz	5.0 Hz	10.0 Hz	25.0 Hz
10	2,782,193	2,915,514	2,960,522	3,042,263	3,069,406	3,099,329
40	1,353,046	1,764,173	1,939,241	2,335,680	2,499,768	2,706,422
70	271,874	475,223	582,928	898,922	1,054,453	1,276,462
100	37,951	77,569	106,527	215,615	288,188	414,927
130	11,036	18,644	24,272	48,183	68,820	109,736

Plots Generated for Parametric Analysis in AASHTO MEPDG 1.0 Software

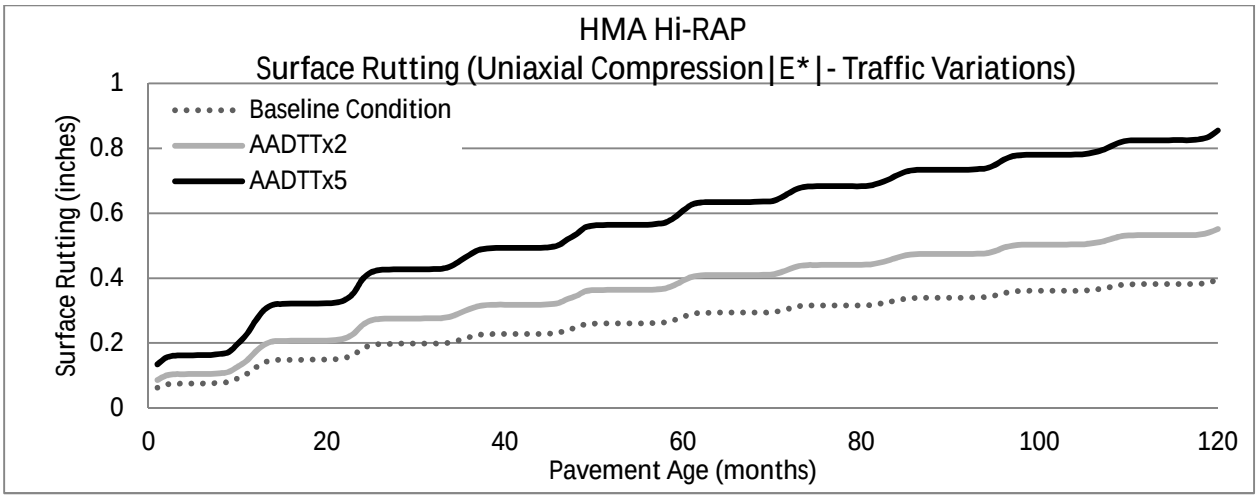
HMA Hi-RAP
Surface Rutting (Uniaxial Compression|E*|- Traffic Variations)
Baseline Condition
AADTTx2
AADTTx5
Surface Rutting (inches)
Pavement Age (months)
0
0.2
0.4
0.6
0.8
1
0
20
40
60
80
100
120

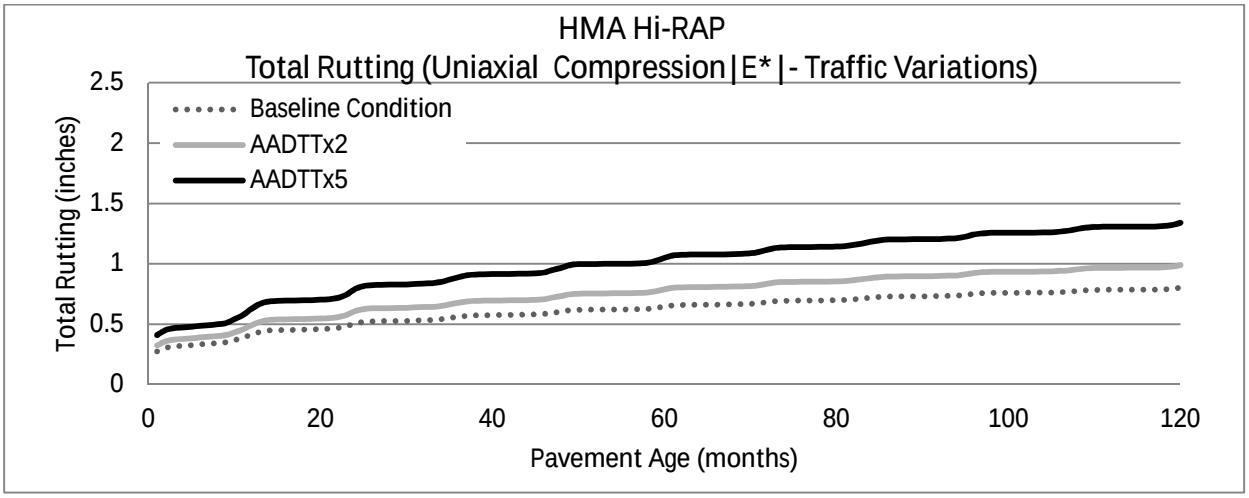
HMA Hi-RAP
Total Rutting (Uniaxial Compression|E*|- Traffic Variations)
Baseline Condition
AADTTx2
AADTTx5
Total Rutting (inches)
Pavement Age (months)
0
0.5
1
1.5
2
2.5
0
20
40
60
80
100
120

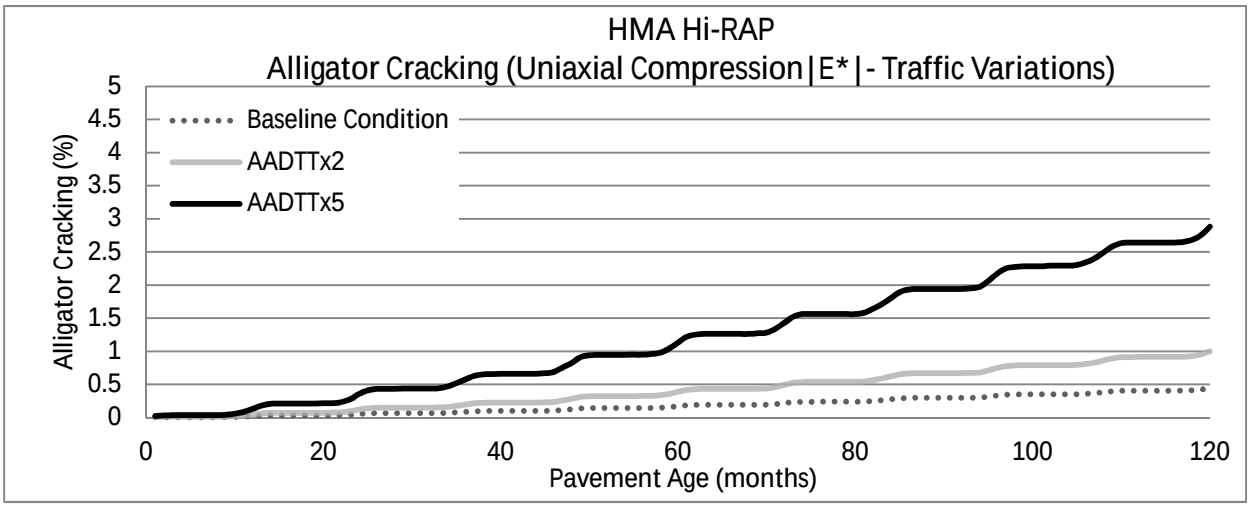
HMA Hi-RAP
Alligator Cracking (Uniaxial Compression|E*|- Traffic Variations)
Baseline Condition
AADTTx2
AADTTx5
Alligator Cracking (%)
Pavement Age (months)
0
0.5
1
1.5
2
2.5
3
3.5
4
4.5
5
0
20
40
60
80
100
120

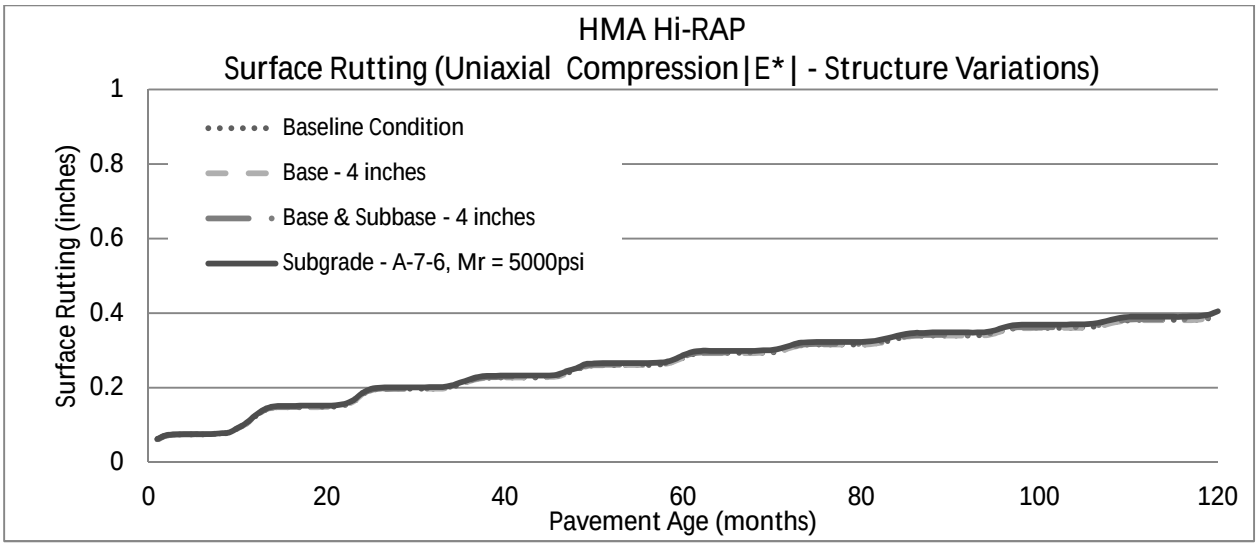
HMA Hi-RAP
Surface Rutting (Uniaxial Compression|E*| - Structure Variations)
Surface Rutting (inches)
Pavement Age (months)
Baseline Condition
Base - 4 inches
Base & Subbase - 4 inches
Subgrade - A-7-6, Mr = 5000psi
0
0.2
0.4
0.6
0.8
1
0
20
40
60
80
100
120

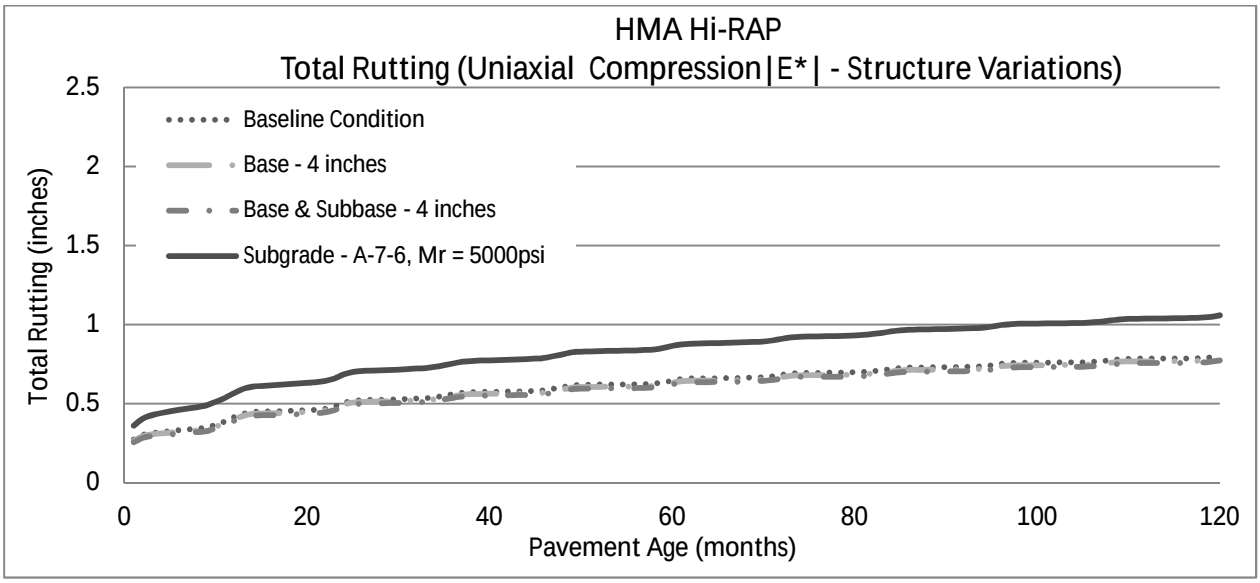
HMA Hi-RAP
Total Rutting (Uniaxial Compression|E*| - Structure Variations)
Total Rutting (inches)
Pavement Age (months)
Baseline Condition
Base - 4 inches
Base & Subbase - 4 inches
Subgrade - A-7-6, Mr = 5000psi
0
0.5
1
1.5
2
2.5
0
20
40
60
80
100
120

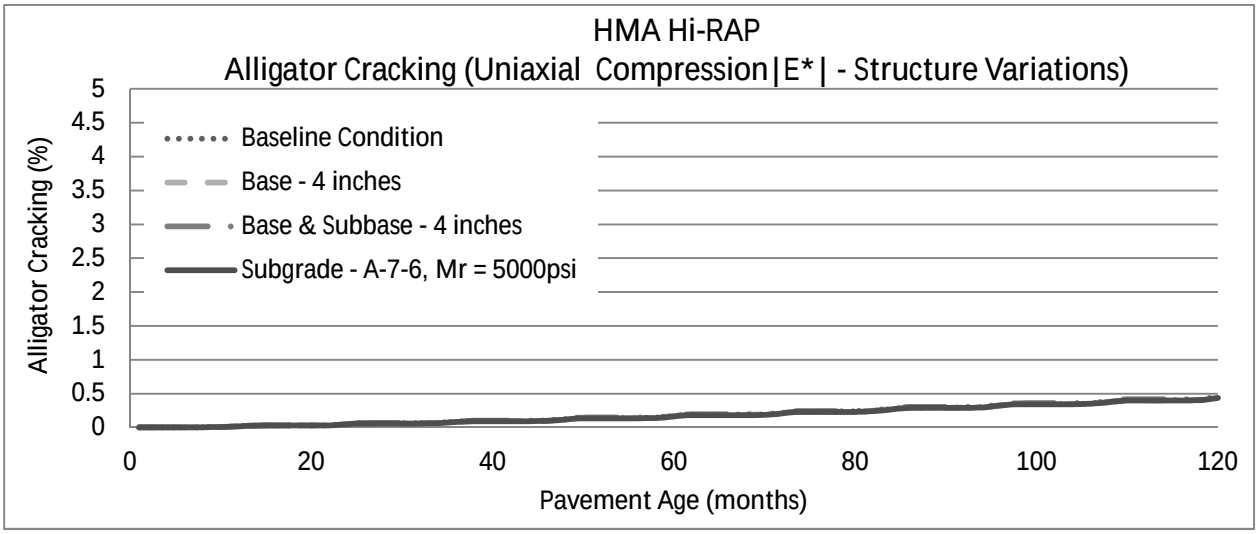
HMA Hi-RAP
Alligator Cracking (Uniaxial Compression|E*| - Structure Variations)
Alligator Cracking (%)
Pavement Age (months)
Baseline Condition
Base - 4 inches
Base & Subbase - 4 inches
Subgrade - A-7-6, Mr = 5000psi
0
0.5
1
1.5
2
2.5
3
3.5
4
4.5
5
0
20
40
60
80
100
120

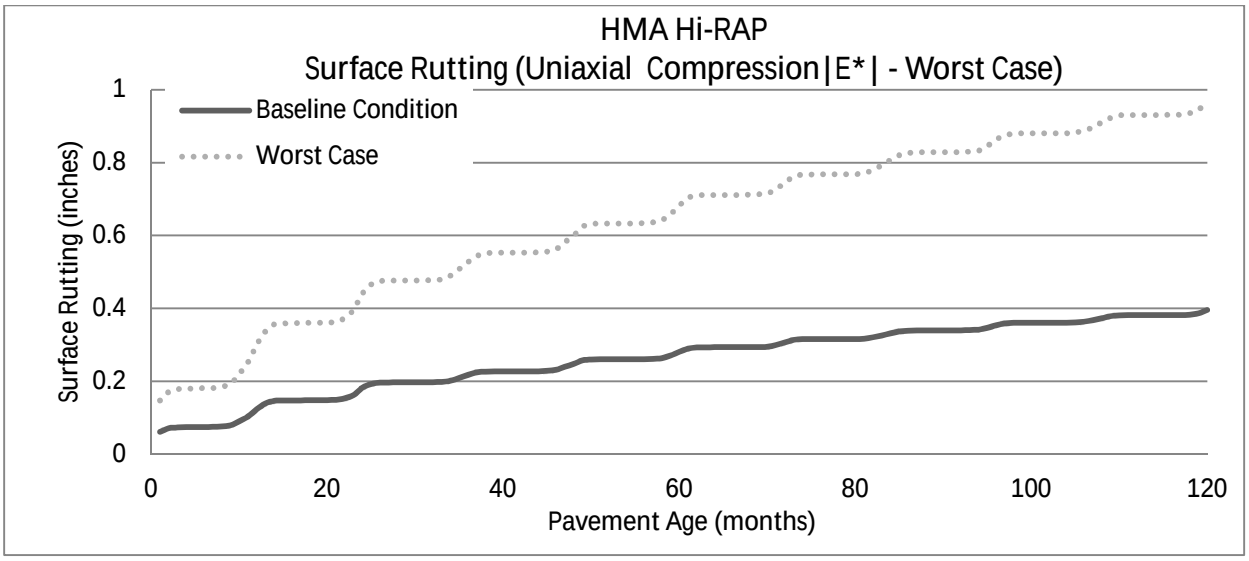
HMA Hi-RAP
Surface Rutting (Uniaxial Compression|E*| - Worst Case)
Baseline Condition
Worst Case
Surface Rutting (inches)
0
0.2
0.4
0.6
0.8
1
0
20
40
60
80
100
120
Pavement Age (months)

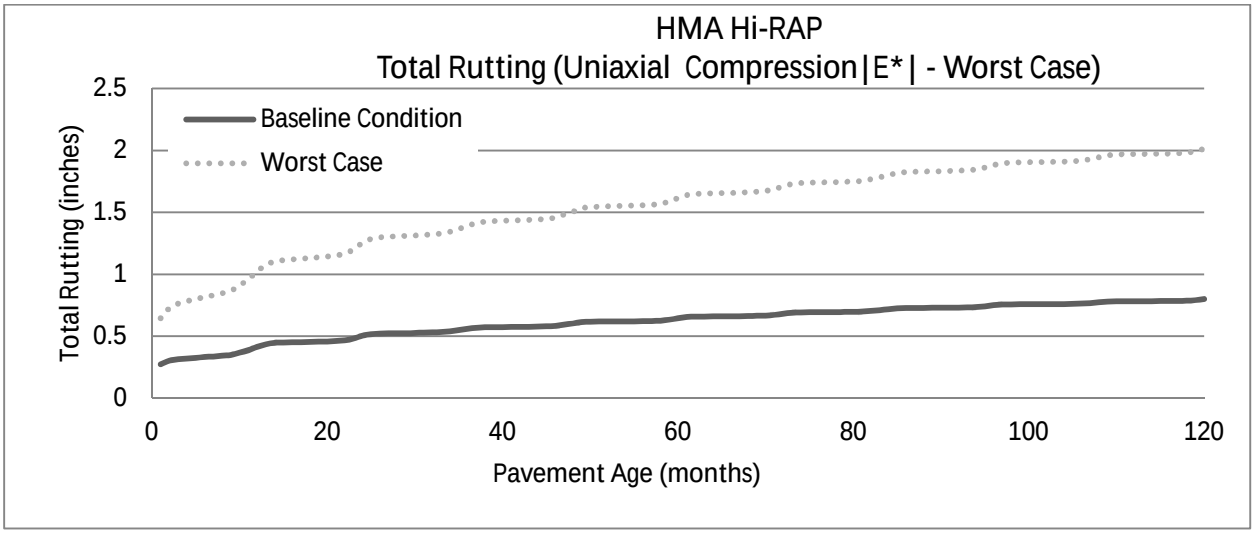
HMA Hi-RAP
Total Rutting (Uniaxial Compression|E*| - Worst Case)
Baseline Condition
Worst Case
Total Rutting (inches)
0
0.5
1
1.5
2
2.5
0
20
40
60
80
100
120
Pavement Age (months)

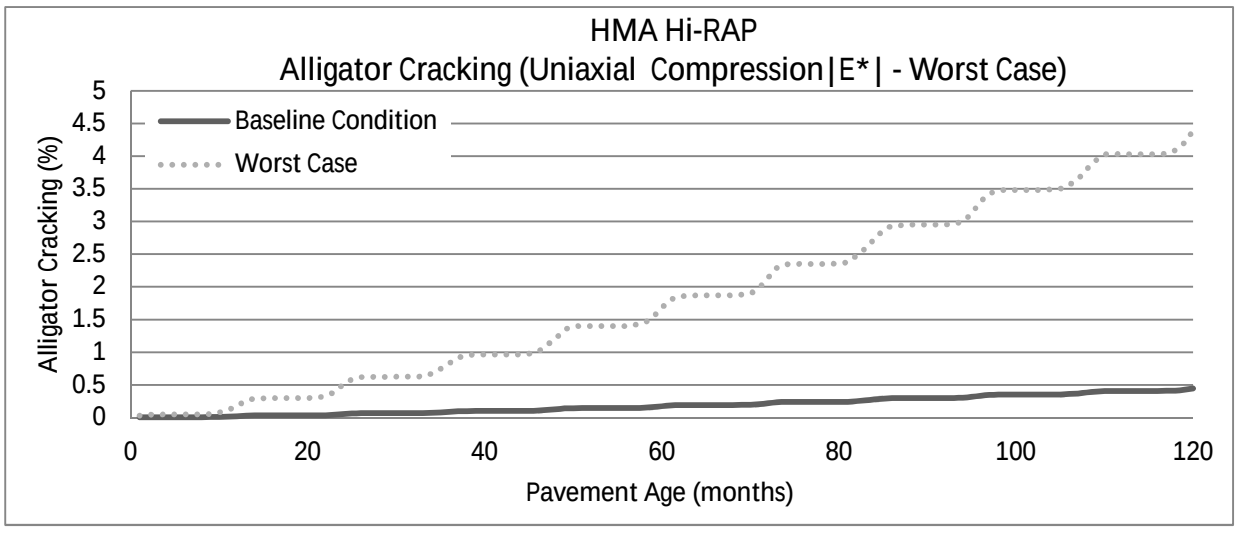
HMA Hi-RAP
Alligator Cracking (Uniaxial Compression|E*| - Worst Case)
Baseline Condition
Worst Case
Alligator Cracking (%)
0
0.5
1
1.5
2
2.5
3
3.5
4
4.5
5
0
20
40
60
80
100
120
Pavement Age (months)

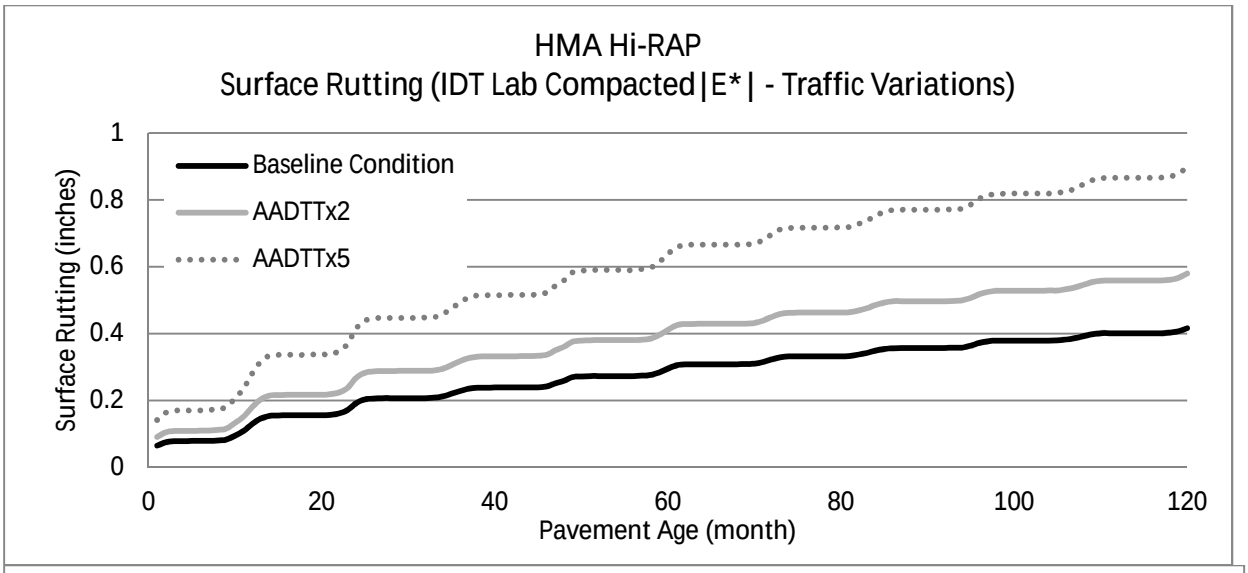
HMA Hi-RAP
Surface Rutting (IDT Lab Compacted|E*| - Traffic Variations)
Surface Rutting (inches)
Baseline Condition
AADTTx2
AADTTx5
Pavement Age (month)

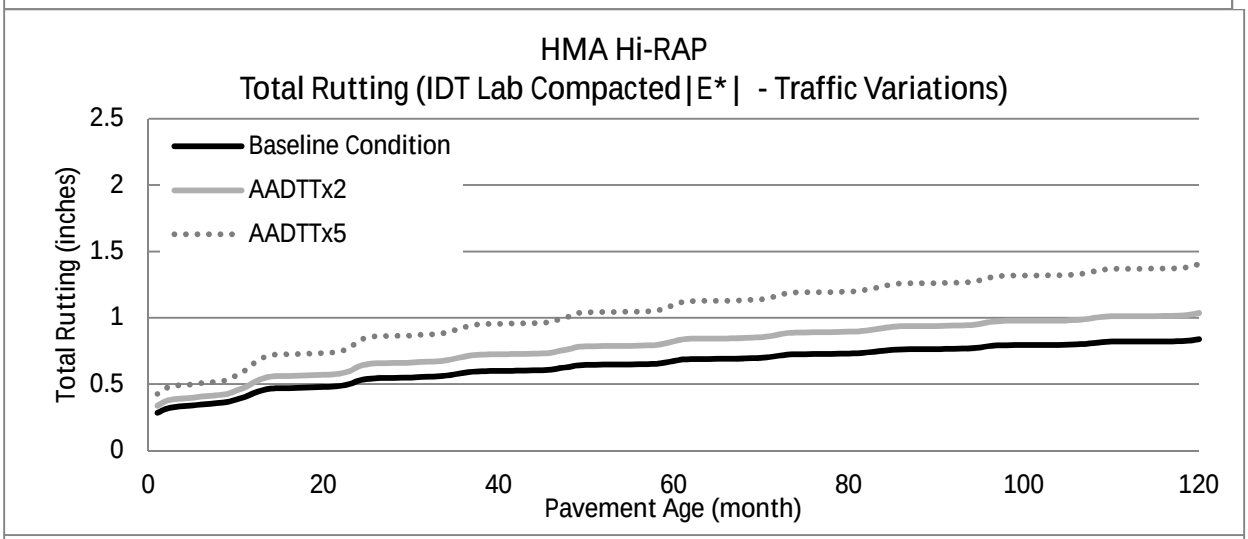
HMA Hi-RAP
Total Rutting (IDT Lab Compacted|E*| - Traffic Variations)
Total Rutting (inches)
Baseline Condition
AADTTx2
AADTTx5
Pavement Age (month)

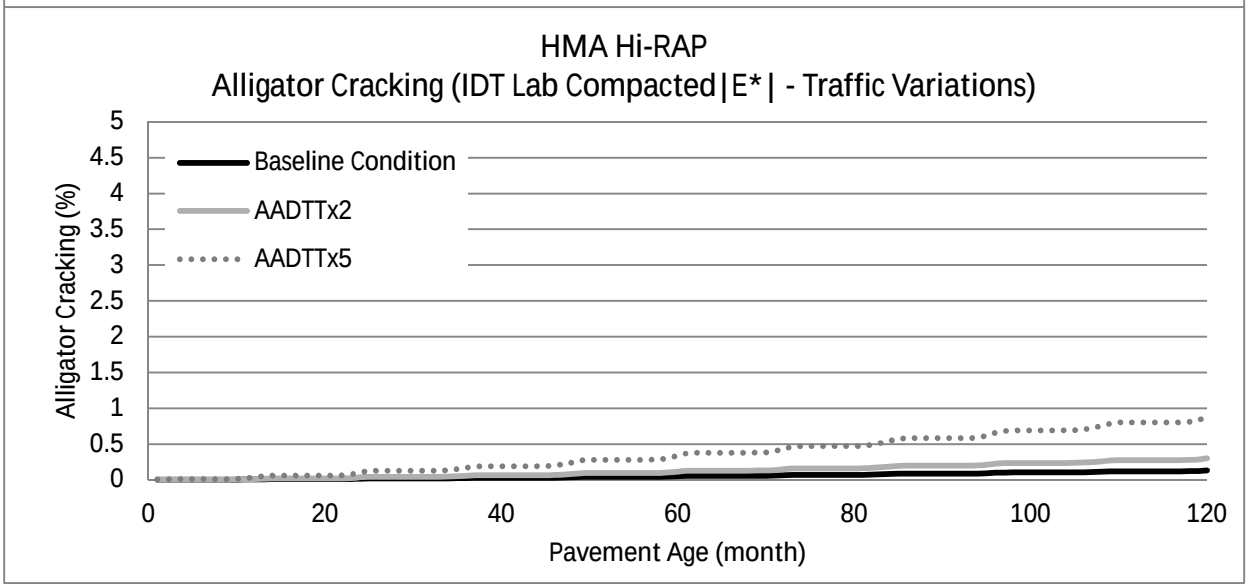
HMA Hi-RAP
Alligator Cracking (IDT Lab Compacted|E*| - Traffic Variations)
Alligator Cracking (%)
Baseline Condition
AADTTx2
AADTTx5
Pavement Age (month)

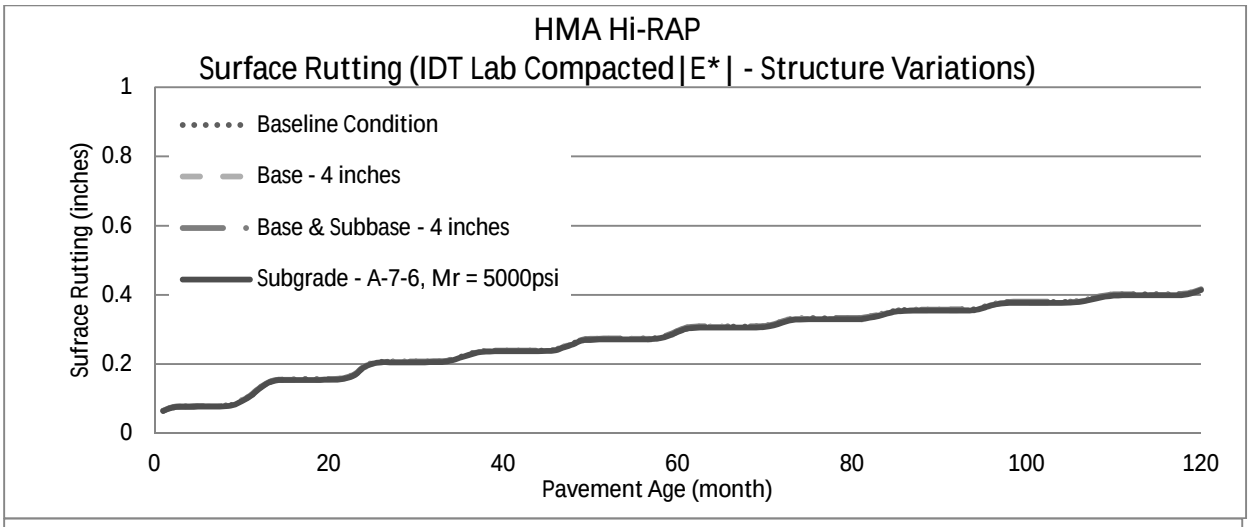
HMA Hi-RAP
Surface Rutting (IDT Lab Compacted|E*| - Structure Variations)
Baseline Condition
Base - 4 inches
Base & Subbase - 4 inches
Subgrade - A-7-6, Mr = 5000psi
Sufrace Rutting (inches)
Pavement Age (month)
0
0.2
0.4
0.6
0.8
1
0
20
40
60
80
100
120

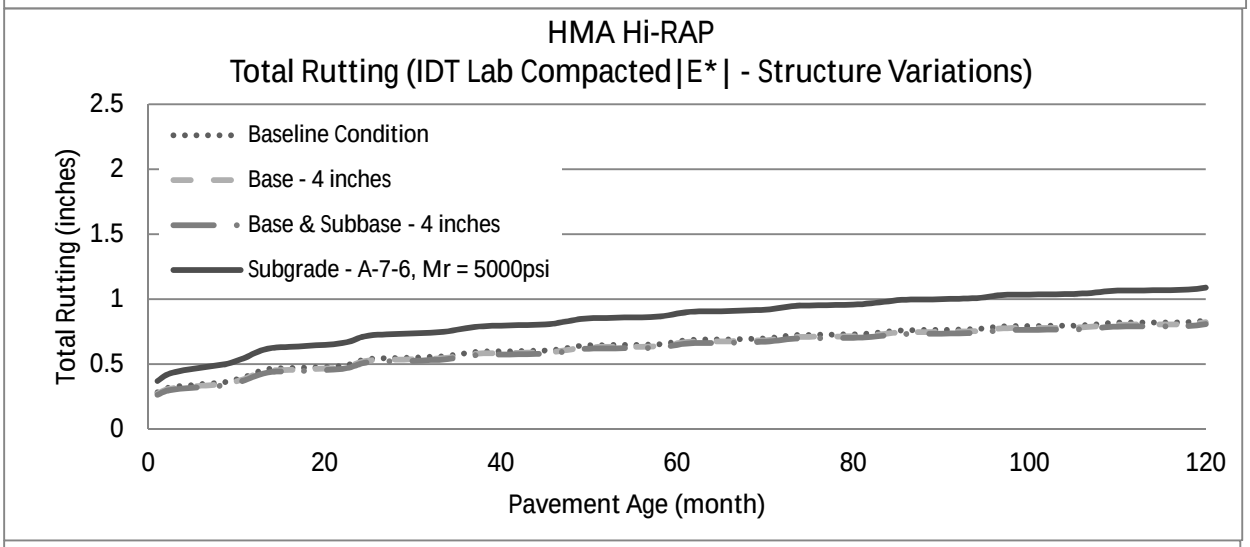
HMA Hi-RAP
Total Rutting (IDT Lab Compacted|E*| - Structure Variations)
Baseline Condition
Base - 4 inches
Base & Subbase - 4 inches
Subgrade - A-7-6, Mr = 5000psi
Total Rutting (inches)
Pavement Age (month)
0
0.5
1
1.5
2
2.5
0
20
40
60
80
100
120

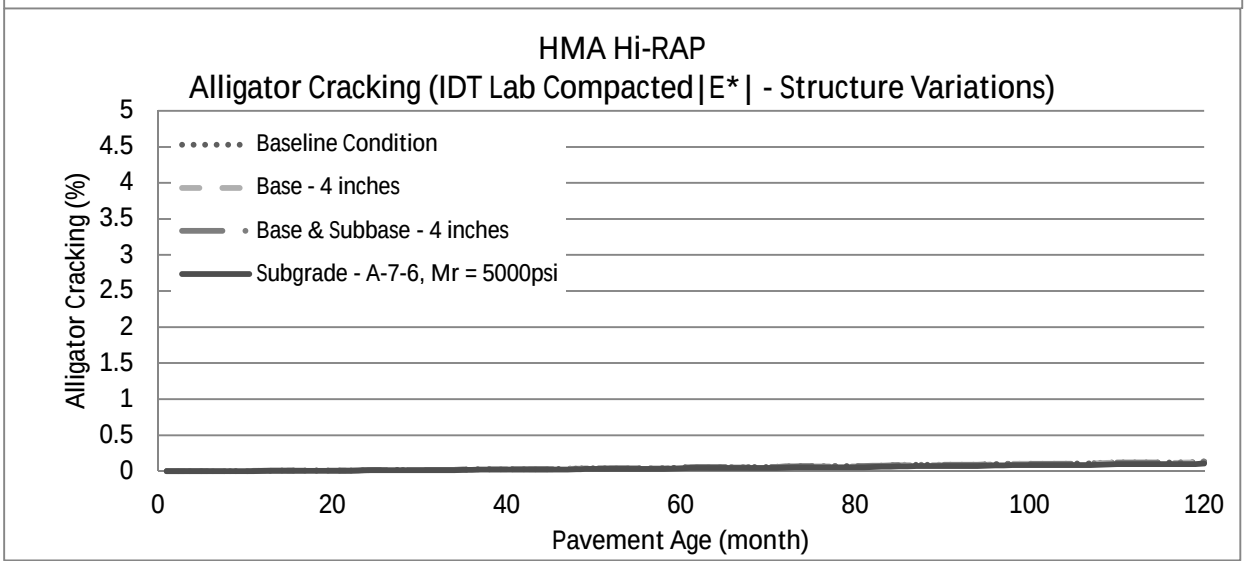
HMA Hi-RAP
Alligator Cracking (IDT Lab Compacted|E*| - Structure Variations)
Baseline Condition
Base - 4 inches
Base & Subbase - 4 inches
Subgrade - A-7-6, Mr = 5000psi
Alligator Cracking (%)
Pavement Age (month)
0
0.5
1
1.5
2
2.5
3
3.5
4
4.5
5
0
20
40
60
80
100
120

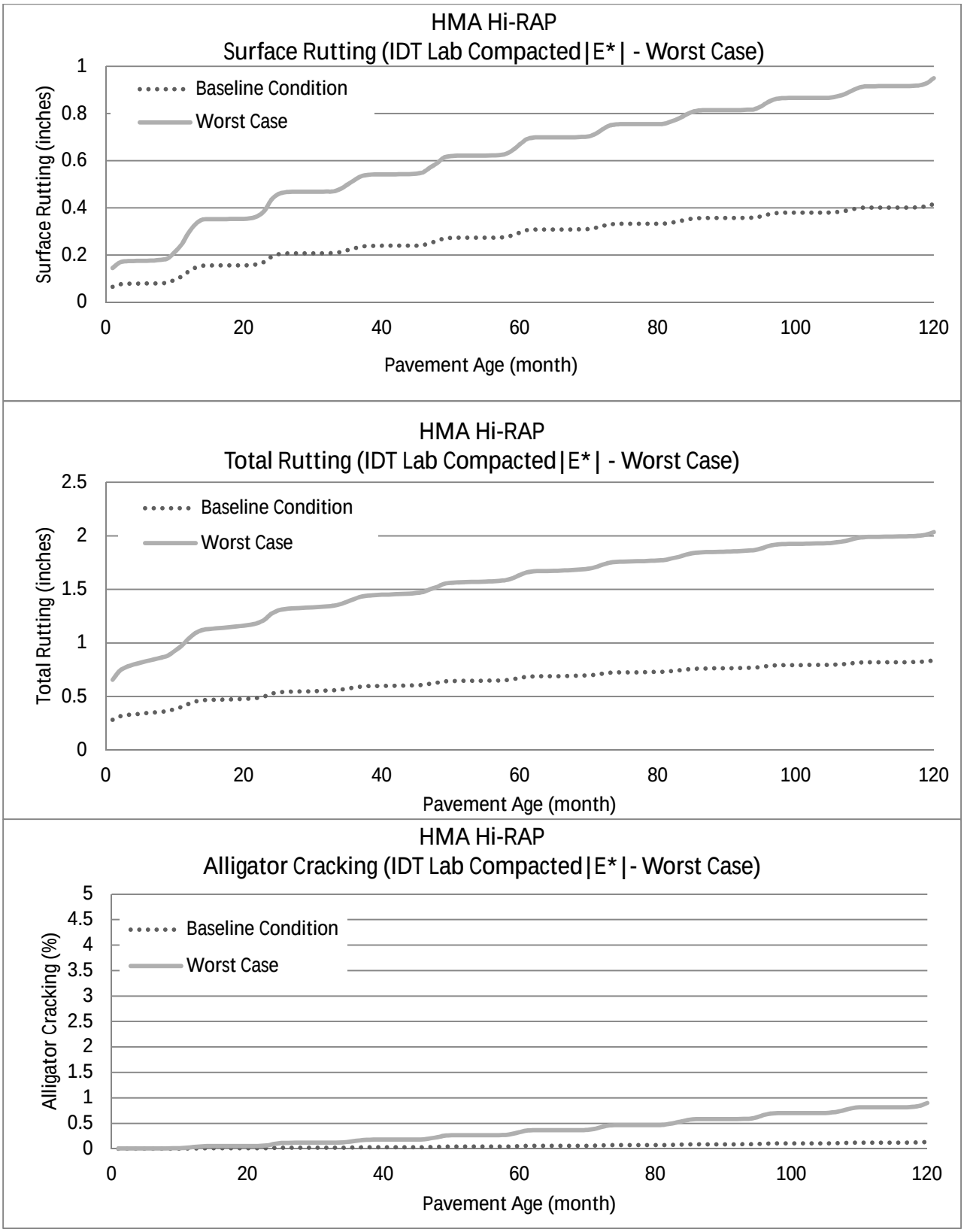
HMA Hi-RAP
Surface Rutting (IDT Lab Compacted|E*| - Worst Case)
Surface Rutting (inches)
Baseline Condition
Worst Case
0
0.2
0.4
0.6
0.8
1
0
20
40
60
80
100
120
Pavement Age (month)
HMA Hi-RAP
Total Rutting (IDT Lab Compacted|E*| - Worst Case)
Total Rutting (inches)
Baseline Condition
Worst Case
0
0.5
1
1.5
2
2.5
0
20
40
60
80
100
120
Pavement Age (month)
HMA Hi-RAP
Alligator Cracking (IDT Lab Compacted|E*|- Worst Case)
Alligator Cracking (%)
Baseline Condition
Worst Case
0
0.5
1
1.5
2
2.5
3
3.5
4
4.5
5
0
20
40
60
80
100
120
Pavement Age (month)

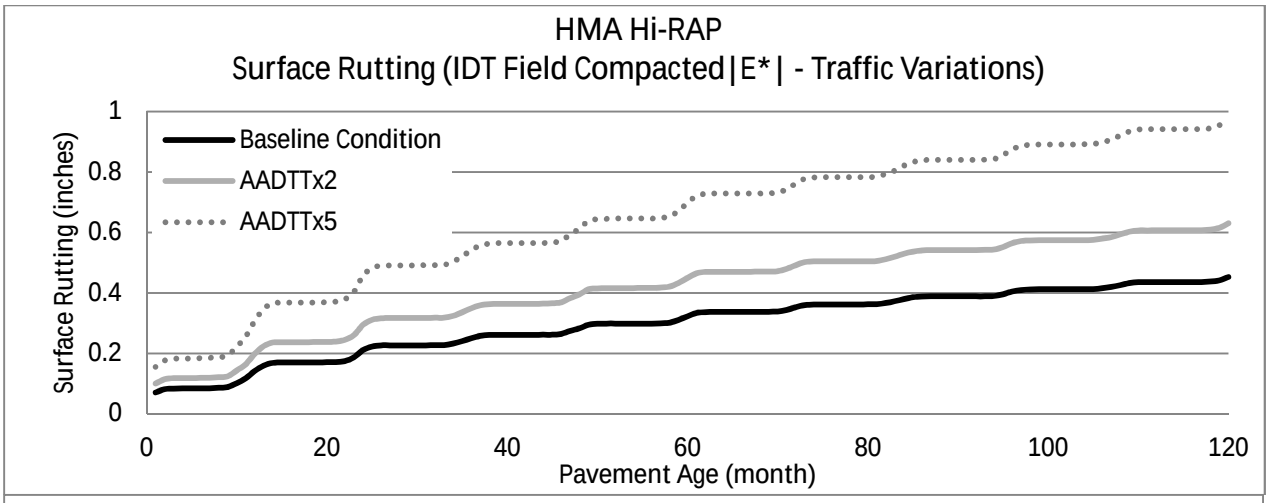
HMA Hi-RAP
Surface Rutting (IDT Field Compacted|E*| - Traffic Variations)
Surface Rutting (inches)
Baseline Condition
AADTTx2
AADTTx5
Pavement Age (month)

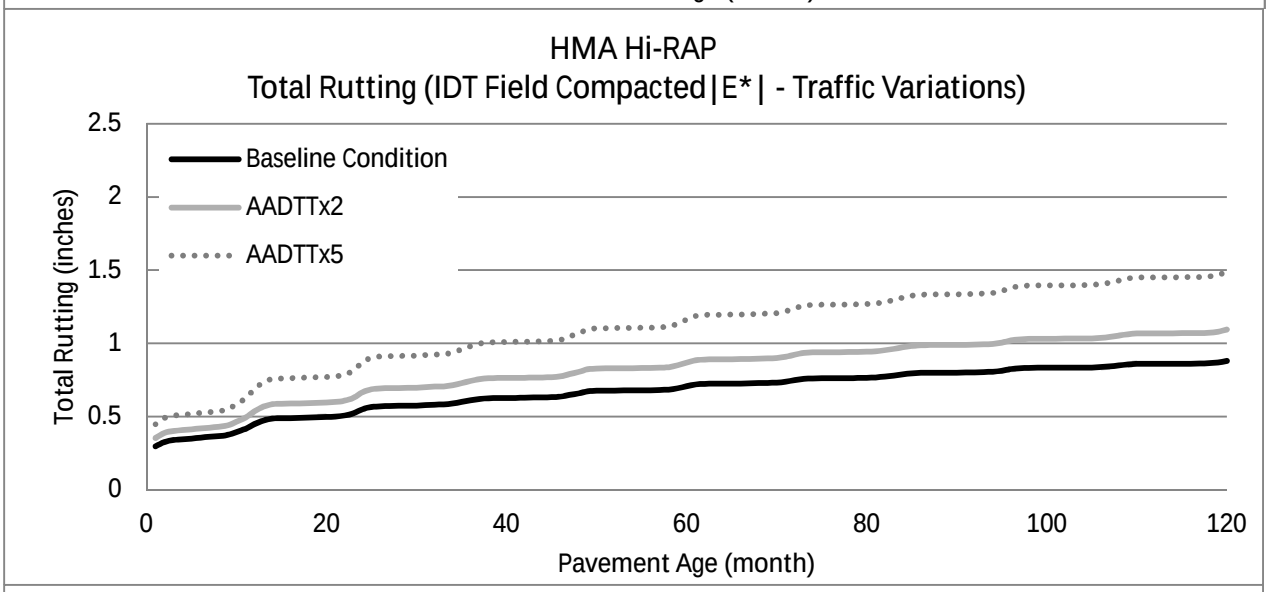
HMA Hi-RAP
Total Rutting (IDT Field Compacted|E*| - Traffic Variations)
Total Rutting (inches)
Baseline Condition
AADTTx2
AADTTx5
Pavement Age (month)

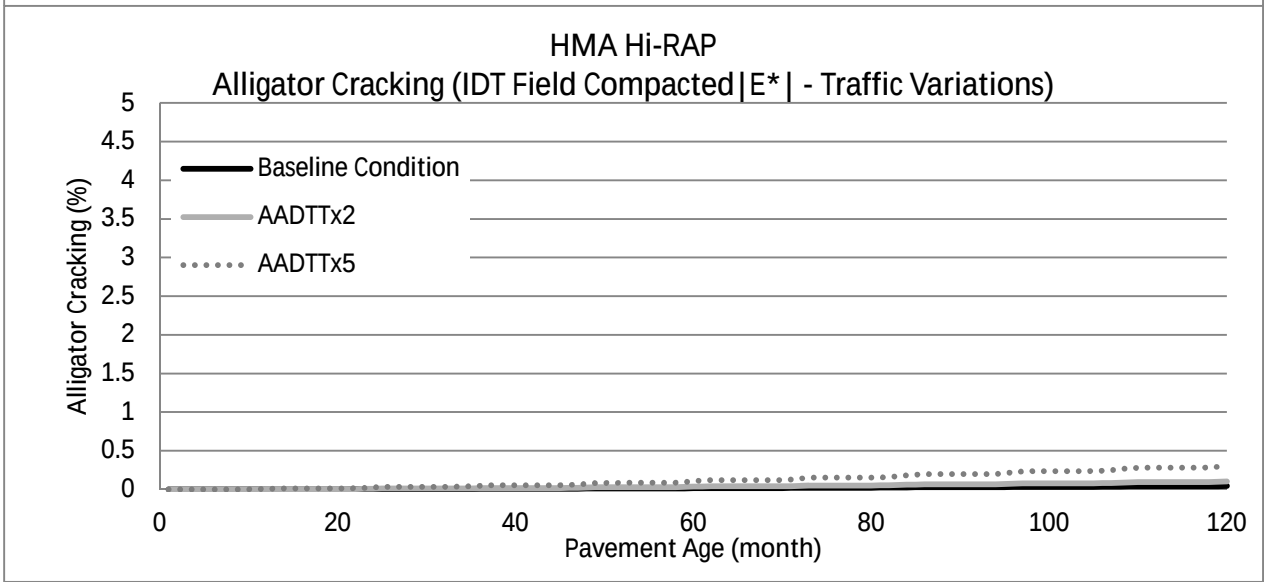
HMA Hi-RAP
Alligator Cracking (IDT Field Compacted|E*| - Traffic Variations)
Alligator Cracking (%)
Baseline Condition
AADTTx2
AADTTx5
Pavement Age (month)

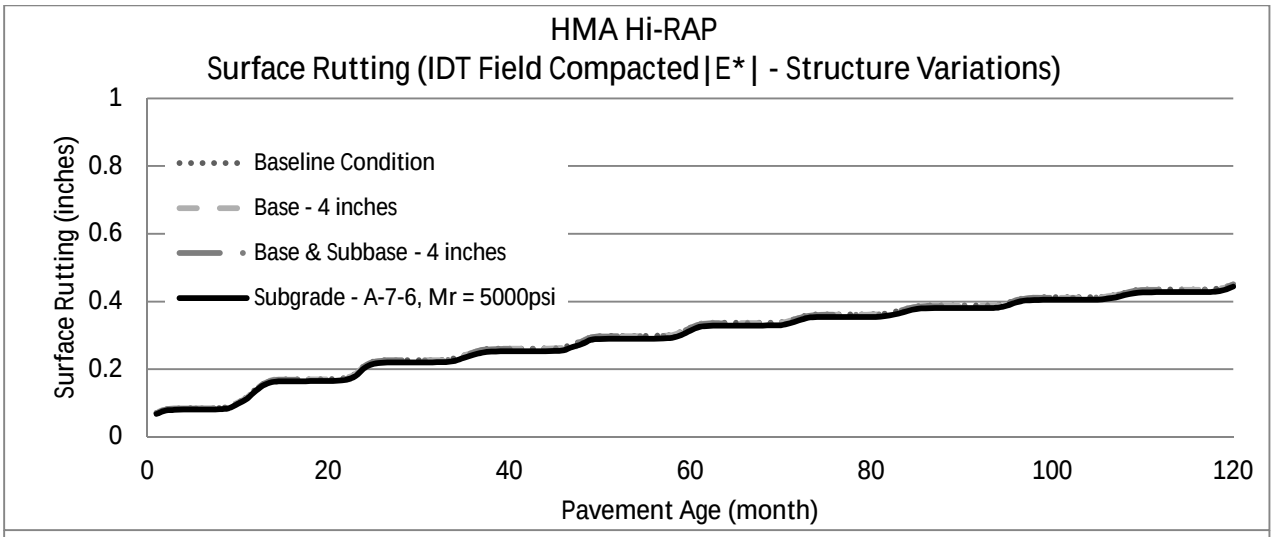
HMA Hi-RAP
Surface Rutting (IDT Field Compacted |E*| - Structure Variations)
Surface Rutting (inches)
Pavement Age (month)
Baseline Condition
Base - 4 inches
Base & Subbase - 4 inches
Subgrade - A-7-6, Mr = 5000psi
0
0.2
0.4
0.6
0.8
1
0
20
40
60
80
100
120

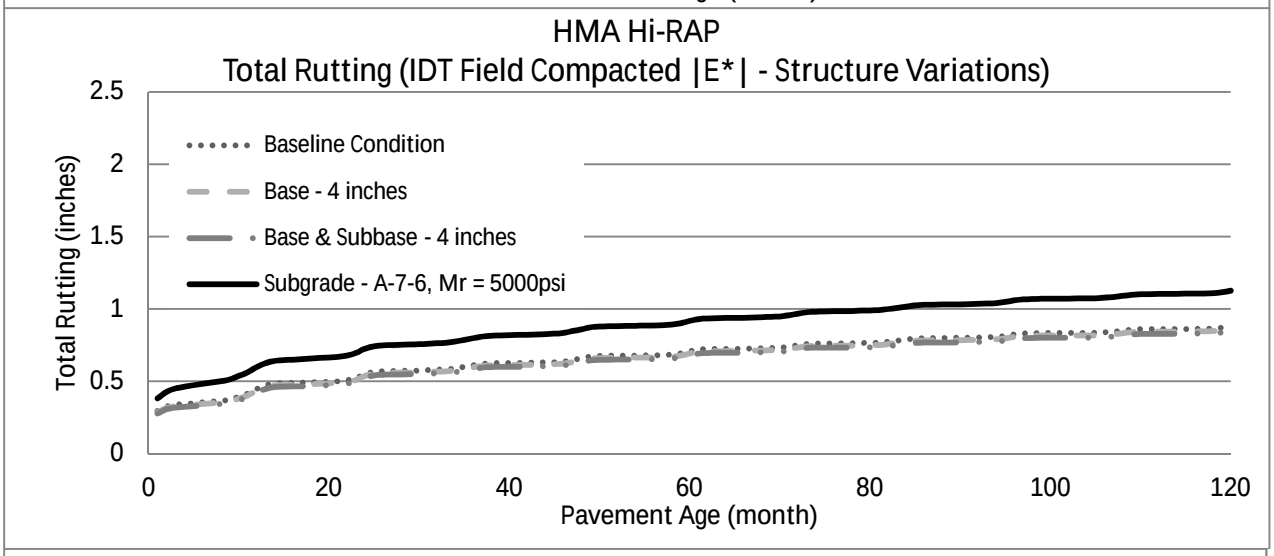
HMA Hi-RAP
Total Rutting (IDT Field Compacted |E*| - Structure Variations)
Total Rutting (inches)
Pavement Age (month)
Baseline Condition
Base - 4 inches
Base & Subbase - 4 inches
Subgrade - A-7-6, Mr = 5000psi
0
0.5
1
1.5
2
2.5
0
20
40
60
80
100
120

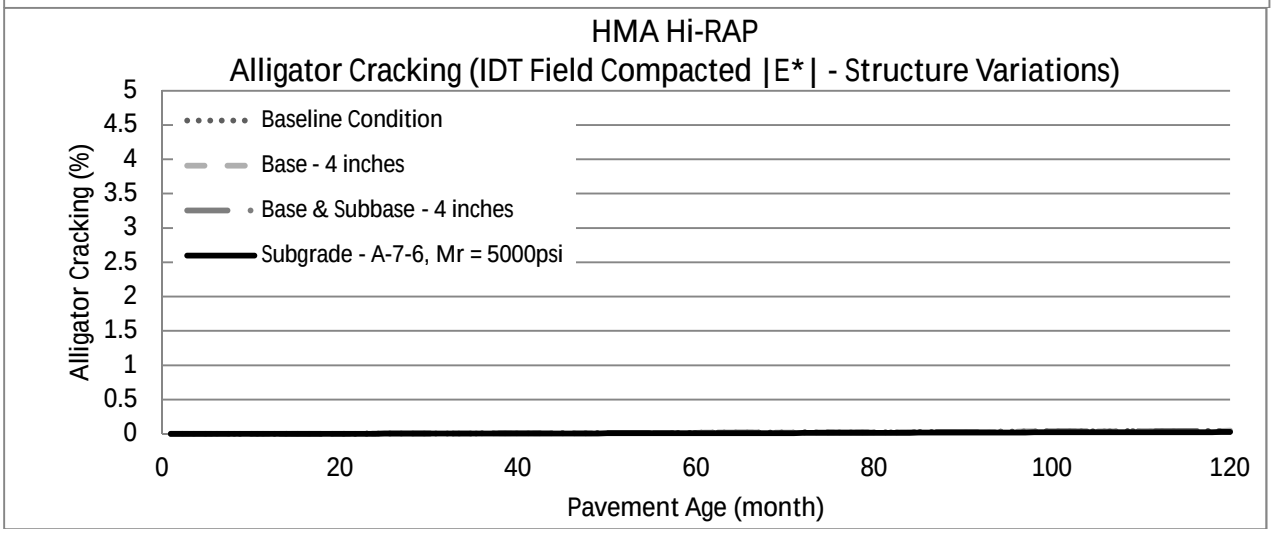
HMA Hi-RAP
Alligator Cracking (IDT Field Compacted |E*| - Structure Variations)
Alligator Cracking (%)
Pavement Age (month)
Baseline Condition
Base - 4 inches
Base & Subbase - 4 inches
Subgrade - A-7-6, Mr = 5000psi
0
0.5
1
1.5
2
2.5
3
3.5
4
4.5
5
0
20
40
60
80
100
120

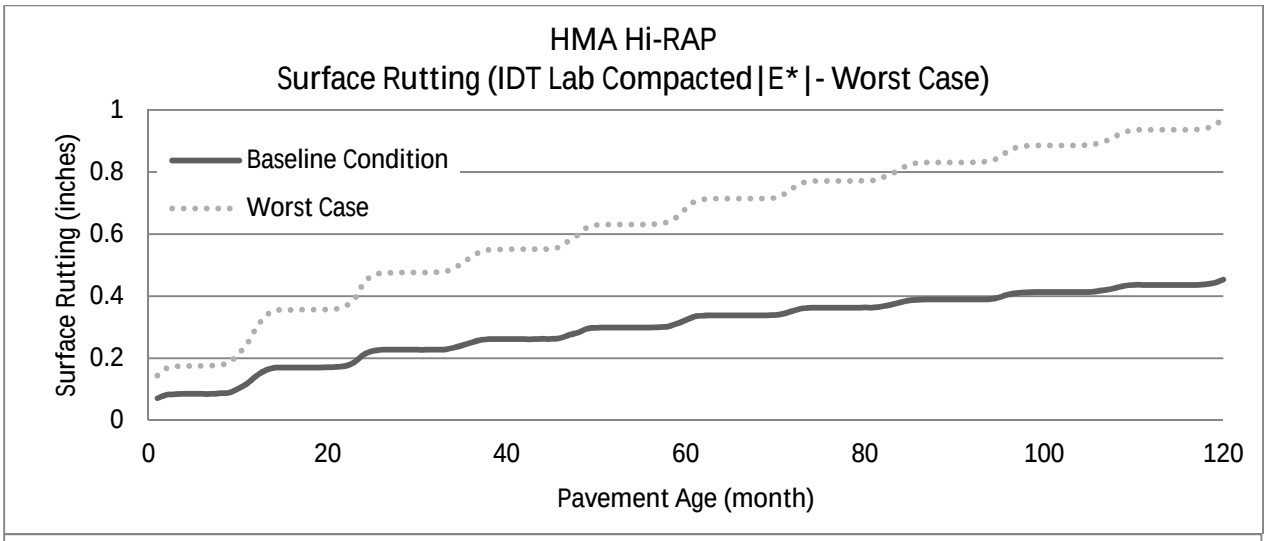
HMA Hi-RAP
Surface Rutting (IDT Lab Compacted|E*|- Worst Case)
Surface Rutting (inches)
Baseline Condition
Worst Case
Pavement Age (month)

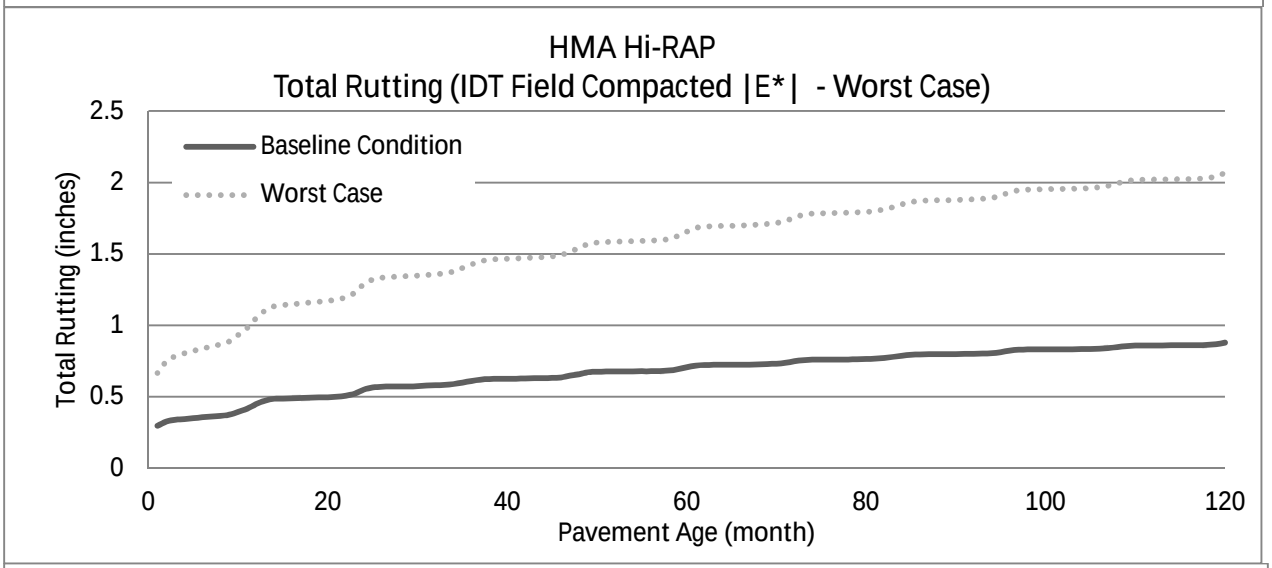
HMA Hi-RAP
Total Rutting (IDT Field Compacted |E*| - Worst Case)
Total Rutting (inches)
Baseline Condition
Worst Case
Pavement Age (month)

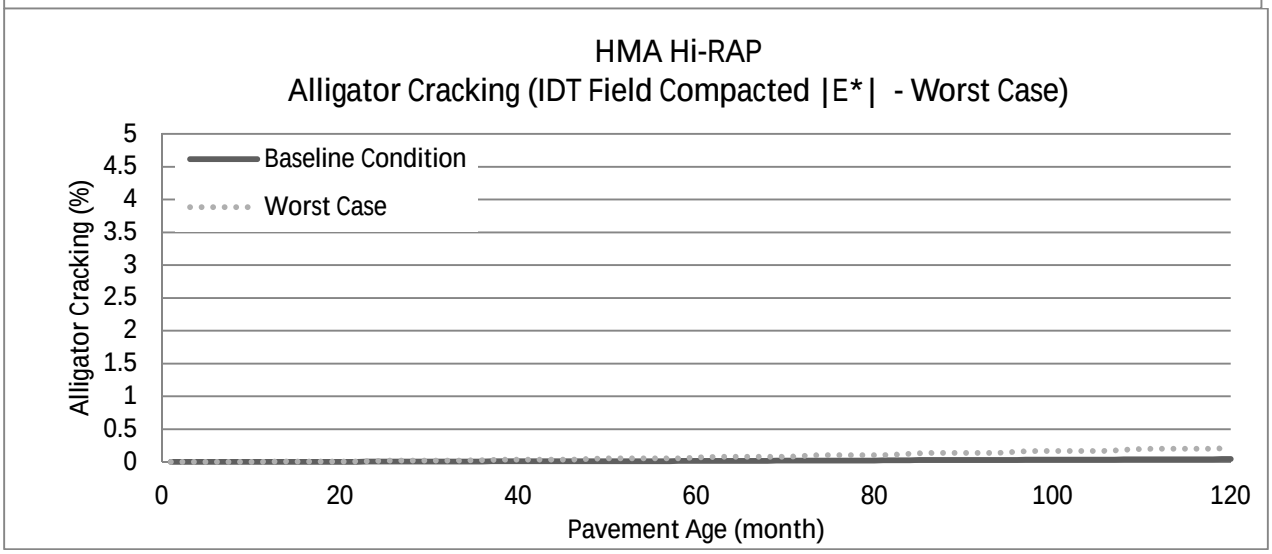
HMA Hi-RAP
Alligator Cracking (IDT Field Compacted |E*| - Worst Case)
Alligator Cracking (%)
Baseline Condition
Worst Case
Pavement Age (month)

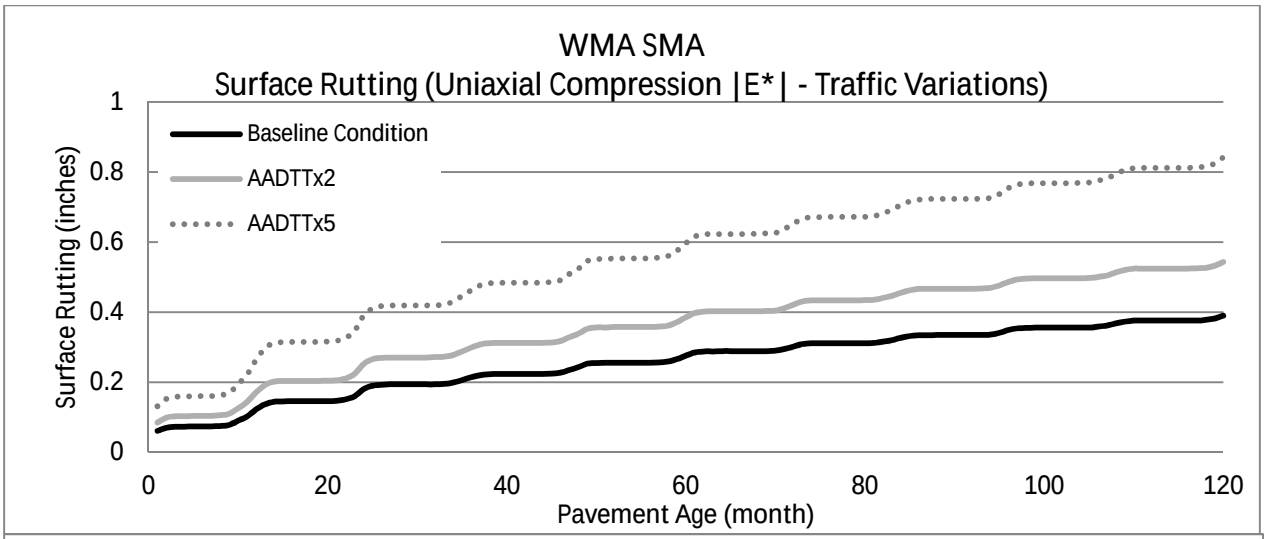
WMA SMA
Surface Rutting (Uniaxial Compression |E*| - Traffic Variations)
Surface Rutting (inches)
Baseline Condition
AADTTx2
AADTTx5
0
0.2
0.4
0.6
0.8
1
0
20
40
60
80
100
120
Pavement Age (month)

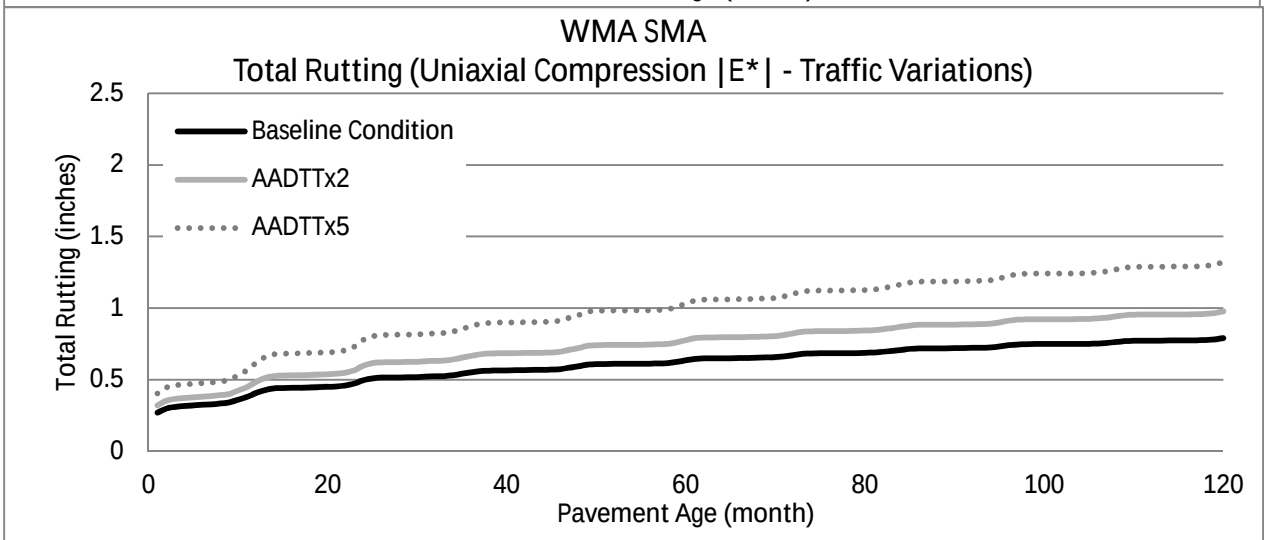
WMA SMA
Total Rutting (Uniaxial Compression |E*| - Traffic Variations)
Total Rutting (inches)
Baseline Condition
AADTTx2
AADTTx5
0
0.5
1
1.5
2
2.5
0
20
40
60
80
100
120
Pavement Age (month)

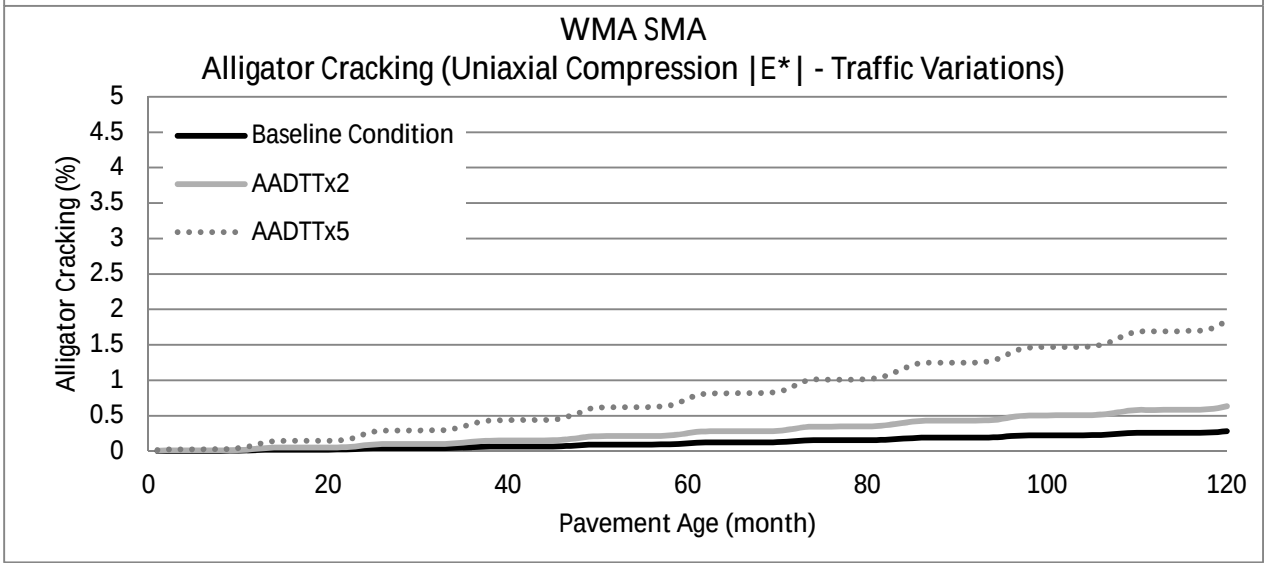
WMA SMA
Alligator Cracking (Uniaxial Compression |E*| - Traffic Variations)
Alligator Cracking (%)
Baseline Condition
AADTTx2
AADTTx5
0
0.5
1
1.5
2
2.5
3
3.5
4
4.5
5
0
20
40
60
80
100
120
Pavement Age (month)

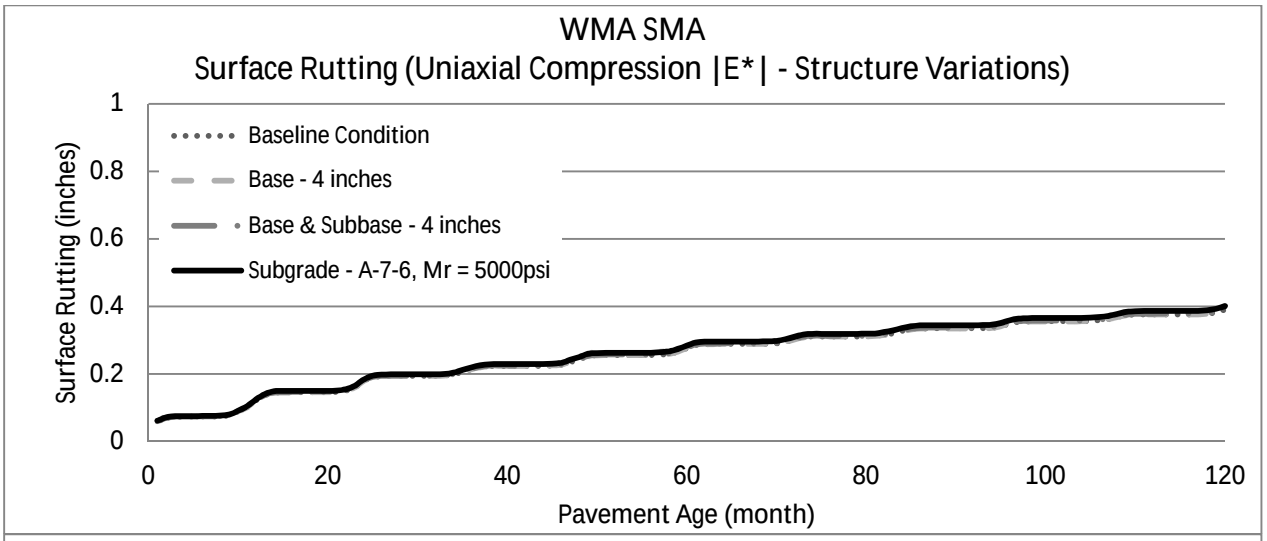
WMA SMA
Surface Rutting (Uniaxial Compression |E*| - Structure Variations)
Surface Rutting (inches)
Baseline Condition
Base - 4 inches
Base & Subbase - 4 inches
Subgrade - A-7-6, Mr = 5000psi
Pavement Age (month)

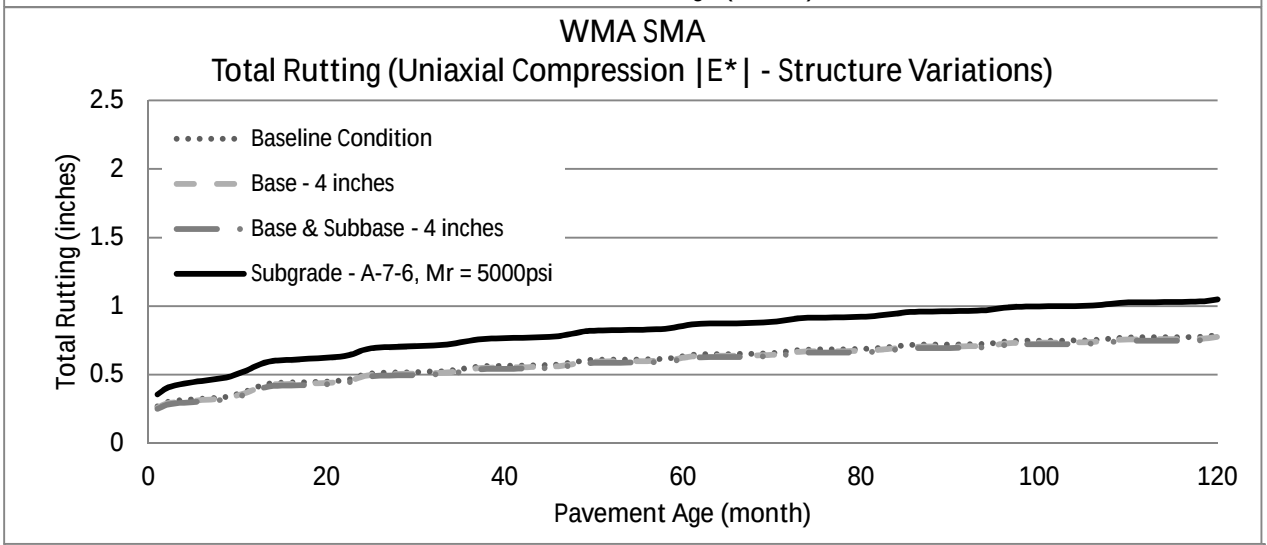
WMA SMA
Total Rutting (Uniaxial Compression |E*| - Structure Variations)
Total Rutting (inches)
Baseline Condition
Base - 4 inches
Base & Subbase - 4 inches
Subgrade - A-7-6, Mr = 5000psi
Pavement Age (month)

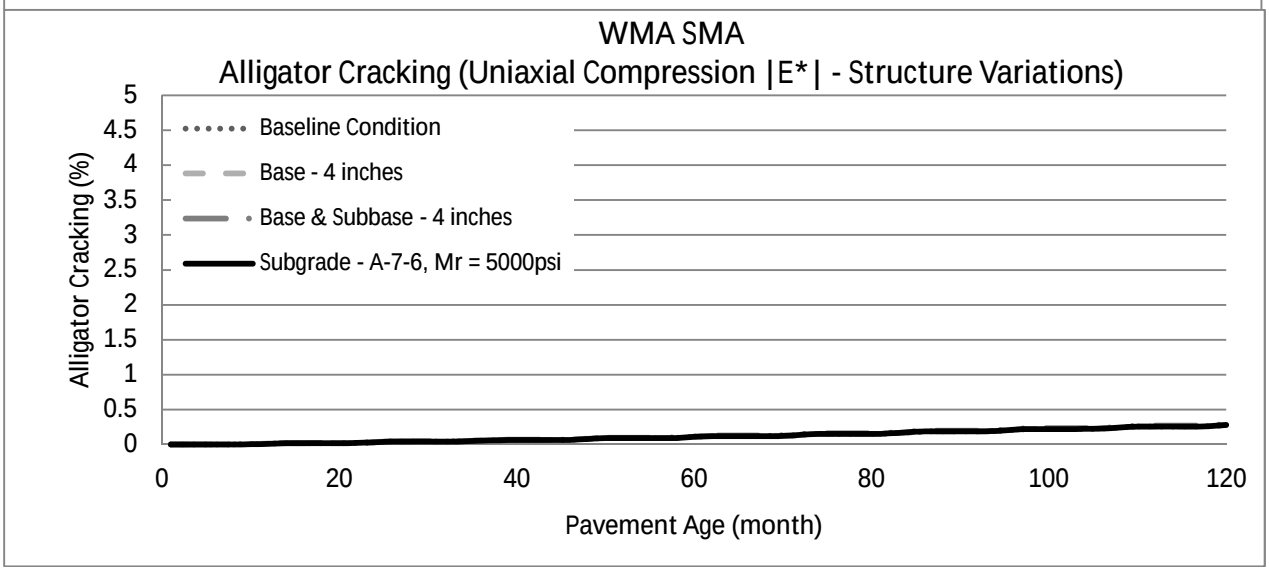
WMA SMA
Alligator Cracking (Uniaxial Compression |E*| - Structure Variations)
Alligator Cracking (%)
Baseline Condition
Base - 4 inches
Base & Subbase - 4 inches
Subgrade - A-7-6, Mr = 5000psi
Pavement Age (month)

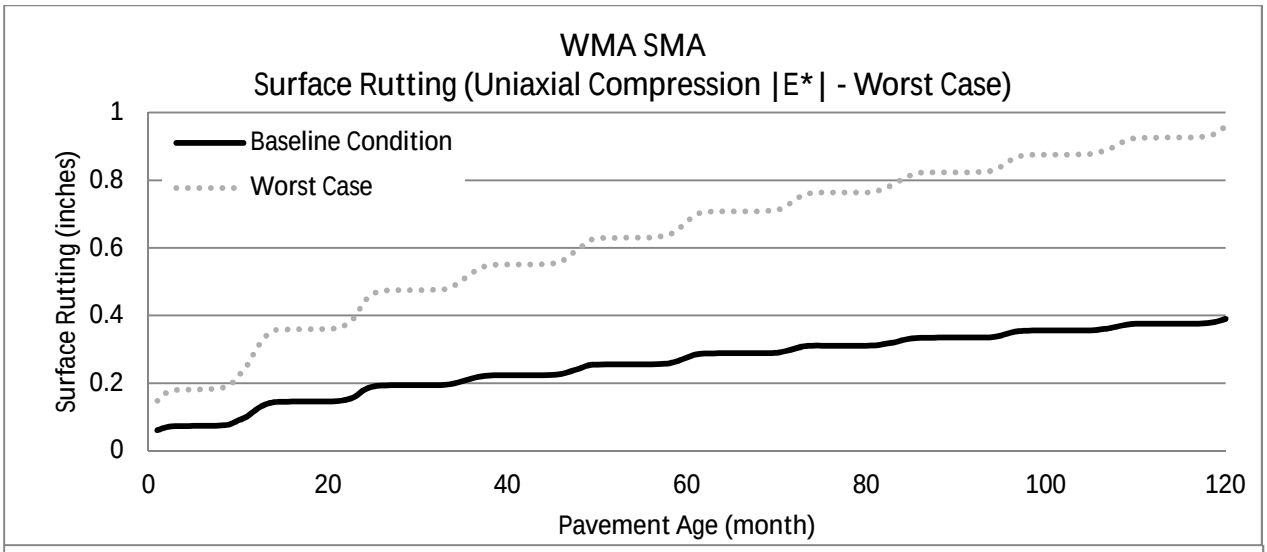
WMA SMA
Surface Rutting (Uniaxial Compression |E*| - Worst Case)
Surface Rutting (inches)
Baseline Condition
Worst Case
0
0.2
0.4
0.6
0.8
1
0
20
40
60
80
100
120
Pavement Age (month)

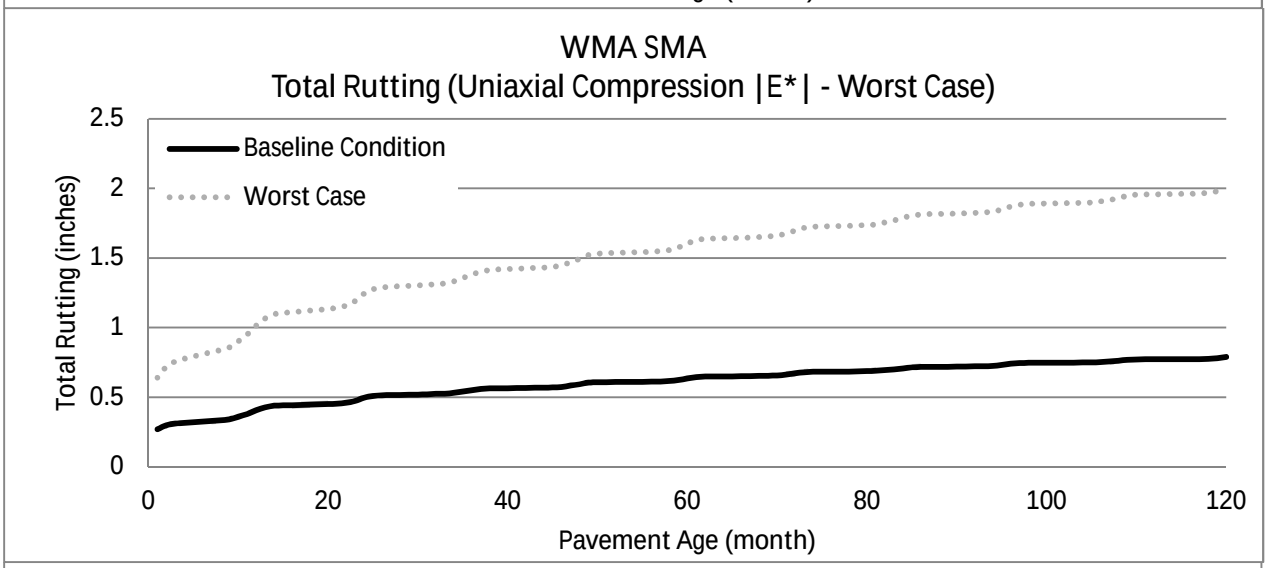
WMA SMA
Total Rutting (Uniaxial Compression |E*| - Worst Case)
Total Rutting (inches)
Baseline Condition
Worst Case
0
0.5
1
1.5
2
2.5
0
20
40
60
80
100
120
Pavement Age (month)

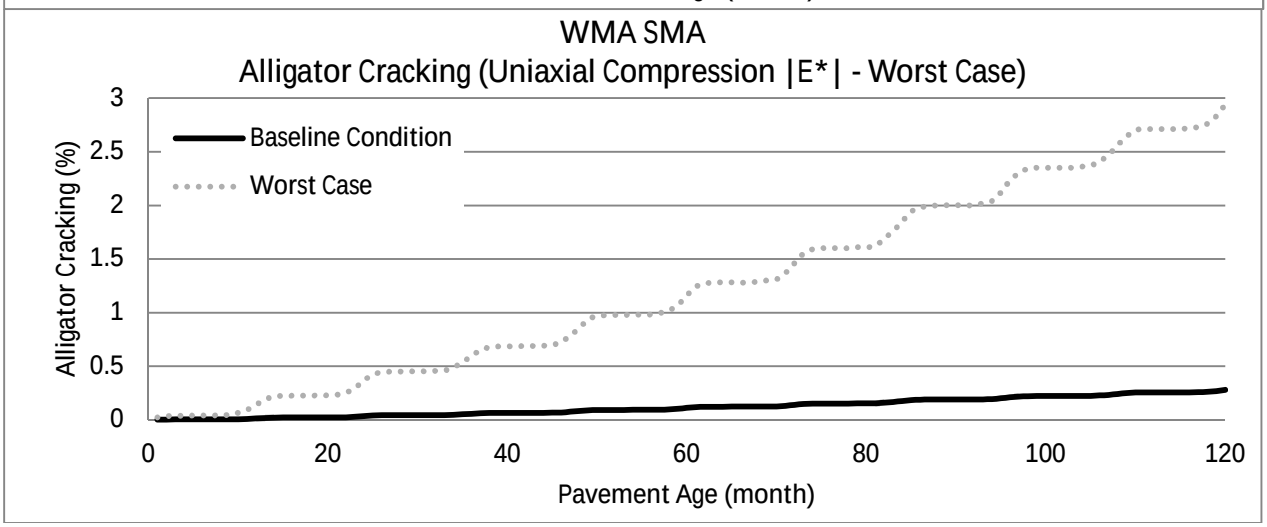
WMA SMA
Alligator Cracking (Uniaxial Compression |E*| - Worst Case)
Alligator Cracking (%)
Baseline Condition
Worst Case
0
0.5
1
1.5
2
2.5
3
0
20
40
60
80
100
120
Pavement Age (month)

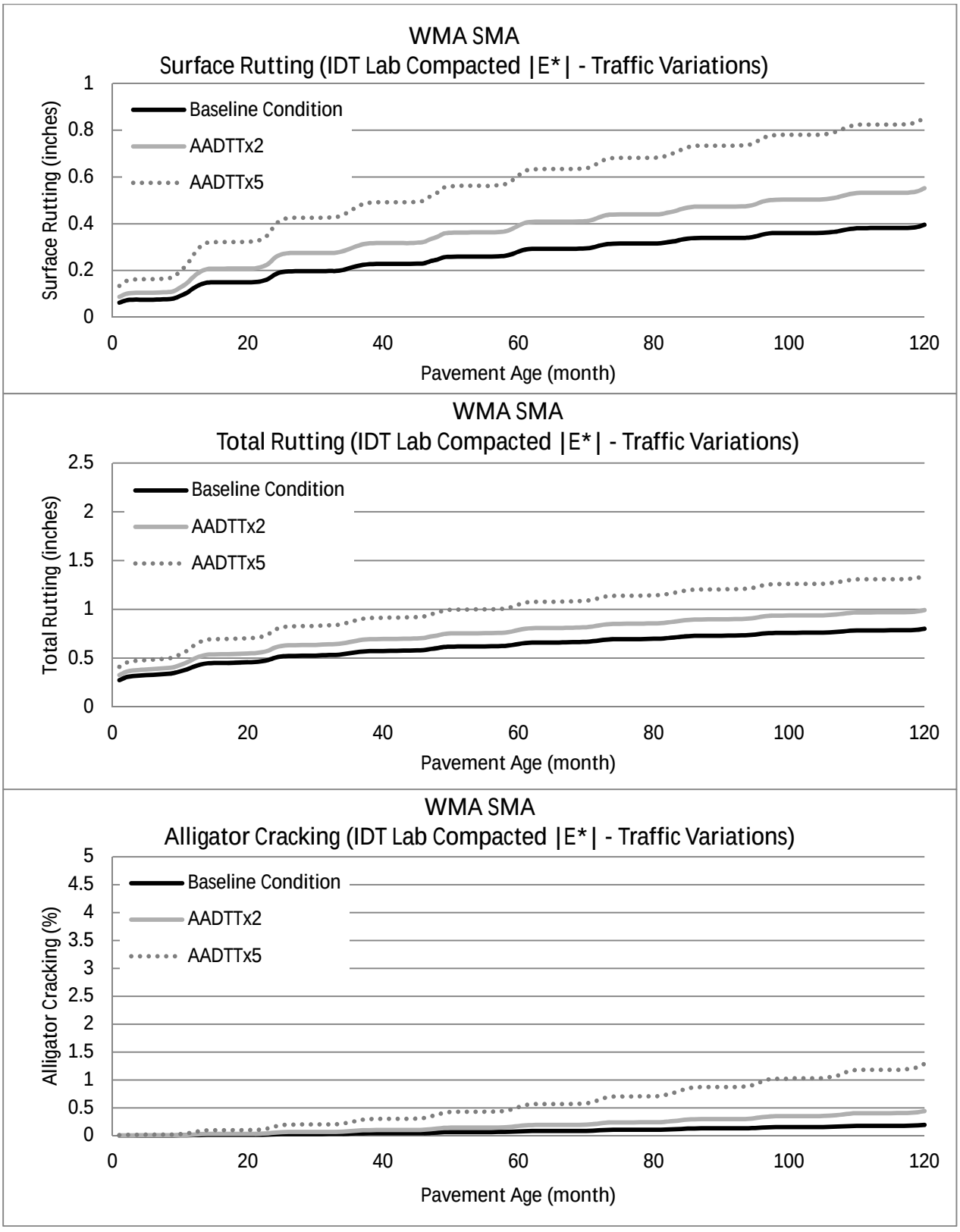
WMA SMA
Surface Rutting (IDT Lab Compacted |E*| - Traffic Variations)
Surface Rutting (inches)
Baseline Condition
AADTTx2
AADTTx5
Pavement Age (month)
WMA SMA
Total Rutting (IDT Lab Compacted |E*| - Traffic Variations)
Total Rutting (inches)
Baseline Condition
AADTTx2
AADTTx5
Pavement Age (month)
WMA SMA
Alligator Cracking (IDT Lab Compacted |E*| - Traffic Variations)
Alligator Cracking (%)
Baseline Condition
AADTTx2
AADTTx5
Pavement Age (month)

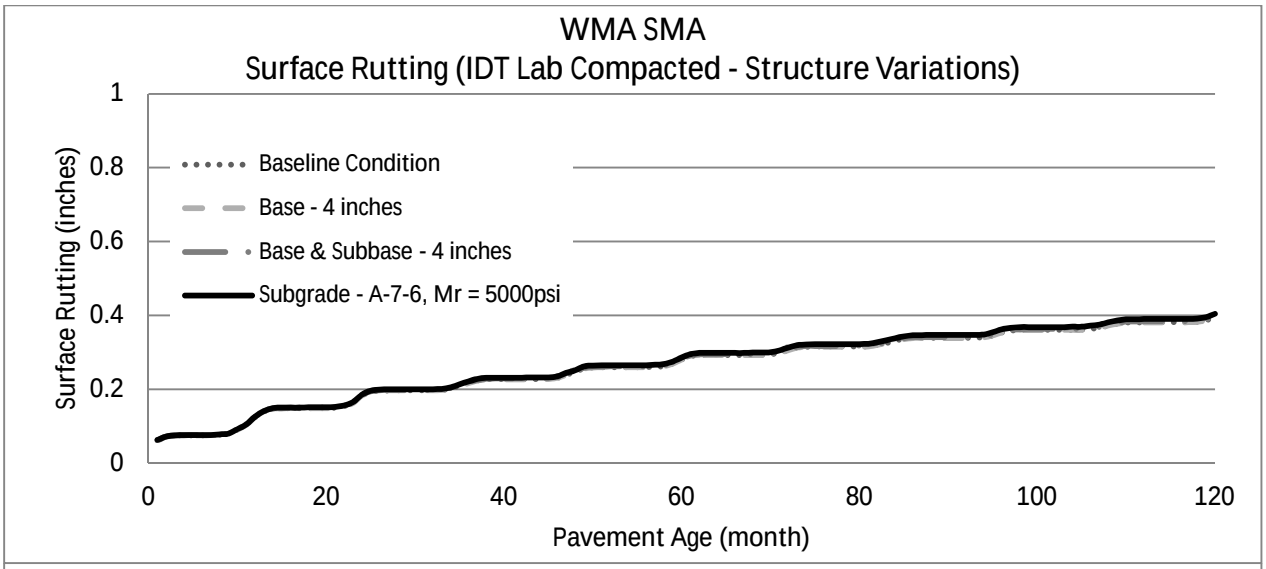
WMA SMA
Surface Rutting (IDT Lab Compacted - Structure Variations)
Surface Rutting (inches)
1
0.8
0.6
0.4
0.2
0
Baseline Condition
Base - 4 inches
Base & Subbase - 4 inches
Subgrade - A-7-6, Mr = 5000psi
0
20
40
60
80
100
120
Pavement Age (month)

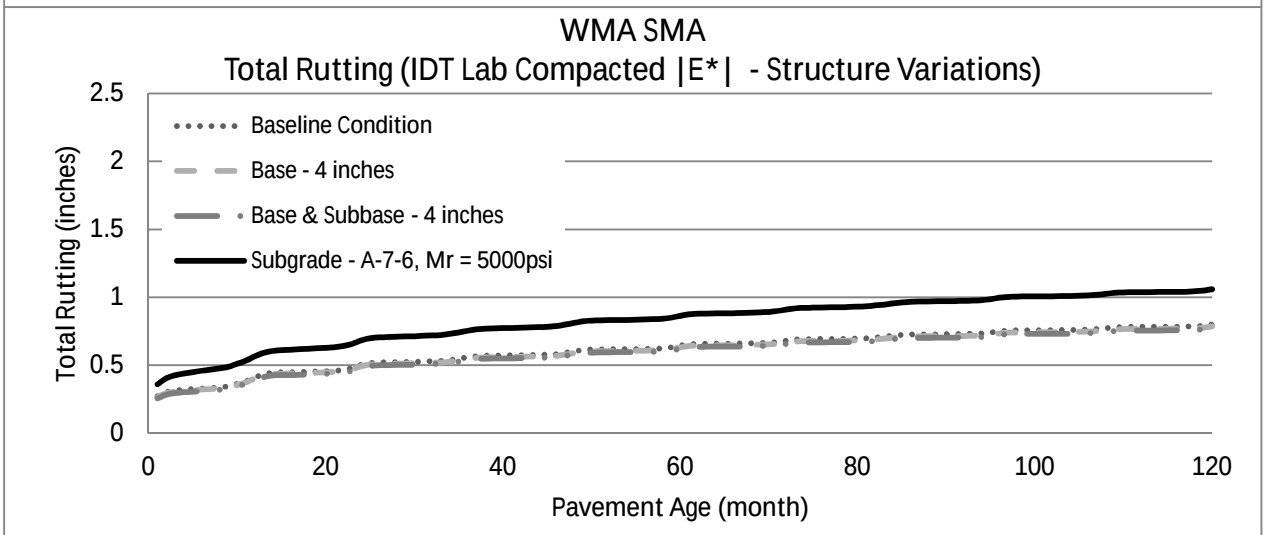
WMA SMA
Total Rutting (IDT Lab Compacted |E*| - Structure Variations)
Total Rutting (inches)
2.5
2
1.5
1
0.5
0
Baseline Condition
Base - 4 inches
Base & Subbase - 4 inches
Subgrade - A-7-6, Mr = 5000psi
0
20
40
60
80
100
120
Pavement Age (month)

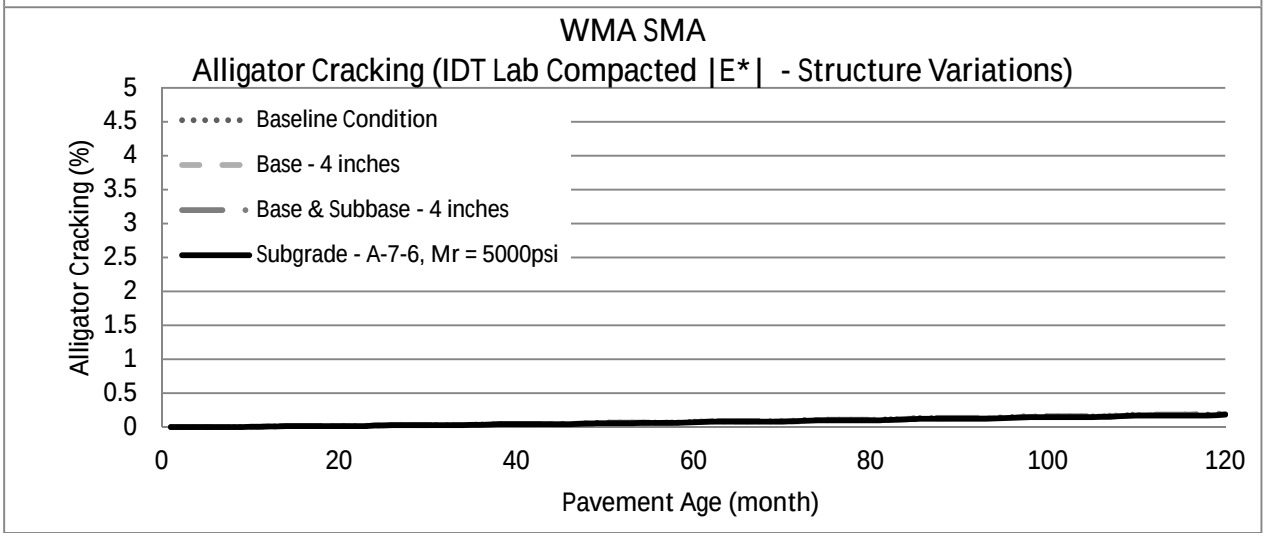
WMA SMA
Alligator Cracking (IDT Lab Compacted |E*| - Structure Variations)
Alligator Cracking (%)
5
4.5
4
3.5
3
2.5
2
1.5
1
0.5
0
Baseline Condition
Base - 4 inches
Base & Subbase - 4 inches
Subgrade - A-7-6, Mr = 5000psi
0
20
40
60
80
100
120
Pavement Age (month)

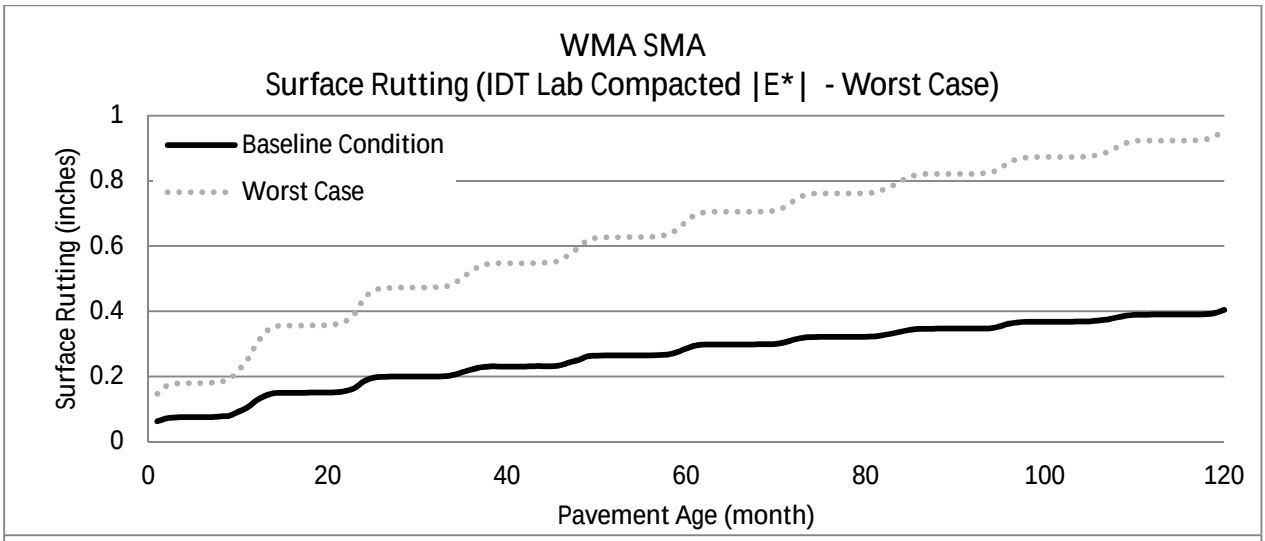
WMA SMA
Surface Rutting (IDT Lab Compacted |E*| - Worst Case)
Surface Rutting (inches)
Baseline Condition
Worst Case
0
0.2
0.4
0.6
0.8
1
0
20
40
60
80
100
120
Pavement Age (month)

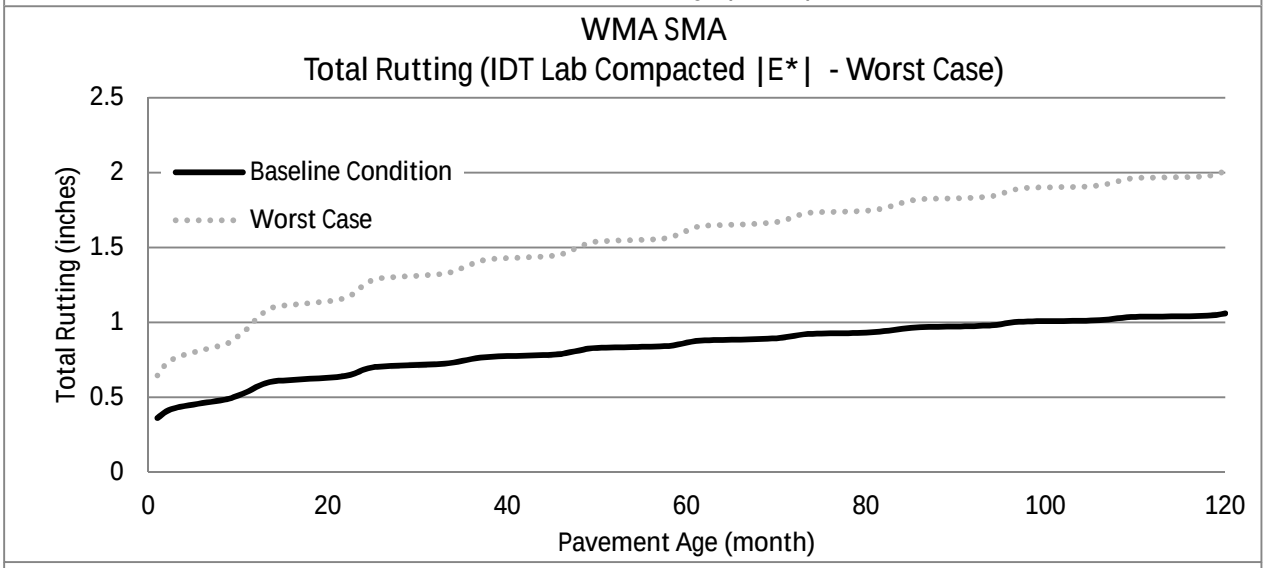
WMA SMA
Total Rutting (IDT Lab Compacted |E*| - Worst Case)
Total Rutting (inches)
Baseline Condition
Worst Case
0
0.5
1
1.5
2
2.5
0
20
40
60
80
100
120
Pavement Age (month)

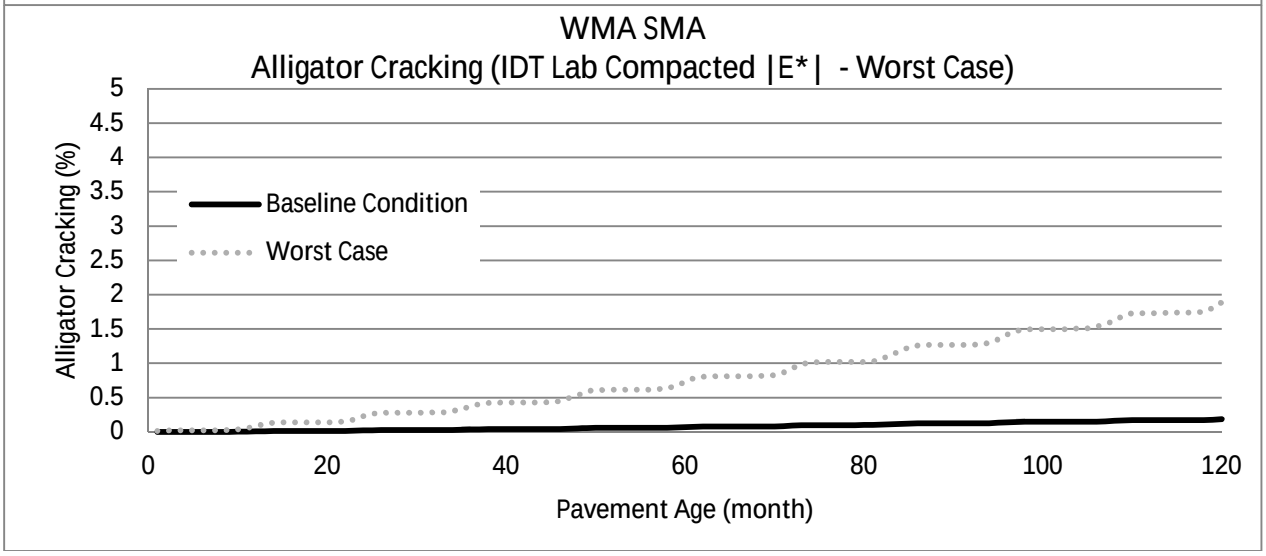
WMA SMA
Alligator Cracking (IDT Lab Compacted |E*| - Worst Case)
Alligator Cracking (%)
Baseline Condition
Worst Case
0
0.5
1
1.5
2
2.5
3
3.5
4
4.5
5
0
20
40
60
80
100
120
Pavement Age (month)

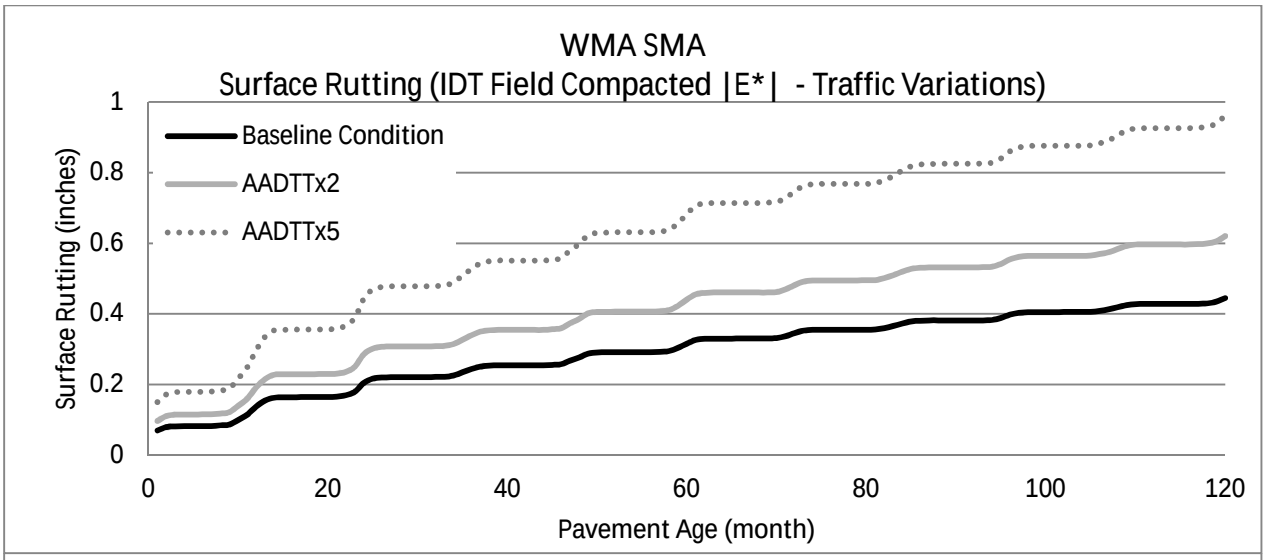
WMA SMA
Surface Rutting (IDT Field Compacted |E*| - Traffic Variations)
Surface Rutting (inches)
Baseline Condition
AADTTx2
AADTTx5
0
0.2
0.4
0.6
0.8
1
0
20
40
60
80
100
120
Pavement Age (month)

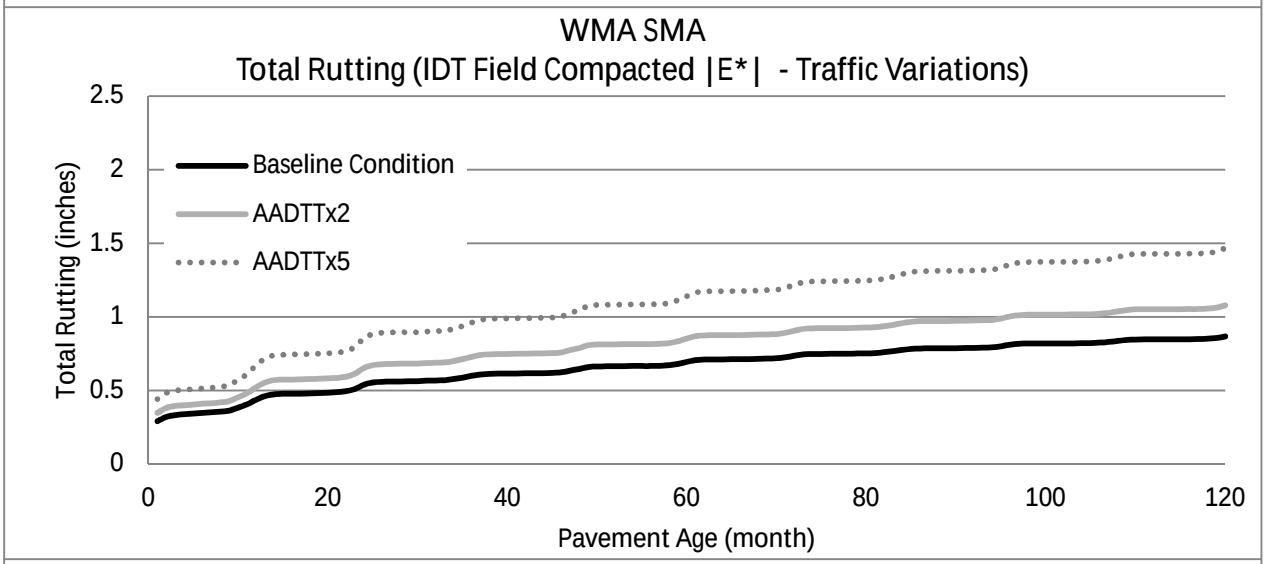
WMA SMA
Total Rutting (IDT Field Compacted |E*| - Traffic Variations)
Total Rutting (inches)
Baseline Condition
AADTTx2
AADTTx5
0
0.5
1
1.5
2
2.5
0
20
40
60
80
100
120
Pavement Age (month)

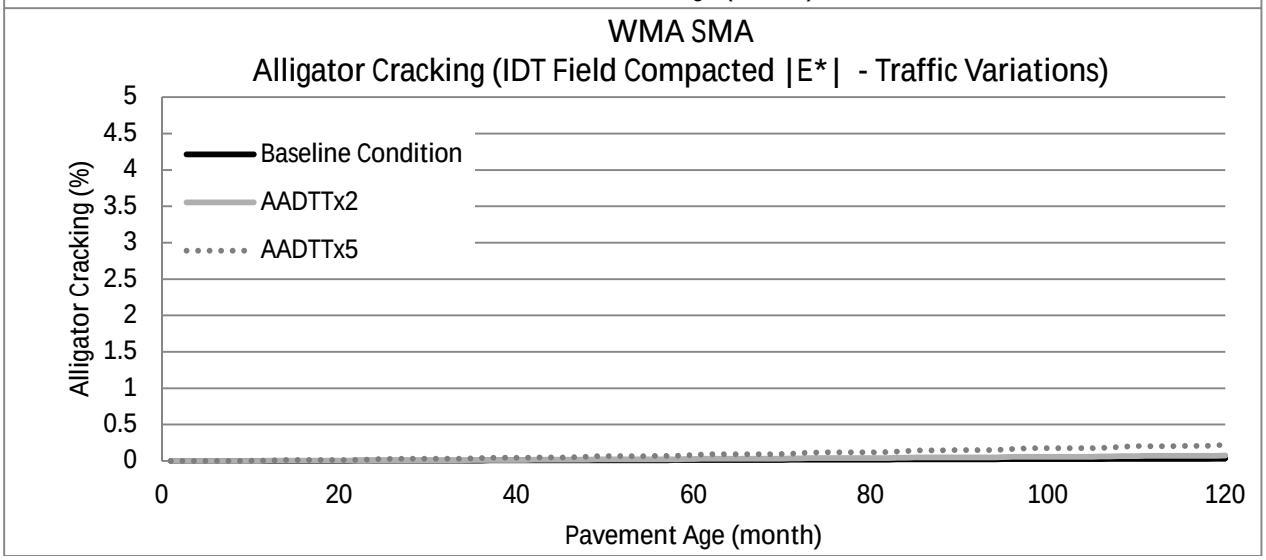
WMA SMA
Alligator Cracking (IDT Field Compacted |E*| - Traffic Variations)
Alligator Cracking (%)
Baseline Condition
AADTTx2
AADTTx5
0
0.5
1
1.5
2
2.5
3
3.5
4
4.5
5
0
20
40
60
80
100
120
Pavement Age (month)

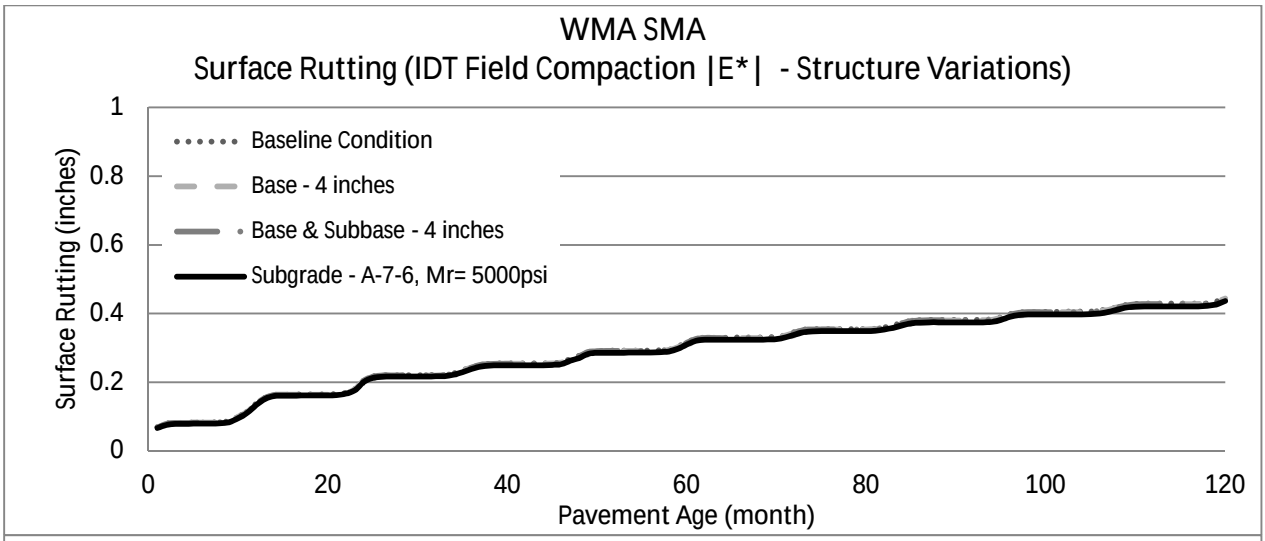
WMA SMA
Surface Rutting (IDT Field Compaction |E*| - Structure Variations)
Surface Rutting (inches)
Pavement Age (month)
Baseline Condition
Base - 4 inches
Base & Subbase - 4 inches
Subgrade - A-7-6, Mr= 5000psi
0
0.2
0.4
0.6
0.8
1
0
20
40
60
80
100
120

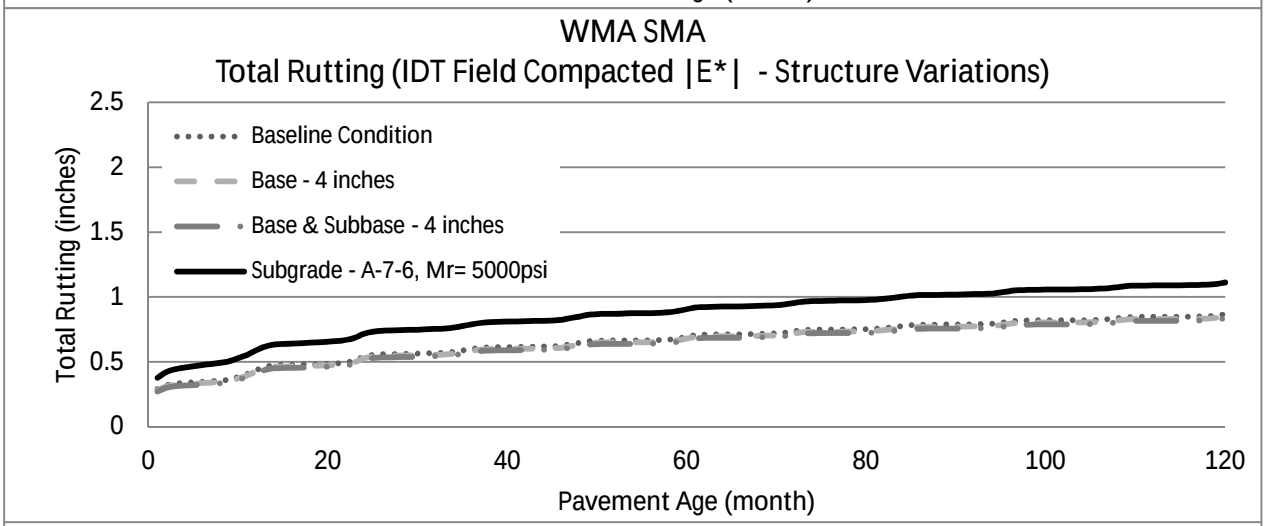
WMA SMA
Total Rutting (IDT Field Compacted |E*| - Structure Variations)
Total Rutting (inches)
Pavement Age (month)
Baseline Condition
Base - 4 inches
Base & Subbase - 4 inches
Subgrade - A-7-6, Mr= 5000psi
0
0.5
1
1.5
2
2.5
0
20
40
60
80
100
120

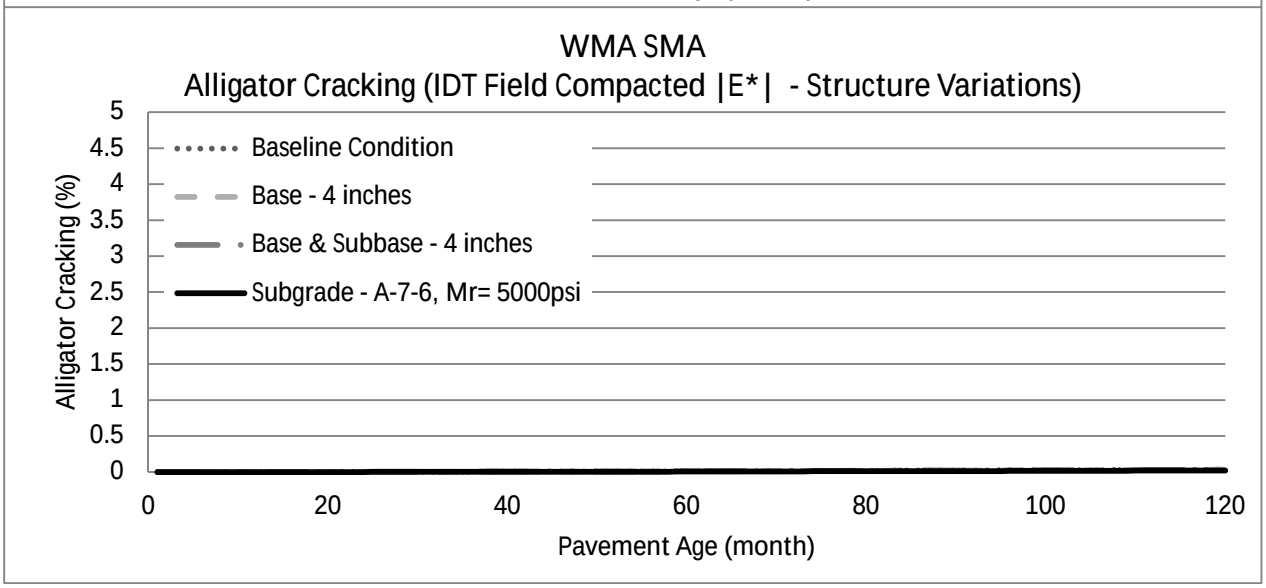
WMA SMA
Alligator Cracking (IDT Field Compacted |E*| - Structure Variations)
Alligator Cracking (%)
Pavement Age (month)
Baseline Condition
Base - 4 inches
Base & Subbase - 4 inches
Subgrade - A-7-6, Mr= 5000psi
0
0.5
1
1.5
2
2.5
3
3.5
4
4.5
5
0
20
40
60
80
100
120

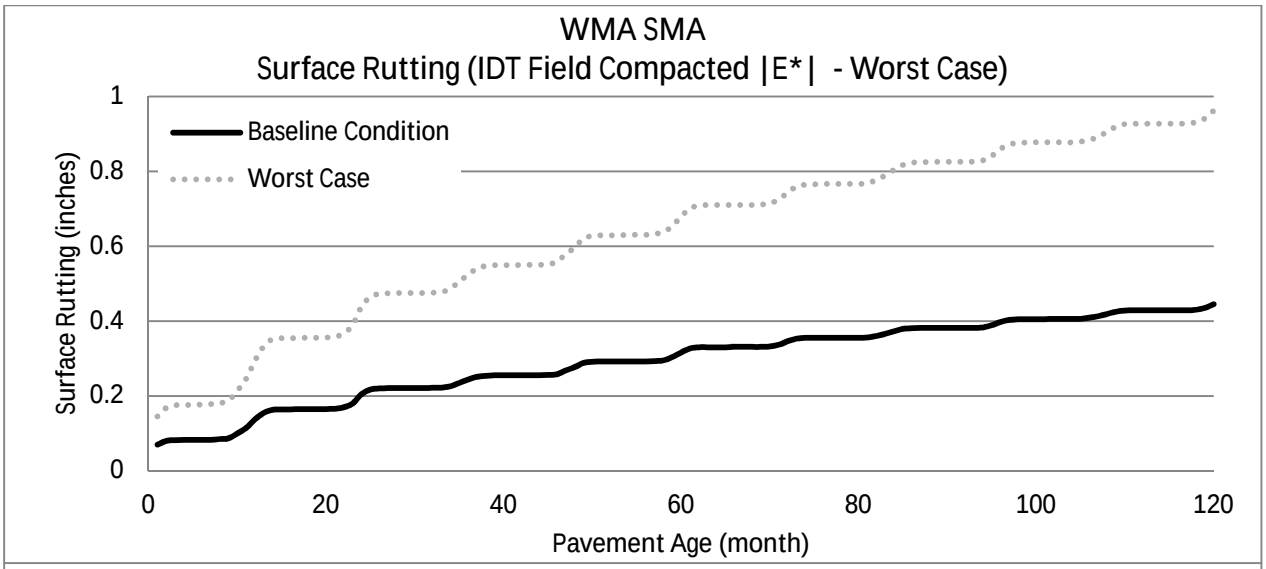
WMA SMA
Surface Rutting (IDT Field Compacted |E*| - Worst Case)
Baseline Condition
Worst Case
Surface Rutting (inches)
Pavement Age (month)
0
0.2
0.4
0.6
0.8
1
0
20
40
60
80
100
120

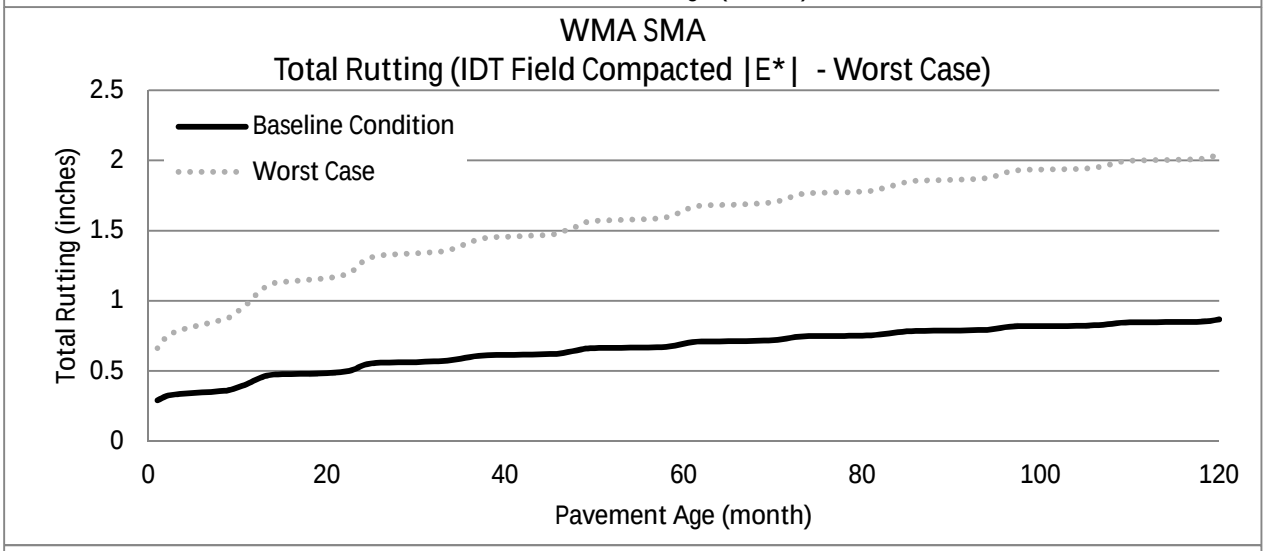
WMA SMA
Total Rutting (IDT Field Compacted |E*| - Worst Case)
Baseline Condition
Worst Case
Total Rutting (inches)
Pavement Age (month)
0
0.5
1
1.5
2
2.5
0
20
40
60
80
100
120

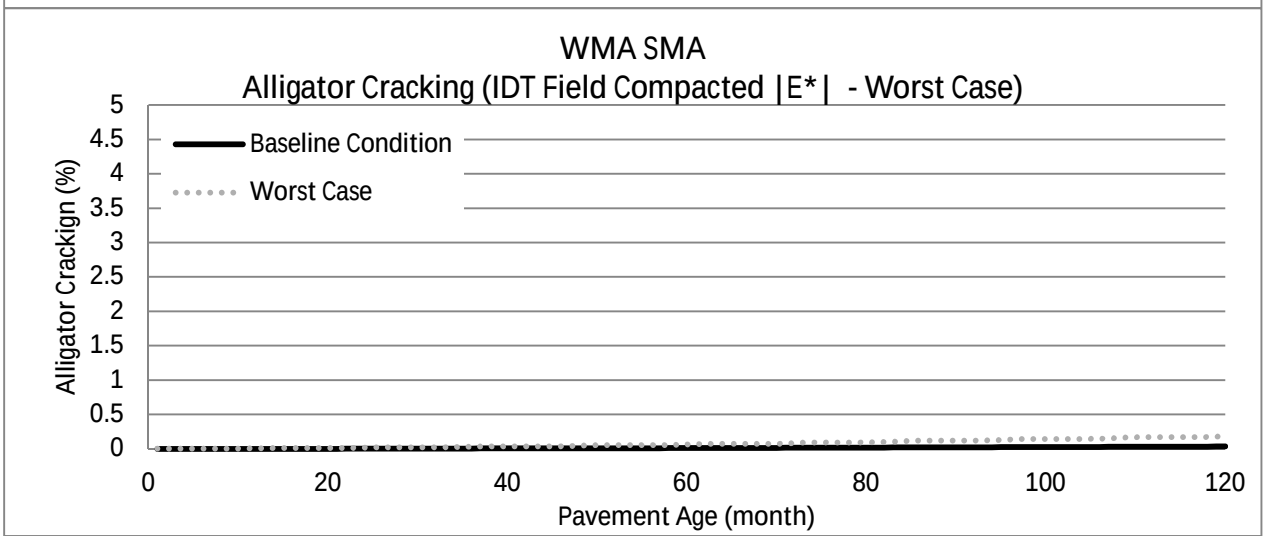
WMA SMA
Alligator Cracking (IDT Field Compacted |E*| - Worst Case)
Baseline Condition
Worst Case
Alligator Crackign (%)
Pavement Age (month)
0
0.5
1
1.5
2
2.5
3
3.5
4
4.5
5
0
20
40
60
80
100
120

UNPUBLISHED APPENDIXES

Appendixes A, B, and D to the contractor's final report for NCHRP Project 09-22B are not published herein but are available on the TRB website at http://apps.trb.org/cmsfeed/TRBNetProjectDisplay.asp?ProjectID=3122.

The appendix titles are the following:

- APPENDIX A Dynamic Modulus Master Curve Data
- APPENDIX B QRSS and SPT Program Input Files
- APPENDIX D: Confidence Interval Analysis